ČESKÉ VYSKOVÉ UČENÍ TECHNICKÉ V PRAZE
FAKULTA STROJNÍ
ÚSTAV ENERGETIKY

DISERTAČNÍ PRÁCE

PREDIKČNÍ MODELY NO_X PRO FLUIDNÍ KOTLE

Jiří Štefanica

Doktorský studijní program: Strojní inženýrství

Studijní obor: Energetické stroje a zařízení

Školitel: *prof. Ing. František Hrdlička, CSc.*

Praha únor 2020

Čestné prohlášení

Čestně prohlašuji, že jsem disertační práci s názvem "Predikční modely NO_X pro fluidní kotle" vypracoval samostatně, a že veškeré použité prameny jsou uvedeny v seznamu literatury (References).

Disertační práce byla dle pokynů zkušební komise opravena a odevzdána v únoru 2020.

Poděkování

Rád bych poděkoval v první řadě prof. Ing. Františku Hrdličkovi, CSc. za odborné vedení práce, za cenné rady, připomínky, konzultace a za pomoc v průběhu celého doktorského studia. Dále bych rád poděkoval doc. Ing. Janu Hrdličkovi, Ph.D. za vedení týmu pro návrh a realizaci experimentálního zařízení Minifluid. Velký dík také patří všem kolegům z doktorského studia, kteří se na realizaci Minifluidu podíleli.

Zvláštní poděkování bych rád věnoval Ing. Olze Ubré, DrSc., se kterou jsem měl tu čest pracovat a která mi předala mnoho svých odborných znalostí.

V neposlední řadě patří také dík mému otci, který je mi svou pracovitostí a poctivostí životním vzorem, a mé matce, která mi vždy byla ochotna podat pomocnou ruku. Děkuji také své sestře Kristýně, za její podporu a povzbuzování. Velký dík patří mé snoubence Alis Muse za její trpělivost, obětavost a za to, že je mi ve všem oporou a motivací zároveň.

Anotace

Cílem předložené práce je zkoumání mechanismů tvorby emisí oxidů dusíku ve fluidních kotlích na tuhá paliva a porovnání těchto mechanismů pro spalování uhlí a biomasy. Dále je cílem práce vyhodnocení současného stavu modelování a predikce emisí NO_X ve fluidních kotlích a formulace návrhů a doporučení, jejichž účelem je predikční modely zefektivnit. Současný stav problematiky mechanismů tvorby NO_X i problematiky predikčních modelů je zpracován v kapitole 2. V Kapitole 3 jsou definovány cíle práce. Kapitola 4 obsahuje vlastní přínos práce k zefektivnění predikčních modelů. Součástí práce je také experimentální část, která je popsaná v kapitolách 5 a 6.

Klíčová slova: NO_X, NO, emise, predikční modely, predikce emisí, fluidní spalování, fluidní kotle

Annotation

The goal of this work is to investigate the mechanisms of nitrogen oxides formation in fluidized bed combustors for solid fuels. The formation mechanisms of nitrogen oxides are compared for the case of coal combustion and for the case of biomass combustion. Another goal is to evaluate the current state of modeling NO_X emissions in fluidized bed boilers and to propose improvements that would make the models more effective. Current state of the problematics of NO_X formation and prediction is described in chapter 2. The goals of this work are defined in chapter 3. The new contributions of this work are in chapter 4. This work also contains experimental part which is described in chapters 5 and 6.

Keywords: NO_X, NO, emissions, prediction models, prediction of emissions, fluidized bed combustion, fluidized bed boilers

Obsah

Abbreviations

B	biomass
BFBC	bubbling fluidized bed combustor
CCS	CO_2 capture and sequestration
CFBC	circulating fluidized bed combustor
CTU	Czech technical university in Prague
$DENO_X$	denitrification, NO_X removal from flue gas
FBC	fluidized bed combustor
FC	fixed carbon
FR	fuel ratio
HC	hard coal
LC	lignite coal
NO_X	NO and NO_2
PCC	pulverized coal combustor
SCR	selective catalytic reduction
SNCR	selective non-catalytic reduction

Used symbols

α [W/m^2·K]	convective heat transfer coefficient
$\alpha_{11} - \alpha_{ml}$ [-]	exponents of fundamental units in the dimension matrix **A**, used in dimensional analysis
β_{1-4} [-]	coefficients expressing the conversion of volatile nitrogen to different parts of volatiles
γ [-]	coefficient expressing the conversion of fixed nitrogen to NO
ξ_C [-]	combustion loss due to unburned carbon
κ [-]	coefficient expressing the part of nitrogen released from fuel in volatile form
λ [W/m·K]	thermal conductivity of the fuel
λ_{comb} [-]	excess air ratio
μ [kg/m·s]	dynamic viscosity
μ_{1-2} [-]	coefficients expressing the conversion of volatile nitrogen (1) and fixed nitrogen (2) to NO
π_1 *to* π_{m-l} [-]	dimensionless complexes, used in dimensional analysis
ρ_f [kg/m^3]	density of the fuel
ρ_g [kg/m^3]	density of gas
ρ_s [kg/m^3]	density of solids (fluidized bed particles)
σ	standard deviation
ϕ [-]	sphericity
φ_{1-2} [-]	coefficients expressing the conversion of different parts of volatile nitrogen to one another
φ_3 [-]	coefficient expressing the conversion of NH_3 to NO

A [g.MJ^{-1}.K^{0,5}]	coefficient
A	dimension matrix, used in dimensional analysis
$\mathbf{A_B}$	square submatrix of the dimension matrix, used in dimensional analysis
$\mathbf{A_R}$	redundant submatrix of the dimension matrix, used in dimensional analysis
a_{1-m} [b_{1-l}]	physical quantities labelled a_1 to a_m with basic dimensions labelled b_1 to b_l, used in dimensional analysis
A^r [-]	ash content of the fuel in raw(non-dried) state, mass fraction
B	solution matrix consisting of solution vectors $\mathbf{x_1}$ to $\mathbf{x_{m-l}}$, or vector elements x_{11} to $x_{m-l,l}$, used in dimensional analysis
C [s^{-1}]	velocity constant of combustion
C^{daf} [-]	carbon content of the fuel, mass fraction
c [%vol/s]	change in reactants volumetric concentration over time
c_p [J/kg·K]	specific heat capacity of the fuel
CO [ppm]	concentration of CO
d [m]	diameter of the particle
D [m]	diameter of the bed
E_a [J/kg]	energy of activation
FC [-]	fixed carbon content
Fr_p [-]	Froud number based on particle diameter

FR [-]	fuel ratio, non-volatile part of fuel
g [m/s^2]	gravitational acceleration
H [m]	height of the bed
H^{daf} [-]	hydrogen content of the fuel, mass fraction
$HRBZA$ [MW/m^3]	heat release per burner zone area
HRC [-]	heat recovery correction parameter for Pohl´s model
K, k [-]	parameter or coefficient
l [-]	number of fundamental dimensions, used in dimensional analysis
m [kg]	mass
m [-]	number of physical quantities, used in dimensional analysis
M_{NOX} [g/s]	formation rate of NO_X
$M_{steam.nom}$ [t/h]	nominal steam output
M_F [kg/s]	mass flow of fuel
N^{daf} [wt%]	nitrogen content in dry de-ashed fuel (similarly for other elements)
N^{d} [wt%]	nitrogen content in dry fuel (similarly for other elements)
NO [ppm]	concentration of NO
NO_{eq} [ppm]	NO concentration in flue gas if all nitrogen in fuel converts to NO
NOX [ppm]	concentration of NO_X
NOX^* [ppm]	concentration of NO_X measured by the flue gas analysed and corrected to standard oxygen concentration
$\frac{NO}{NO_{eq}}$ or $\frac{NOX}{NO_{eq}}$ [-]	conversion factor of fuel nitrogen to NO or NO_X, for 0 % O2 and dry basis
$O2$ [%vol]	primary concentration of O_2 in flue gas, volumetric
$O2_{total}$ [%vol]	total O_2 concentration used in case of staged combustion
O^{daf} [-]	oxygen content of the fuel, mass fraction
p [MPa]	pressure
P_e [MW_e]	electrical power output, can be expressed in MWe or in % of maximum power output electrical
P_{th} [MW_{th}]	thermal power output, can be expressed in MWt or in % of maximum power output thermal
$P_{MAX,\,e}$ [MW_e]	maximum power output electrical
$P_{MAX,\,th}$ [MW_{th}]	maximum power output thermal
Q_i^r [MJ/kg]	lower heating value
R [J/kg·K]	universal gas constant
r [-]	flue gas recirculation coefficient, calculated as flow of recirculated flue gas relative to primary flow
R^2 [-]	coefficient of determination, the proportion of dependent variable that is predictable from the independent variable
Re_p [-]	Reynolds number based on particle diameter
S^{daf} [-]	sulphur content of the fuel, mass fraction
$SO2$ [ppm]	concentration of SO_2
T [K]	thermodynamic temperature
t [°C]	temperature
t [s]	residence time
u [m/s]	superficial velocity

U	uncertainty of the measured value, unit is corresponding to the physical value
u_{mf} [m/s]	minimal fluidization velocity
VM [-]	volatile matter content
V_{fd} [m^3/kg]	volume of dry flue gas from combustion of 1 kg of fuel
W^r [-]	water content of the fuel in raw(non-dried) state, mass fraction
$\bar{x}$	average value of the quantity x, unit is corresponding to the averaged physical quantity
x_i	measured values of the physical quantity, used in determination of measurements uncertainty, unit is corresponding to the averaged physical quantity
$\mathbf{x}_1$ - $\mathbf{x}_{m-l}$ [-]	solution vectors labelled $\mathbf{x}_1$ to $\mathbf{x}_{m-l}$, used in dimensional analysis
x_{11} - $x_{m-l,l}$ [-]	elements of the solution vectors, number of vectors is m-l and each vector has l elements, used in dimensional analysis
XAC [-]	oxygen concentration correction parameter for Pohl´s model

List of tables

List of figures

1 Introduction

This work consists of 7 chapters. Chapter 1 is introduction.

Chapter 2 consists mostly of information obtained from studying the relevant literature. It provides the basic information about combustion technologies with emphasis on fluidized bed combustion and it describes the basic boiler types. The main part of chapter 2 is dealing with the formation mechanisms of nitrogen oxides. The literature review of parameters influencing emissions of NO_X is provided. Short mentions are included regarding the possibilities of NO_X abatements and regarding the special case of oxy-fuel combustion and its impact on NO_X emissions. In the end of chapter 2 the NO_X prediction models are investigated.

Chapter 3 is stating the goals of the work and is advocating their utility, applicability and originality

Chapter 4 is aimed at describing new contributions of this work to the field of NO_X prediction. Two contributions are shown. A theoretical approach to parameter selection of empirical models by the means of the dimensional analysis was done. Secondly, modifications were proposed to the current PCC empirical models for NO_X prediction to be applicable to prediction of NO_X emissions of the FBC.

Chapter 5 is aimed at the experimental part. Firstly, the laboratory unit Minifluid, the fuels used during experiment, the start-up and the shut-down procedures are described. The experiment´s methodology and plan are explained. The measurement uncertainty is addressed.

Chapter 6 is presenting the experimental results and their evaluation. Firstly, the repeatability of results is discussed. Later, correlation analysis is done, the findings are presented, the conclusions are drawn and, in the end, extensively discussed.

Chapter 7 is summarizing the work done.

2 Theoretical part

2.1 Combustion technologies

Even though the basic mechanism of combustion reactions is the same, several types of combustion can be distinguished. The main categorization of the combustion processes is based on the combustion velocity [1]. The combustion consists of physical and chemical processes. The physical processes being mostly the transport of mass (fuel and oxidizer) and heat. The chemical processes being combustion reactions themselves. All processes are running simultaneously and are characterized by time duration. If the duration of physical transport processes is significantly longer than the duration of chemical processes the combustion is called diffusive and the velocity constant of combustion is high. If it is the other way around the combustion is called kinetic and the velocity constant of combustion is low. These combustion types have characteristic temperature intervals, see Figure 1. Kinetic combustion takes place at combustion temperatures under 600 °C and diffusive combustion over 1300 °C.

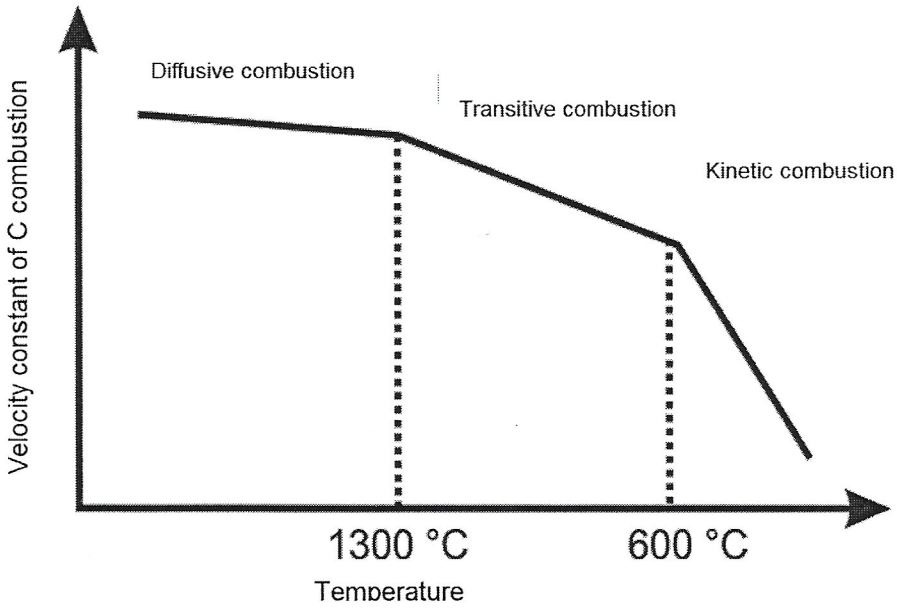

Figure 1: Types of combustion [1]

Furthermore, the combustion process can be categorized based on the state of fuel and oxidant. If both have the same phase (combustion of gaseous fuels) the combustion is called homogeneous. If the phase of fuel and oxidant are different the combustion is heterogeneous.

During the combustion of solid fuels, the combustion of fixed carbon is heterogeneous diffusive, and the combustion of volatile combustible is homogeneous kinetic.

Another way how to categorize the combustion processes is based on the relative velocity of fuel and oxidant [2]. The categorization is as follows:

1. Filtration combustion – pieces of fuel are brought to a grate and combusted by oxidizer flowing through the gaps. The relative velocity of fuel and oxidant is about 1,5 m/s, the combustion process is mostly diffusive. The grate consists of the support construction, grate bars and possibly a moving mechanism. Other parts of the combustor are fuel hopper, slide, clinker hopper, combusting area, ignition arch and the equipment for air

inlet. The purpose of the grate is to support fuel, allowing its drying, degassing and combustion as well as ensuring the inflow of necessary air and outlet of ashes.

2. Drift combustion – typical for combustion of pulverized coal and liquid fuels. Despite the very high velocity of oxidant, the relative velocity of fuel and oxidant is very low. Compared to grated coal, the pulverized coal has up to 1000 times greater surface area and therefore also the combustion velocity. Fuel is led to the combustion chamber by burners that ensure optimal mixing with oxidant. The flow in the combustion chamber is influenced by the shape of the chamber and number of burners and their placement which must be chosen with respect to boiler reliability and heat exchanger placement.
3. Suspended combustion – fuel is suspended by flowing through oxidant. Relative velocity of fuel and oxidant is high. More detailed description will be provided in chapter 2.1.1.
4. Whirling combustion – typical for cyclone combustors. Very high relative velocity of fuel and oxidant is achieved through centrifuge effect and particle deceleration on the walls. The combustion velocity is even higher than at drift combustion due to higher velocity and turbulence. [2]

2.1.1 Fluidized bed combustion

Fluidized bed combustion takes place in the bed of an inert material brought to a state of fluidization by passing though air usually at temperature 800 – 950 °C. For more information on the phenomenon of fluidization see e.g. Fluidization Engineering [3]. Fluidized bed combustors (FBC) can be using stationary bubbling bed or circulating bed. The combustors can be pressurized; however, atmospheric option is more common.

FBC are an alternative to pulverized coal combustors (PCC) used in classical power plant units with medium and high power output. Contrary to PCC the FBC are more suitable for medium power output of tens to several hundreds of MWe. FBC can combust fuel of low quality – low heating value, high water content – and allow much more variation of fuel properties than PCC. Fuel size in FBC is usually between 0 – 5 mm and the fuel is combusted in the bed of inert material. Inert material can be its ash in case of coal combustion. In case of biomass, that has very low ash content (usually under 1 %), external material is needed – dolomite or sand are the usual choices. Inert material is major component of the bed, while fuel usually represents only 5 – 10 % of bed mass. [2]

2.1.2 Advantages of FBC

1. Fuel requirements

   The main advantage of FBC is their low sensitivity on fuel quality and fuel preparation which reduces the fuel associated costs and allows combustion of fuels that are not suitable for other combustion technologies. Larger fuel particle size is reducing the energy consumption for grinding compared to PCC. Another big advantage is low sensitivity to fuel switching.

2. Mass and heat transfer

   Intensive mixing of solid and gaseous phase in the fluidized bed is enhancing the transfer of mass and heat which allows the combustion process to be realized at much lower temperature, compared to PCC and grate combustors, without the drop of combustion efficiency. Convective heat transfer in the combustion chamber of a FBC is 2 – 3 x higher than in the PCC.

3. SO_2 reduction

Due to the low combustion temperature and intensive mass transfer the FBC are suitable for dry method of desulphurization (dosing of milled lime stone directly in the bed) which is the cheapest technology of SO_2 removal from flue gas. Low combustion temperature is necessary for reaching high efficiency of SO_2 removal.

4. NO_X reduction

Another benefit of low combustion temperature is elimination of thermal NO_X. The NO_X emission limit is usually abode by primary measures only (no need for flue gas denitrification). [2]

2.1.3 Disadvantages of FBC

1. Power output

The FBC are not suitable for large power plant blocks. Stationary bubbling bed boilers are suitable for power output 1 – 40 MWe, circulating bed boilers are suitable up to 200 MWe. The FBC are generally limited by the dimension of the combustion chamber. Large combustion chamber brings difficulties with maintaining the whole bed uniformly fluidized. Large power output can be obtained by modular design and combination of smaller units.

On the other hand, FBC are also not suitable for small units and household heating where grate boilers are much more economical.

2. Blower consumption

The bed needs to be maintained suspended in the state of fluidization which requires a lot of energy. The blower consumption is larger compared to PCC.

3. SO_2 and NO_X reduction

The dry SO_2 reduction method is less efficient than the wet method which is commonly used at the PCC. The efficiency of SO_2 removal of 70 % can be achieved with Ca/S = 3 using the dry method. Increasing the efficiency is possible by further increasing the Ca/S ratio. The dry method is simple and cheap but requires larger amount of lime stone for the same efficiency.

In case of legislation changes and emission limit decrease the dry method might not be sufficient and wet method implementation could become a necessity at FBC as well. The same point stands for NO_X reduction, in case of legislation changes and emission limit decrease the implementation of denitrification technology can become obligatory. This is not a disadvantage per se; however, this would represent a loss of an advantage.

4. Heat transfer

Due to the low combustion temperature the heat transfer through radiation is also low. This is partially compensated by greater convective heat transfer (one of the advantages). Another effect that can complicate the heat transfer is coating of the heat transfer surfaces which was observed in the experimental part of the work.

5. Elutriation

Both stationary and circulating FBC have large elutriation of fine particles from the bed which can cause abrasion of the heating surfaces and which needs to be separated before the flue gas is recirculated or discharged. [2]

2.1.4 Basic types of the FBC

1. Bubbling (stationary) fluidized bed combustor

Bubbling fluidized bed combustor (BFBC) is suitable for P_e = 1 – 40 MWe and steam output max 265 t/h. Equipment of the BFBC with elutriated particles recirculation is

optional. The bed temperature can be controlled by recirculated particles (external heat exchanger) or by submerged or side heat exchanger (usually evaporator, possibly the superheater). See Figure 2. [3]

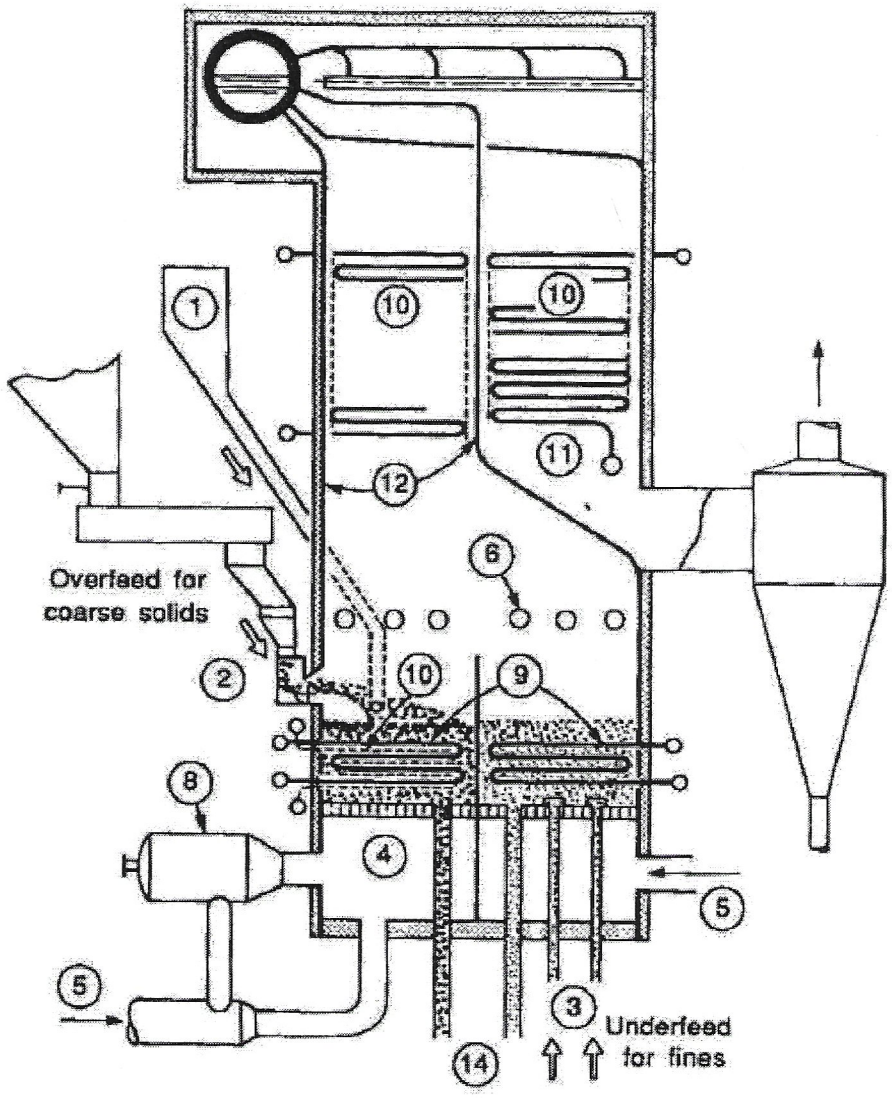

Figure 2: BFBC with stationary bubbling bed and a cyclone separator of particles; 1 – lime stone inlet, 2 – fuel inlet – coarse particles (on the top of the bed), 3 – fuel inlet – fine particles (under the bed), 4 – distributor, 5 – primary air inlet, 6 – secondary air nozzle, 7 – Fluidization air, 8 – air heater, 9 – evaporator, 10 – superheater, 11 – economizer, 12 – Membrane wall, 14 – ash discharge [3]

2. Circulating (fast) fluidized bed combustor

Circulating fluidized bed combustor (CFBC) is suitable for P_e = 40 –200 MWe. Equipment with external heat exchanger, cyclone and separator grid is optional. Bed temperature is usually regulated by external heat exchanger, flue gas recirculation or fluidization air preheating. See Figure 3. [3]

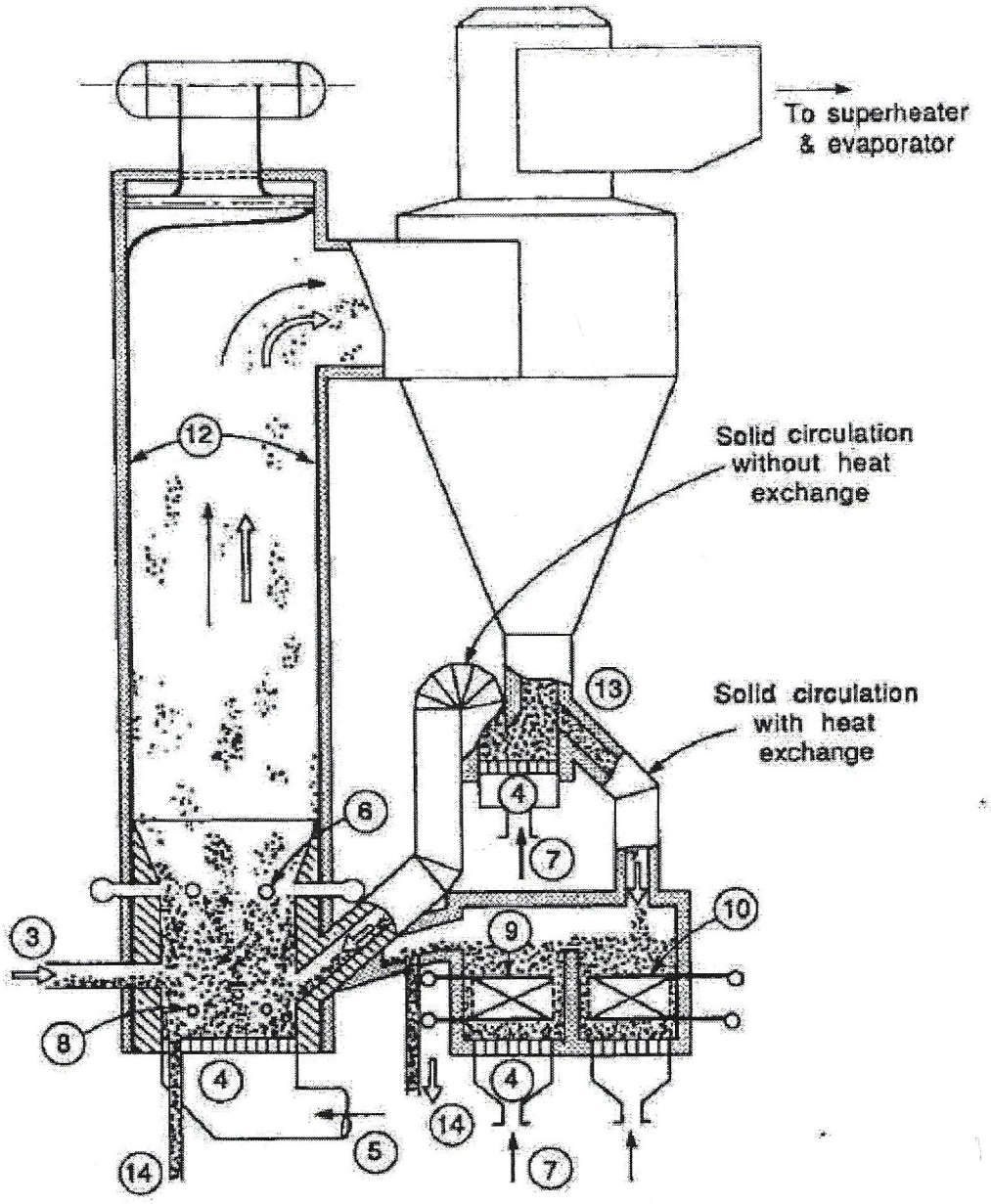

Figure 3: CFBC with cyclone separator and external heat exchanger; 3 Fuel inlet – fine particles (under the bed), 4 – distributor, 5 – primary air inlet, 6 – secondary air nozzle, 7 – fluidization air, 8 – air heater, 9 – evaporator, 10 – superheater, 12 – membrane wall, 13 – circulator, 14 – ash discharge [3]

3. Fluidized bed combustor with the expanding bed

Fluidized bed combustor with the expanding bed is a special case of the BFBC. It´s characteristic feature is the diameter of the fluidized bed which is increasing with the height. See Figure 4 for a variant of the FBC equipped with primary combustion chamber with expanding bed. This type of combustor is suitable for heating and technology purposes in the scope of several MWe. The main advantage is larger fuel variety and regulation range. [3] [4]

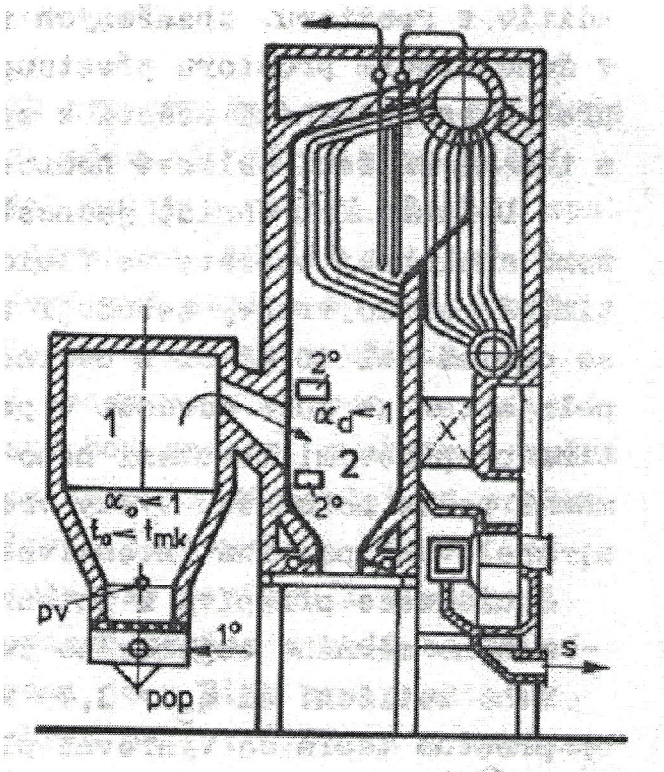

Figure 4: FBC with the expanding bed; 1 – primary combustion chamber with the expanding fluidized bed, 2 – secondary combustion chamber [4]

2.2 NO_X emissions from combustion of solid fuels

Electric power and heat generation by coal, biomass and other solid fuels combustion is indispensable in the Czech Republic as well as all over the world. On the other hand, it releases large amounts of noxious gases that are harmful to humans and all ecosystem of Earth. One of these gases is referred to as NO_X, it refers to nitrogen compounds NO and NO_2. These pollutants cause photochemical smog, acid rain, ground level ozone and damage to respiratory systems of organisms. Therefore, the emitters must abide to the emission limits. Current Czech legislation (edict 415/2012) sets the NO_X emission limit to 300 mg/m^3 for new boilers combusting solid fuels with P_{th} > 50 MW_{th}. Considering the BFBC lower power range should be also considered. The boilers combusting solid fuels with thermal power input 0,3 – 50 MW_{th} have the emission limit 600 mg/m^3. [5]

2.2.1 NO_X formation chemistry

2.2.1.1 Origin of Nitrogen in the combustion process

The nitrogen in the combustion process can originate either in the fuel or in the combustion air. Nitrogen content of biomass is much lower compared to coal (coal having usually 0,5 – 2 wt% and biomass 0,1 – 1 wt%). The nitrogen content of air is 78 vol%. [6]

2.2.1.2 Forms of Nitrogen in solid fuels

Nitrogen is very important part of biomass and is present in the form of proteins, nitrates, ammonium, chlorophyll and nucleic acids. The exact composition is varying strongly, depending not only on the type of biomass but also on local conditions.

The nitrogen in coal comes mostly from the biomass that has undergone coalification and it takes form of pyridinic, pyrrolic, and quaternary functional groups in polycyclic aromatic

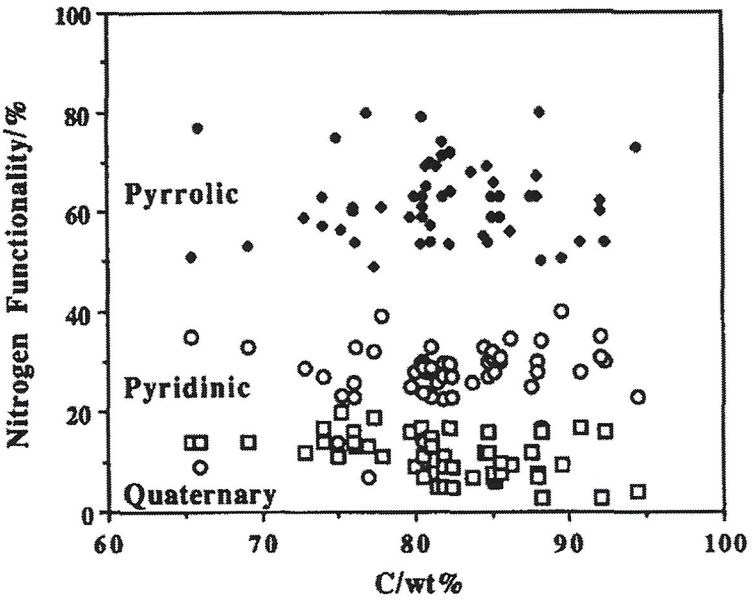

Figure 5: Division of nitrogen functional groups in coal with carbon content [7]

compounds. Fractional division of these compounds is independent on coal rank and reaches 0 – 20 % for quaternary, 20 – 40 % for pyridinic and 50 – 80 % for pyrrolic compounds, as can be seen in Figure 5. Occurrence of inorganic nitrogen in coal coming from mineral matter is very rare but can substitute up to 20 % of total nitrogen in some anthracites. [6]

2.2.1.3 Forms of nitrogen in flue gas

It is now widely accepted that none of the nitrogen contained in coal or biomass is in any way chemically bonded in the ash, meaning all fuel-nitrogen will be eventually released as part of the flue gas (with exception of nitrogen in unreacted residue).

The nitrogen contained in the combustion air remains mostly unreacted and leaves the process as N_2; however, small part is also converted to nitrogen oxides.

Nitrogen can be present in emitted flue gas as NO, NO_2, N_2 or N_2O (considering there are no unburned volatiles – NH_3 and HCN). The chemistry determining whether the nitrogen will be released in the end as N_2 or oxidized into one of the above-mentioned oxides is very complex. It is not sufficient to take in account only the formation mechanisms of nitrogen oxides but it is necessary to keep in mind also the reduction mechanisms – homogenous and heterogeneous.

It is often considered that overall NO_X emissions from combustion of solid fuels consist from 95% of NO and just 5% of NO_2 making the NO chemistry much more important. [6]

2.2.1.4 NO formation mechanisms during combustion

There are altogether three mechanisms that are generally accepted to be responsible for NO emissions. "Thermal NO" are formed by oxygen and hydroxyl radicals' oxidation of air nitrogen. "Fuel NO" have the origin in nitrogen contained in the fuel that reacts with hydrocarbon radicals followed by further oxidation. And the "prompt NO" are formed from the air nitrogen through the similar path as the fuel NO. [6] [7]

Thermal NO

Thermal NO formation mechanism can be considered independent on the fuel because both the nitrogen and oxygen are provided with the combustion air. The mechanism consists of reactions (1), (2) and (3).

$$N_2 + O \cdot \rightarrow NO + N \cdot \quad (1)$$

$$N \cdot + OH \cdot \rightarrow NO + H \cdot \quad (2)$$

$$N \cdot + O_2 \rightarrow NO + O \cdot \quad (3)$$

The reaction (1) is the most important one and is responsible for virtually all thermal NO. The reaction (2) takes place mostly in fuel rich conditions where OH radical is present in larger quantities.

The air nitrogen is oxidized either with O or OH radicals that are also responsible for fuel oxidation. This means that although this mechanism does not involve fuel it is not independent on the combustion process. However, the thermal NO are in most cases considered independent on the combustion process, as was suggested by Zeldovich, because this mechanism is very slow compared to the fuel combustion. Based on Zeldovich approximation the thermal NO concentration can be calculated considering the steady state and temperature equilibrium concentrations of O, O_2, N_2 and OH. This approximation underestimates the real values in most cases with a very high relative deviation at low temperatures. Raising the combustion temperature makes the calculated values more precise which is very favourable because thermal NO formation mechanism is considered significant just at high temperature (starting at 1500 K), the dependence on temperature is very strong. [6] [8]

Prompt NO

Air nitrogen can be converted to NO also through the prompt formation path that was proposed by Fenimore [6]. These NO are called prompt because their formation is very rapid – occurs only in the fuel rich zone close to the flame. NO formed by thermal mechanism in concentration higher than the equilibrium are by some authors also considered to have the prompt origin. Not considering this the formation mechanism is initiated by the reaction of air nitrogen with hydrocarbon radicals as can be seen in equation (4), (5) and (6). Reaction (4) is the most important one under most of combustion conditions.

$$CH\cdot + N_2 \rightarrow HCN + N\cdot \qquad (4)$$

$$CH_2\cdot + N_2 \rightarrow HCN + NH\cdot \qquad (5)$$

$$CH_2\cdot + N_2 \rightarrow H_2CN\cdot + N\cdot \qquad (6)$$

Reaction (7) is not very significant at low temperature but as temperature raises this reaction also becomes not negligible.

$$C\cdot + N_2 \rightarrow CN\cdot + N\cdot \qquad (7)$$

Subsequently formed radicals are all converted to HCN by reactions (8) and (9).

$$H_2CN\cdot + M \rightarrow HCN + H\cdot + M \qquad (8)$$

$$CN\cdot + H_2 \rightarrow HCN + H\cdot \qquad (9)$$

HCN is then oxidized to NO as is shown by reactions (10), (11), (12) and (2).

$$HCN + O\cdot \rightarrow NCO\cdot + H\cdot \qquad (10)$$

$$NCO\cdot + H\cdot \rightarrow NH\cdot + CO \qquad (11)$$

$$NH \cdot + H \cdot \rightarrow N \cdot + H_2 \qquad (12)$$

Reaction (12) can be also followed by reactions (13) and (14) instead of (2) and lead to N_2 and H_2CN instead of NO.

$$N \cdot + NO \rightarrow N_2 + O \cdot \qquad (13)$$

$$N \cdot + CH_3 \cdot \rightarrow H_2CN \cdot + H \cdot \qquad (14)$$

Obviously, reactions (2),(13) and (14) are competing. N_2 formed by reaction (13) leaves in the flue gas without reacting any further. H_2CN resulting from reaction (14) is reduced to HCN by reaction (8) and must undergo the rest of the process again. NO formed by reaction (2) can either leave the process in the flue gas or be recycled to HCN by reaction (15) followed by (9).

$$NO + C \cdot \rightarrow CN \cdot + O \cdot \qquad (15)$$

These are the most important reactions that take part in the prompt NO formation. However, there are many other possible reactions following formation of HCN that are of smaller importance; see complete overview in Figure 6. Highlighted (bold) processes are of major importance and were mentioned in this chapter. [6]

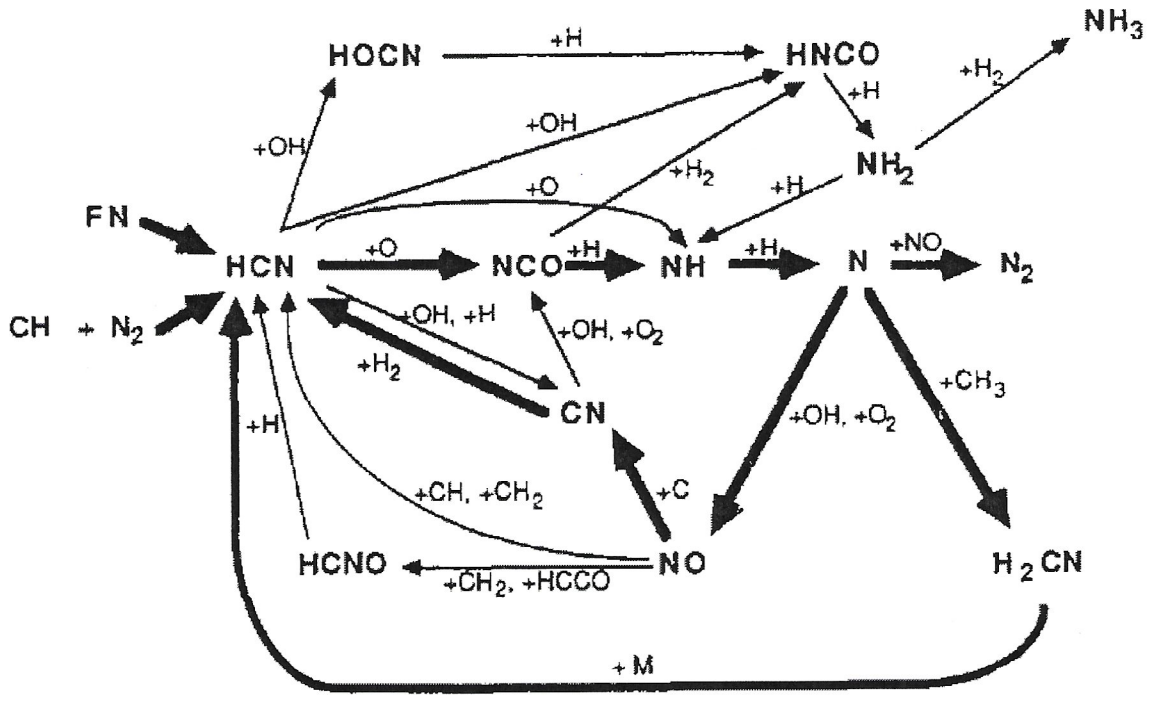

Figure 6: Overview of NO formation via prompt mechanism [6]

Fuel NO

Another source of NO emissions is the nitrogen contained in the fuel. Usually, coal has a nitrogen content of 0,5 – 2 wt% and biomass even less (0,2 – 1 wt%) but there are also exceptions like dewatered sewage sludge (6,5 wt%) with very high nitrogen content. Coal nitrogen content increases with coal rank until the carbon content cca 85 wt%. Then it starts to decrease as seen in Figure 7.

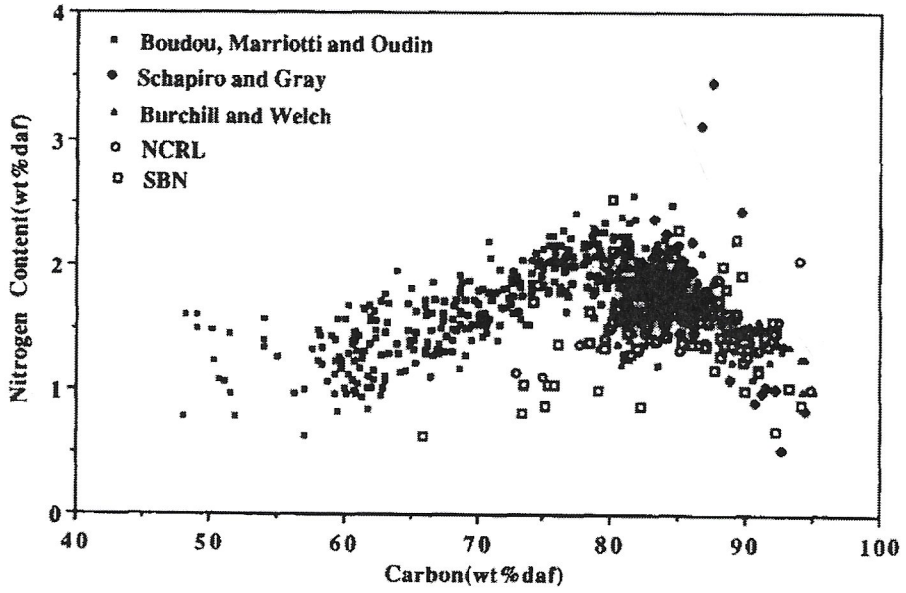

Figure 7: Dependence of nitrogen content on carbon content [7]

The amount of nitrogen oxides released is dependent not only on nitrogen content of fuel but also on the form of nitrogen compounds and combustion conditions (temperature, excess air and residence time). The NO emissions usually increase with increasing the fuel nitrogen content; however, the fuel nitrogen conversion to NO generally decreases. See in Figure 8.

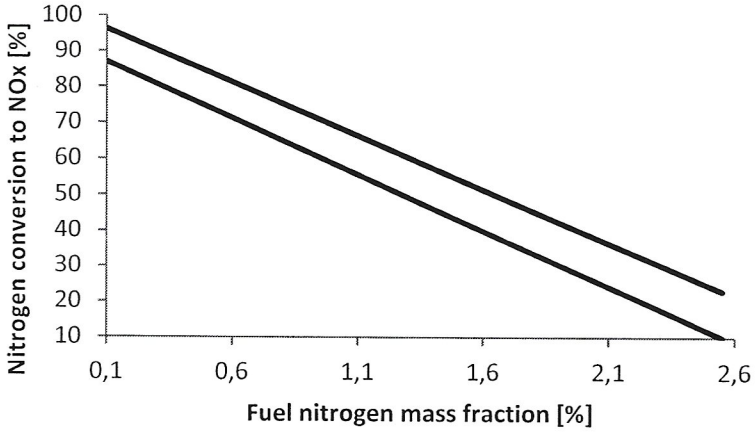

Figure 8: Dependence of nitrogen conversion to NO on nitrogen mass content in combustible for fossil fuels [8]

Conversion of fuel nitrogen to NO strongly depends on combustion parameters, fuel and air staging. The fuel nitrogen conversion to NO can be significantly lowered after combustion parameters´ optimization. Simplified reaction mechanism of nitrogen oxides

formation and reduction is shown on Figure 9 (although HCN can also react with H_2O vapor at higher temperatures to form CO and NH_3).

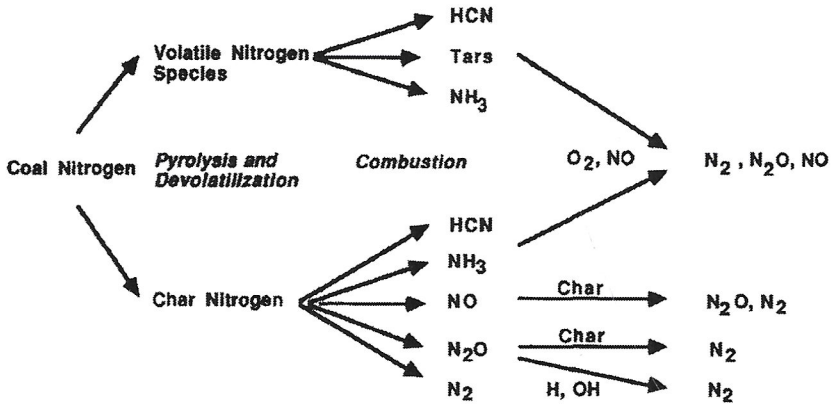

Figure 9: Coal nitrogen conversion [7]

Combustion process starts with devolatilization. During devolatilization the fuel particle breaks down into gases, tars and the remaining char. If tar is the primary product it further breaks down into gaseous volatiles. The tar yield of coal decreases with increasing temperature and can be expected between 10 – 30 %. Released volatiles are then combusted.

Fuel nitrogen that is released in the volatiles consists mostly of two final compounds: NH_3 and HCN. HCN has the origin in the aromatic rings bound nitrogen, it does not arise directly but comes from secondary cracking of tar and other volatile nitrogen compounds. NH_3 comes from amines but can also have origin in HCN, equations (10) and (11) followed by further hydrogenation. The division between HCN and NH_3 is also influenced by temperature and residence time.

The rest of the fuel nitrogen stays bound to char. These two are usually referred to as volatile nitrogen and char nitrogen. However, the amount of volatile/char nitrogen does not depend just on the fuel type. It was observed to depend also on many parameters such as: temperature, heating rate and residence time (also indirectly on particle size and feeding method); however, the volatile content seems to be the most important from these parameters. The observed dependence was increasing volatile nitrogen release with increasing temperature and residence time. Release of volatile nitrogen is not proportional to other volatiles release because high temperatures are needed to break the nitrogen compounds´ bonds. At lower temperatures (600 – 1200 K) and low residence time the resulting char is enriched by nitrogen and vice versa (lower rank coals show greater enrichment). The process of releasing volatile combustible is considered to play an important role in nitrogen chemistry because oxidation mechanisms for volatile nitrogen and char nitrogen (and also different compounds in volatile nitrogen) are different. At low rank coals about 55 % of fuel NO can be attributed to volatile nitrogen while at high rank coals it can fall to 25 %. At biomass combustion volatile nitrogen is usually responsible for majority (60 – 75 %) of NO emissions; however, contribution of char cannot be neglected and in some cases up to 50 % of NO can originate from char.

General observation can be made that biomass and low rank coals release more NH_3 (due to higher amine content) and high rank coals release more HCN. With increasing temperature HCN importance increases. The HCN yield also increases with decreasing particle size.

Biomass´ release of nitrogen compounds during devolatilization is highly dependent on the biomass type. During the biomass combustion NH_3 comes from the aromatic pyridine

structures. HCN has the origin in aliphatic and pyrrolic/pyridinic structures. The ratio of HCN/NH_3 release seems to be related to the H/N and O/N ratio of the biomass. Biomass with high O/N ratio will release more OH radicals that are responsible for conversion of HCN to NH3, see Figure 10. [7-14]

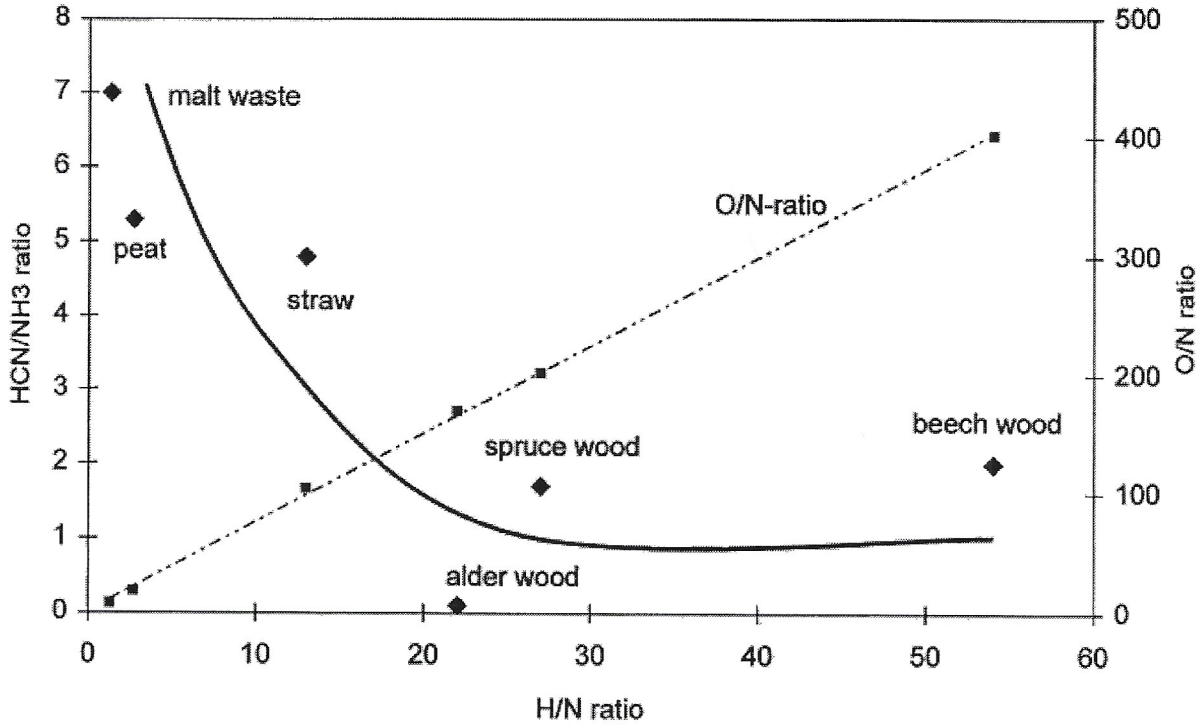

Figure 10: Volatile nitrogen distribution for biomass [9]

Volatile-nitrogen conversion

The conversion of HCN to NO or N_2 has the same mechanism that was described earlier in reactions (2) and (4) – (15) and Figure 6.

The conversion of NH_3 starts with abstracting hydrogen mostly by OH radical as shown in reaction (16) but also possibly by H or O radicals - reactions (17) and (18).

$$NH_3 + OH \cdot \rightarrow NH_2 \cdot + H_2O \qquad (16)$$

$$NH_3 + H \cdot \rightarrow NH_2 \cdot + H_2 \qquad (17)$$

$$NH_3 + O \cdot \rightarrow NH_2 \cdot + OH \cdot \qquad (18)$$

Further hydrogen abstraction occurs with OH and H radicals forming free radicals NH_{i-1} (possibly N) as is shown by a general reaction (19).

$$NH_i + H \cdot (OH \cdot) \rightarrow NH_{i-1} \cdot + H_2\ (H_2O) \qquad (19)$$

Each amine free radical and nitrogen radical can either be oxidized to NO or react with NO to form N_2. NH_2 is oxidized by reaction (20) followed by (21), (22) or (23).

$$NH_2 \cdot + O \cdot \rightarrow HNO \cdot + H \cdot \qquad (20)$$

$$HNO \cdot + M \rightarrow NO + H \cdot + M \qquad (21)$$

$$HNO \cdot + OH \cdot \rightarrow NO + H_2O \quad (22)$$

$$HNO \cdot + NH_2 \cdot \rightarrow NO + NH_3 \quad (23)$$

N_2 can be formed from NH_2 either directly by equation (24) or by (25) followed by (26).

$$NH_2 \cdot + NO \rightarrow N_2 + H_2O \quad (24)$$

$$NH_2 \cdot + NO \rightarrow NNH \cdot + OH \cdot \quad (25)$$

$$NNH \cdot + NO \rightarrow N_2 + HNO \cdot \quad (26)$$

NH is oxidized either directly by reaction (27) or (28) as well as indirectly by (29) or (30) followed by (21) – (23).

$$NH \cdot + O_2 \rightarrow NO + OH \cdot \quad (27)$$

$$NH \cdot + O \cdot \rightarrow NO + H \cdot \quad (28)$$

$$NH \cdot + O_2 \rightarrow HNO \cdot + O \cdot \quad (29)$$

$$NH \cdot + OH \cdot \rightarrow HNO \cdot + H \cdot \quad (30)$$

NH reacts with NO to form N_2O by reaction (31) which is subsequently reduced by hydrogen (32) to N_2.

$$NH \cdot + NO \rightarrow N_2O + H \cdot \quad (31)$$

$$N_2O + H \cdot \rightarrow N_2 + OH \cdot \quad (32)$$

Nitrogen atoms are forming NO and N_2 according to the extended Zeldovich mechanism shown in reactions (3), (33) and (34).

$$N \cdot + NO \rightarrow N_2 + O \cdot \quad (33)$$

$$N \cdot + OH \cdot \rightarrow NO + H \cdot \quad (34)$$

Simplified review of NO and N_2 formation from NH_3 can be seen on Figure 11. As we can see for both HCN and NH_3 combustion, there are competing reactions of NO and N_2 formation as well as NO reduction reactions. The reaction velocity is depending on the

combustion parameters and by their adjustment the form of nitrogen emitted can be influenced. [6]

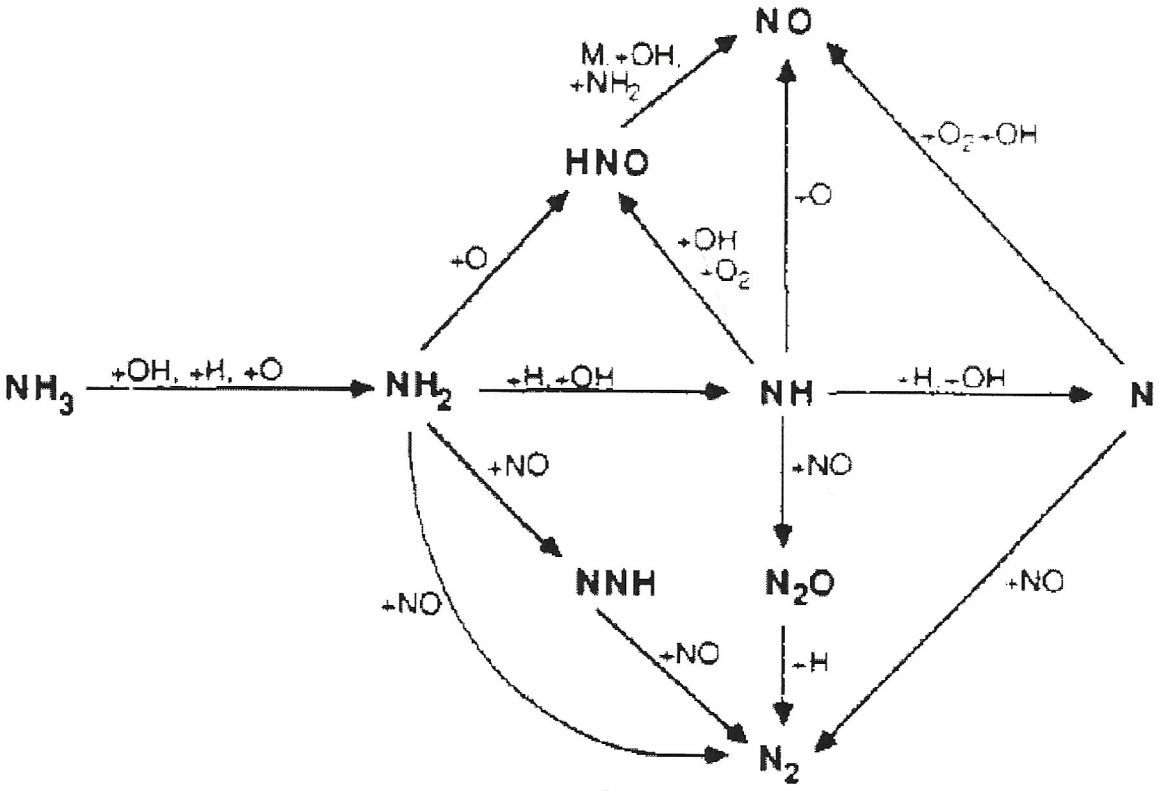

Figure 11: NO formation from NH_3 [6]

Char formation

The char is formed during devolatilization. The char structure and morphology are influenced by temperature, heating rate, petrographic composition, volatile and ash content and tar yield as well as coal rank. The resulting char structure determines the surface area of char particles. Char surface area together with char reactivity influence the char-nitrogen conversion to NO as well as the reduction reactions on char surface (mentioned later). The dependence of char surface on coal volatile content can be seen on Figure 12. The minimal char active surface can be expected from medium volatile bituminous coals.

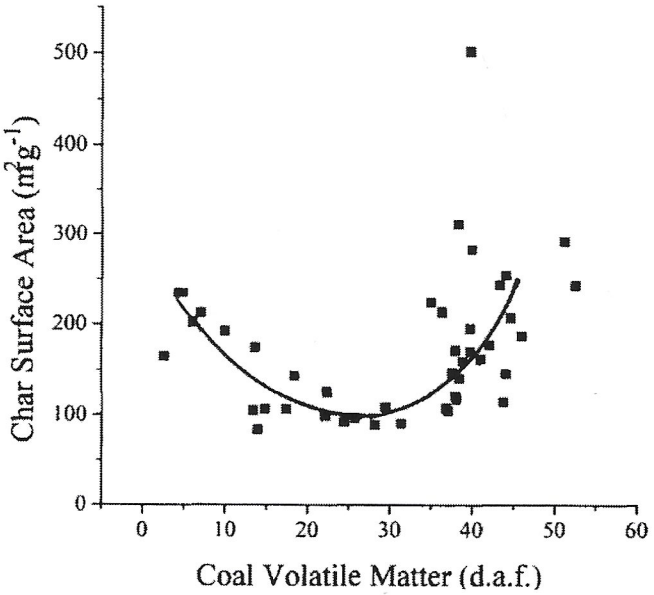

Figure 12: Dependence of char surface area on coal volatile content, devolatilization at 1273 K for 1 s [7]

The temperature gradient for large particles results in char with thick solid outer layer while small particles have much more uniform temperature profile, so the solidified layer is very thin or missing at all, meaning the devolatilization is steadier for smaller particles. [7]

Char-nitrogen conversion

The char nitrogen that stays chemically bonded to char after devolatilization is released during combustion in form of NO, N_2, N_2O where most important product is NO with conversion up to 80 % (data for fluidized bed) depending on conditions. Conversion of char nitrogen to NO is enhanced by increasing the devolatilization and combustion temperature. The mechanism of char nitrogen oxidation and release is assumed to proceed according to equations (35) – (40), where parentheses represent a solid bound species. It is a complex process of surface free active sites interactions. [7] [8] [12]

$$(-CN) + (-CO) \rightarrow (-CNO) + (-C) \qquad (35)$$

$$(-CNO) \rightarrow NO + (-C) \qquad (36)$$

$$2(-CNO) \rightarrow 2(-C) + N_2 + O_2 \qquad (37)$$

$$(-CNO) + (-CN) \rightarrow 2(-C) + N_2O \qquad (38)$$

$$2(-CN) \rightarrow 2(-C) + N_2 \quad (39)$$

$$2(-CNO) \rightarrow N_2O + (-CO) + (-C) \quad (40)$$

NO originating from char is formed in conditions that are favourable for its reduction as mentioned later. [7] [15] [16]

2.2.1.5 NO_2 formation during combustion

In most of the combustion processes the NO_2 presents just a minor part of nitrogen oxides. The formation of majority of NO_2 occurs through reaction (41). NO reacts with HO_2 that is present in significant concentration especially in low temperature regions of the flame.

$$NO + HO_2 \cdot \rightarrow NO_2 + OH \cdot \quad (41)$$

Reduction of NO_2 with O or H radicals is showed in reaction (42).

$$NO_2 + H \cdot (O \cdot) \rightarrow NO + OH \cdot (O_2) \quad (42)$$

All NO formed during combustion is converted to NO_2 after it is released to the atmosphere by reaction with air oxygen. If the flue gas sampling probe is not heated the conversion of NO to NO_2 can occur and influence the measurement. [6]

2.2.2 N_2O formation during combustion

N_2O is another oxide of nitrogen that has harmful effects – especially a strong greenhouse effect. It is not considered to be part of NO_X; however, it deserves some attention because it presents another form in which nitrogen can leave the combustion process. HCN is believed to be the precursor of N_2O formation according to reaction (10) followed by reaction (43).

$$NCO + NO \rightarrow N_2O + CO \quad (43)$$

N_2O can be also formed from ammonia by reactions (16) – (19) followed by reactions (44) and (45).

$$NH \cdot + NO \rightarrow N_2O + H \cdot \quad (44)$$

$$NH_2 \cdot + NO \rightarrow N_2O + H_2 \quad (45)$$

N_2O emissions are very high at FBC due to low combustion temperatures, except for biomass combustion where almost no N_2O is formed. [6] [9]

2.2.3 NO_X formation in a fluidized bed combustor

The fuel nitrogen is considered to be the main source of NO_X in FBC (about 90 %). The significance of thermal NO_X is very low and usually considered negligible because of the low temperature (750 – 950 °C). Most of the fuel nitrogen usually remains in char after devolatilization due to relatively low combustion temperatures as well.

Most of the NO_X and other pollutant formation takes place in the oxygen rich zone above the distributor plate. In BFBC the pollutant formation reactions occur just in the particulate

phase and not in bubbles. After the oxygen is consumed in the zone above the distributor the reduction zone follows in which devolatilization and homogeneous and heterogeneous reduction of NO take place. The mixing of gases from emulsion phase and bubbles in BFBC occurs in the splash zone and further homogeneous reduction follows in the freeboard. [11-13]

2.2.4 NO reduction in a fluidized bed combustor

FBC have very good conditions for NO reduction both homogeneous and heterogeneous. In BFBC the NO reduction reactions are taking place in the bed and in the freeboard. In CFBC there is no sharp boundary between the bed and freeboard.

It was observed that the reduction reactions in the freeboard of BFBC are mostly homogenous, caused by volatiles or CO. Heterogeneous reduction on surface of entrained solids in the freeboard is negligible. Inside the bed of FBC (both BFBC and CFBC) homogeneous and heterogeneous reduction reactions occur.

Some homogenous reduction reactions were described earlier in the chapter concerning NO_X formation mechanisms. Further reduction can occur outside of the formation process by CO, NH_3 or hydrocarbons as shown in reactions (46) - (48).

$$NO + CO \xrightarrow{char,ash,bed\ material} \frac{1}{2}N_2 + CO_2 \quad (46)$$

$$NO + \frac{2}{3}NH_3 \rightarrow \frac{5}{6}N_2 + H_2O \quad (47)$$

$$NO + CH \cdot \rightarrow HCN + O \cdot \quad (48)$$

Reaction (47) represents an example and NH_3 can be substituted by any species of NH_i group. HCN formed by reduction with hydrocarbons reacts further in a way described by reactions (10) – (15) and it can be converted again to NO. However, the final product for the part on the nitrogen will be N_2.

Heterogeneous reactions can occur on the surface of char, sorbent and bed material. Heterogeneous reduction on char surface is believed to involve chemisorption on free carbon active sites. First step in the process is formation of surface complex (-CNO) on a free carbon active site (49). The release of N_2 follows in two possible ways by reactions (50) or (51) followed by (52).

$$NO + (-C) \rightarrow (-CNO) \quad (49)$$

$$2(-CNO) \rightarrow 2(-CO) + N_2 \quad (50)$$

$$(-CNO) \rightarrow (-CN) + (-CO) \quad (51)$$

$$2(-CN) \rightarrow N_2 + 2(-C) \quad (52)$$

Another mechanism was proposed by de Soete, which involves chemisorption of NO on two free carbon active sites, reactions (53) and (52). The chemisorbed oxygen complexes can be regenerated by (54), (55).

$$NO + 2(-C) \rightarrow (-CN) + (-CO) \quad (53)$$

$$(-CO) \rightarrow CO \quad (54)$$

$$(-CO) + CO \rightarrow CO_2 + (-C) \quad (55)$$

The presence of excess oxygen in the combustion process increases the reduction reaction rate by creating more oxygen surface complexes. However, it also causes combustion of char leading to rapid decrease of reduction after a short time. It was not yet clarified if the char-nitrogen can be affected by this process or not.

The role of char in NO reduction is very important. In heterogeneous reduction it is the reducing element and in homogeneous reduction it has strong catalytic effect. Lignite and brown coal have usually high active surface of char. Calcined limestone is a catalyst for both NO production and reduction and its overall effect depends on other conditions. Sulphated sorbent has no effect on NO emissions.

Usually, increase of NO_X emissions was observed after limestone addition at CFBC because there is an oxygen rich atmosphere above the secondary air injection level and the unreacted limestone stays in the form of CaO that catalytically enhances formation of NO from HCN. In the BFBC the sorbent is kept in the reduction atmosphere in the bed and does not enter the oxygen rich atmosphere above the secondary air inlet. If the oxygen concentration is lower than 0,5 vol% the CaO catalysed oxidation reaction is strongly inhibited and the sulphur capture leads to CaS rather than $CaSO_4$. CaS catalyses the reduction of NO according to equation (46) that balances the increased NO formation by unreacted sorbent. For BFB no sorbent influence or (in case of low volatile fuel) even slight decrease in NO can be observed. CO (and also N_2O) promotes the reduction reactions especially at low temperatures. [7] [12] [13] [15-20]

2.3 The literature review – parameters influencing NO_X emissions

Pereira et al. [13] investigated the NO_X emissions from coal combusted in a fluidized bed of shale in a temperature range of 700 – 850 °C. Excess air was varied between 0,93 – 1,2 and a constant fluidizing air flow rate was kept providing a superficial air velocity of 0,92 m/s at 800 °C. The experiment was conducted also with argon as a fluidization gas followed by air injection in a freeboard to separately investigate the NO_X emissions from combustion of volatiles. The experiment showed an oxygen-rich zone near the distributor plate even for overall sub stoichiometric conditions. This zone is responsible for most of the NO_X emissions. NO_X concentration drop contributed to the reduction was observed in the freeboard. It was found that for the bed temperature below 750 °C most of the NO_X emissions have an origin in char-nitrogen. This is caused by a fact that under these temperatures the level of devolatilization is low and most of the nitrogen stays bound to the char. For higher temperatures the importance of volatile nitrogen increases and becomes a ruling factor near 950 °C. NO_X emissions were found to increase with the bed temperature until cca 800 °C and then stagnation (or slight decrease) was observed.

Hampartsoumian et al. [16] investigated the NO_X emissions from combustion of different fuels in a silica sand (0,5 – 1 mm) bed operated at fixed fluidization velocity of 1 m/s. The temperature was varied between 750 – 900 °C and the excess air between 0,2 – 1,2. Dependence of NO_X on combustion conditions was evaluated. Anthracite and bituminous coal showed an increase in NO_X with temperature (about 1,5 ppm/°C) while peat showed no temperature dependence at all. This is contributed to the fact that volatile nitrogen release is increasing with temperature. Almost complete devolatilization occurs in the case of peat even at lower temperatures. The nitrogen conversion to NO_X was found to increase with increasing

excess air and with decreasing reactivity of the fuel (volatile content). NO_X reduction in the freeboard was also investigated. The observed dependency was increasing reduction with decreasing excess air and with increasing volatile content. Reduction on the surface of entrained char particles in the freeboard was concluded to be not significant. NO emissions between 200 – 600 ppm and fuel nitrogen conversion of 5 – 45 % were observed depending on operation conditions

Lin et al. [18] presented a simple model to predict NO_X emissions that incorporated following parameters: coal and sorbent particle size, weight fraction of nitrogen/carbon, volatile nitrogen and char reactivity. The excess air ratio was varied between 0,7 – 1,7. The bed temperatures tested were from 750 to 1000 °C. Results showed an increase in NO_X emissions with increasing excess air, temperature and increasing nitrogen/carbon weight fraction. With increasing volatile nitrogen, char reactivity and coal particle size the NO_X were found to decrease. The influence of sorbent was found just for large coal particles and as the coal particle size decreased the significance of added sorbent fell. NO emissions were found in a wide range 150 – 1000 ppm depending on other parameters.

Åmand et al. [15] investigated the impact of different fuel properties as well as combustion parameters on NO emissions of a CFBC with superficial air velocity 3 – 6 m/s. Temperature range was 800 – 900 °C and excess air 1,1 – 1,4 (primary air stoichiometry 0,4 – 1,2). Brown coal, bituminous coal and petroleum coke were used. Bed temperature, excess air ratio, primary air stoichiometry, fluidization velocity, fuel fixed carbon content and sort of bed material and its size were identified as primary parameters that influence NO_X. It was observed that the ash of brown coal coats the bed material and has a strong NO reducing effect in contrast of other fuels. Fuel nitrogen conversion to NO_X increased with increasing temperature; however, the slope was different for every fuel. The reason is believed to be in the decrease of CO and char concentrations in the bed at higher temperatures which play an important role in NO_X reduction. Different slope suggests that each fuel has either different char activity for NO_X reduction or different dependence of bed char content on temperature, most likely both principles. Another factor can be that in CFBC the temperature has much lower uniformity and it may not be enough to choose just one measuring point. This fact can be very strong especially for lab scale models. The air stoichiometry measurements were influenced by temperature changes in the bed and will not be considered relevant. This mistake was corrected in their later work [21], which showed it is irrelevant whether the stoichiometry change is achieved by changing the air flow or fuel feed. NO_X were found to increase with both primary and overall air stoichiometry while the influence of overall stoichiometry is stronger. Effect of secondary air injection height was found but without a definite conclusion. Nitrogen conversion to NO was measured between 0,5 – 4,5 %.

Lin et al. [22] made a fixed bed experiment to evaluate the effect of limestone on NO_X emissions in a CFBC. In the experiment superficial gas velocities between 0,8 – 2,5 m/s were used and temperature was held at 850 °C. It was found that calcined limestone has a strong catalytic activity on NH_3 oxidation to NO while sulphated limestone has no effect. As a result, increasing the Ca/S ratio (limestone feed) during desulfurization in CFBC leading to increased sulphur capture also leads to increasing NO emissions because it increases the amount of unreacted CaO.

Lu et al. [23] investigated the influence of pressure combustion and air staging on NO_X emissions. Primary air ratio was changed between 0,9 – 1,2. They conducted the experiment in a pressurized bed at 1 MPa and concluded that increased pressure has potential to lower the NO_X emissions. Low-oxygen zone in the bed is created by combustion air staging which improves the NO reduction because it leads to increased char and CO content in the bed. The

dependence on primary air ratio was found stronger than on overall excess air. NO concentrations between 15 – 105 ppm were obtained.

Findlay et al. [24] performed several combustion tests in combustors of different sizes to evaluate the influence of combustion conditions and construction parameters on NO_X emissions. From construction parameters bed height and secondary air injection height were observed to have strong influence on NO_X. These parameters have influence on residence time and freeboard temperature. Decreasing bed height and increasing secondary air injection height lowered the NO_X. They also concluded disharmony in NO_X emissions observed at laboratory and industrial size boilers. Big industrial boilers suffer from worse fluidisation homogeneity and contain low oxygen zones where NO reduction is promoted. NO_X emissions of industrial size boilers were about 50% lower; however, the results from small scale combustors are valuable to establish trends. Limestone addition was observed to have effect on increasing NO_X and coarser limestone lead to more increase. Increasing excess air lead to increase of NO_X and lower values were achieved in case of combustion air staging.

Minimal NO_X was achieved for primary/secondary air ratio of 30/70 which not only created good reduction environment in the bed but also led to freeboard temperature increase which promotes reduction in the freeboard as well. The recommendation for fluidized bed boiler design is to make shallow bed and air staging with secondary air inlet positioned high above the bed.

Gulyurtlu et al. [25] investigated the effect of air staging and co-combustion of coal and straw on NO_X emissions in a CFBC boiler. Combustion temperature was between 750 – 900 °C, excess air was kept between 1,2 - 2 and the amount of biomass added was from 5 wt% to 20 wt%. It was concluded that positioning the secondary air inlet higher and increasing the straw amount decreased the NO_X emissions. The reason for the reduction is increased volatile release (mostly NH_3 and hydrocarbons). The best effect was achieved by feeding mixture of coal and straw inside the fluidized bed and not on the top. The effect of co-combustion on NO_X was found much higher than just dilution of flue gas. Adding 5 % of straw decreased the emission by 15 %. In optimal case emissions could be lowered from 400 ppm (coal combustion) to 250 ppm (co-combustion).

Hayhurst et al. [11] observed NO_X emissions from coal of different sizes in a BFBC at temperatures of 800 °C and 900 °C. Experimental results indicated conversion to NO about 30 % for volatile nitrogen and 10 % for char nitrogen. The fraction of NO_X originating from volatiles was between 30 – 80 % and the ruling parameter was coal type and volatile content (higher volatile contend lead to higher fraction of volatile NO). Temperature and coal size had little effect. Increasing temperature decreased the conversion of volatile nitrogen while also increased the fraction volatile/char nitrogen. The resulting effect of temperature was increasing NO_X with temperature. The increase in particle size decreases the amount of volatiles released and their conversion. The large coal particles were observed to stay on top of the bed until end of devolatilization. The residual char then sank in the bed and moved around. The small coal particles sank and devolatilized inside the bed. Also, the volatiles were combusted in the bed. Combustion of volatiles in the freeboard was observed to have positive effect on NO reduction in some cases. In other cases no particle size effect was observed.

Winter et al. [26] investigated the volatile and char nitrogen conversion to NO from bituminous and subbituminous coal and beech wood in a lab scale FBC. The bed temperature was varied between 600 – 900 °C and oxygen partial pressure between 0,05 – 21 kPa, superficial gas velocity was kept at 0,68 m/s. Authors concluded that formation of NO during combustion of both volatile and char are of nearly equal importance. Formation rate during volatile combustion is very rapid compared to char combustion while char combustion takes

much longer. They reported average values of 38 % conversion for volatile nitrogen and just 16 % for char nitrogen. Distribution of fuel nitrogen between volatiles and char was 28 % / 72 %. The increase of temperature from 600 to 900 °C led to increase of volatile and char nitrogen conversion to NO (from 6 to 49 % for volatiles and from 5 to 26 % for char). Increasing oxygen partial pressure from 0,05 – 10 kPa led to increase of volatile nitrogen conversion from 6 to 38 % and decrease of char nitrogen conversion from 31 to 16%. With further increase from 10 – 21 kPa the dependence reversed for both and conversion reached 33 % for volatile and 24 % for char nitrogen.

De Diego et al. [27] investigated the effect of various parameters on NO_X emission from CFBC. The NO_X emissions were found to rise with increasing temperature, the effect was more pronounced with higher excess air. The reason is decreased CO and char concentration in bed at high temperatures and oxygen concentrations which hinders NO reduction. Increase in the secondary air ratio led to decrease of NO_X due to the increased char and CO concentration in the bed as well as increased residence time. NO_X also increased with limestone addition and increasing Ca/S ratio. Slight increase in NO_X was also observed with increasing particle size. Particle size has effect on the heating rate and also location where particle devolatilizes. Fuel was fed to the bottom of the bed and mall particles devolatilized quickly while larger particles devolatilized during their rise to the top of the bed. Larger fuel particles also have less complete devolatilization and leave more char for NO reduction.

Skreiberg et al. [28] performed a fixed bed experiments to evaluate the NO_X emissions from different kinds of wood. The conversion of fuel nitrogen to NO was measured in the range of 11 – 86 %. The conversion increased slightly with decreasing particle size, which was concluded to be in agreement with other authors that observed also slight increase or no change. The most significant influence was found for excess air ratio. Increasing the excess air leads to increased conversion. The effect of temperature was changing with wood type, particle size and temperature interval used so no general conclusion can be made.

Köpsel et al. [29] compared normal and de-ashed coal samples of hard coal and lignite to evaluate the catalytic activity of ash on NO formation. Significantly higher emissions and fuel nitrogen conversion were observed for hard coal. Increasing the combustion temperature increases the nitrogen conversion for hard coal and decreases the conversion for lignite in the temperature range 500 – 900 °C. The effect of ash was dependent on temperature and coal type. De-ashed lignite shows similar temperature dependence as hard coal. For low temperatures the lignite ash seems to enhance NO formation, for temperatures higher than 650 °C the overall reduction of NO was observed. De-ashing has only little effect on hard coal. However, for temperatures higher than 800 °C slight decrease of NO was observed for de-ashed samples. The positive effect of coal ash on NO emissions was concluded in both cases above certain temperature (650 °C for lignite and 800 °C for hard coal).

Hosoda et al. [30] compared the NO_X emissions from a BFBC combusting coal in two different regimes. The compared modes were once through mode (OTM) and exit-gas recycle mode (ERM). Combustion temperature was kept on 1120 K and gas velocity 1 m/s. Results from oxy-fuel experiments confirmed there are no significant amounts of prompt or thermal NO formed in BFBC. In the ERM with the inlet oxygen concentration at 21% the resulting nitrogen conversion was 0,83 % which is about 9 times lower compared to 7,7 % for OTM. The composition of inlet mixture of oxygen, nitrogen/carbon dioxide and water was varied to determine the contribution of these parameters and the same results were obtained for OTM and EMR for the same inlet gas composition. The main contribution to the NO reduction is the in-bed heterogeneous and homogeneous reduction and the longer residence time in the bed. Substitution of nitrogen by carbon dioxide and increasing the water content (flue gas recycle

increased water content of flue gas from 1,5 to 5,5 %) increases the heat capacity leading to decreasing the combustion temperature. This effect was compensated by cooling water flow rate control. Char concentration in the bed during the experiment was 1 – 2 % and was not dependent on inlet gas concentration and mode. Increased carbon dioxide concentration leads to increased concentration of CO due to reaction with char. Water react with char as well to form H_2. Both mechanisms also promote NO reduction.

Winter et al. [9] measured the emissions of NO during combustion of different types of biomass in a FBC. Decreasing conversion to NO was found with increasing fuel nitrogen content. Maximum conversion was found for oxygen partial pressure 10 – 15 kPa and temperatures around 800 °C. The explanation is increased significance of NO reduction for higher oxygen content.

Pilawska et al. [31] observed the methane combustion in a BFBC of sand 0,250 – 0,350 mm. Combustion inhibiting effect of sand were confirmed. The dependence of NO_X on mass of sand in the bed was observed. NO_X increased with increasing sand mass (bed height) for all temperatures until 1250 K. For higher temperatures NO_X was independent on bed height. Linear increase of NO_X with increasing gas velocity was observed until $4U_{mf}$, stagnation followed.

Valentim et al. [32] investigated the influence of petrographic composition of coal on char morphology and NO_X emissions using lab-scale model (80 mm diameter, 500 mm height) with silica sand. Several types of high volatile bituminous coal were used. Char morphotype can be either highly porous – Group 1– or medium and low porous – Group 2 and 3. Petrographic composition has large influence on volatile nitrogen fraction and char structure. All maceral groups can be labelled as precursors of Group 1 or Group 2 and 3 chars. More porous chars of Group 1 were formed with increasing temperature for vitrinite rich coals. No dependence on temperature was found for inertinite rich coals. This fact leads to decreased emissions of NO with increasing temperature for vitrinite rich coals due to enhanced heterogeneous reduction. Increase or stagnation of NO can occur for inertinite rich coals with increasing temperature.

Krzywanski et al. [60] investigated a co-combustion of various types and shares of biomass with coal (lignite) on a CFB combustor with nominal output of 261 MW_e. The biomasses tested were both energy crops and wood biomass and co-combustion ratio was 7 – 15 %. The co-combustion experiments were compared with pure lignite combustion. Significant decrease in NO_X emissions were observed; however, the decrease was relatively lower when the biomass amount was increased over 10 %.

Zhou et al. [61] investigated the conversion on fuel-N, volatile-N and char-N to NO_X and N_2O in a fluidized bed single particle combustion test rig. Single coal particle combustion testing was selected to eliminate interactions between fuel and flue gas. Two fuels were investigated – anthracite and bituminous coal – and the effect of temperature change was studied. The results showed that 70 – 80 % NO_X are formed from the char-N for both fuels. The conversion rates were 80 % (char-N) and 36 % (volatile-N) for anthracite and 45 % (for both char-N and volatile-N) for bituminous coal at 1043 K. Increasing temperature had little effect on anthracite, while it increased the conversion rates of fuel-N, volatile-N and char-N to NO_X of the bituminous coal. Considering the N_2O, cca 45 % was produced by volatile-N in anthracite and 70 % in bituminous coal. The conversion to N_2O was measured to be 4 % (volatile-N) and 5 % (char-N) in anthracite, and 12 % (volatile-N) and 2 % (char-N) in bituminous coal at 1043 K. With increasing temperature, the N_2O was found to decrease.

Xu et al. [62] investigated the formation of N_2O during air and oxy-fuel combustion of bituminous coal. A 50 kW_{th} testing unit was used and concentration profiles along the

combustor height were measured. The influence of air staging was investigated. It was found that the N_2O concentration increase along the combustor height for both air and oxyfuel combustion. The N_2O emissions were much higher in the oxy-fuel setting compared to the air combustion. With introduction of secondary air to the oxyfuel combustion the N_2O concentrations in the dense zone of CFBC further increased; however, it had little effect on the exit flue gas emissions.

Li et al. [63] investigated the NO_X formation in BFB combustion of biomass. The influence of bed temperature, excess air, staged combustion and flue gas recirculation was observed. Ten different types of biomass were used, and a sub-bituminous coal was used as a reference case. The experiments were conducted in three experimental units - in a rectangular unit with thermal load 150 kW_{th}, in a circular unit with thermal load 150 kW_{th} and a rectangular unit with thermal load 12,8 kW_{th}. Authors observed minimal effect of the thermal load, combustor size and boiler design on the NO_X emissions. During the air staging an inert gas or recirculation were used to compensate the primary flow rate to a constant value. The bed temperature was controlled by heat transfer tubes and by spraying water on the bed. The results showed NO_X emissions of most of the biomasses were under 200 ppm at 700 °C. Except for leather waste with cca 250 ppm of NOX at 700 °C with further increase to 450 ppm at 800 °C. Most of the biomass types showed very little temperature influence on NO_X of 12 – 18 ppm/100 °C except for rice husk and soybean which showed 54 – 63 ppm/100 °C, the greatest temperature influence on NO_X was observed for the previously mentioned leather waste. The excess oxygen influence on NO_X emissions was observed higher than the temperature influence, for most biomasses being 8 – 29 ppm/10%O_2 with exception of leather waste with significantly stronger influence of 69 ppm/10%O_2. The effect of air staging on NO_X emissions was found to be inconsistent as contradictory trends were observed for different biomasses when air staging was introduced. The effect of air staging was quite contradictory as well - several types of biomass showed increased NO_X when flue gas recirculation was introduced. The overall dependency of NO_X on recirculation was rather weak. The authors also observed the dependency of fuel nitrogen conversion to NO_X on total fuel nitrogen content. The results showed exponential dependency for the ten biomasses tested. A linear dependency of fuel nitrogen conversion on CH/N ratio was suggested.

Li et al. [64] investigated the conversion factors of volatile-N and char-N in a silica sand 150 kW_{th} fluidized bed combustor. Coke and toluene were used to represent char and volatile matter. Volatile nitrogen compounds - nitrobenzene, pyridine and pyrrole - were added to the fuel during the experiments to represent volatile nitrogen species. Results showed significantly lower temperature dependence on NO_X conversion for char-N in comparison to volatile-N. The conversion to NO_X was observed much higher for volatile-N than char-N (13 – 15,5 % compared to 4 – 7,5 %). All volatile nitrogen compounds that were used showed similar behavior regarding the NO_X concentration profile trends. However, the functionality played an important role in the NO_X emissions and conversion rates. Pyridine and pyrrole addition resulted in lowed NO_X emissions and conversion than the nitrobenzene case.

2.3.1 The literature review - Summary

Some general conclusions can be made from the above-mentioned literature review. Results of some authors can be confusing and contradictive, and a lot of articles had to be discarded because of fundamental experimental flaws. Some authors were not able to keep constant all parameters except the one that was investigated and observed cumulative influence of more parameters as a result. Some did not convert the NO concentrations to

standard excess air. Results were compared in three possible ways: concentrations of NO, NO_X or fuel nitrogen conversion.

Practically all NO_X emissions of FBC boilers are originating from fuel. Emissions of NO_X are strongly dependent on boiler design and combustion parameters. Coal has usually higher NO_X emissions than biomass but the conversion of fuel nitrogen to NO_X is lower. For all fuels the higher the nitrogen content the lower the conversion to NO_X. The NO_X originating from volatile and char nitrogen are of relatively equal importance and neither can be neglected. In case of biomass combustion lower NO reduction effects can be expected compared to coal.

For combusting coal in the BFBC the NO_X emissions were usually in the range of 150 – 1000 ppm, typical values of NO_X can be considered around 200 – 400 ppm (fuel nitrogen conversion over 5 %) but after optimisation the conversion can fall under 150 ppm (conversion below 1 %). Typical emissions of NO_X from biomass combusting BFBC are around 100 – 200 ppm (with fuel nitrogen conversion over 10 %) and after optimisation can reach 50 ppm (conversion less than 5 %). Co-combustion of coal and biomass has a potential to decrease the NO_X more than just the dilution effect; however, not all experiments showed this conclusion. The fuel feeding system may have a strong influence.

From all fuel parameters the volatile content or the fuel factor has the strongest influence on NO_X emissions. The conversion of volatile nitrogen to NO_X is several times larger than conversion of char nitrogen for high volatile fuels such as biomass, lignite and brown coal. Biomass has generally much higher volatile content.

Increasing the temperature usually leads to NO_X increase because high temperature decreases the concentration of CO and char it the bed providing less reduction. Increasing temperature also leads to increased volatile release and change of the conversion of volatile and char nitrogen to NO_X. The effect is usually slightly increased NO_X with increasing temperature. However, this will level of at some point when the complete devolatilization occurs. Some coals can show decrease or no influence of temperature, the reason is the vitrinite that is forming more porous char under higher temperature and providing more active surface for homogeneous reduction. Brown coal can also show slight decrease of NO_X with increasing temperature thanks to NO reducing effect of ash that is enhanced at high temperatures.

Increasing the excess air in sub stoichiometric conditions (oxygen concentration) can lead to decrease of NO_X emissions because of increased amount of NO reducing free radicals. However, in most cases the oxygen concentration increase leads to more complete combustion and decreases the CO and char concentration in the bed. Less reduction of NO and higher emissions of NO_X can be observed. The change of excess air can also lead to change of fluidization velocity providing longer residence time in the bed for lower excess air. Longer residence time increases the reduction effects in the bed and freeboard.

Air staging creates low-oxygen concentration zone in the bed and freeboard before the secondary air inlet. Lower primary air ratio brings lower oxygen concentration in the bed and increased residence time. Increasing the secondary air inlet height also increases residence time resulting in lower NO_X emissions. Although contradictory results might be found in the literature for some non-standard types of biomass.

The fuel particle size has influence on its temperature profile and heating rate resulting in lower volatiles release for larger particles. Larger particles also create more char as a result. All this leads to decreasing NO_X with increasing particle size. Particle size can also influence the place where particles devolatilize and burn and the devolatilization time. This effect combined with the fuel feeding system (on top of the bed, inside the bed) can have very

significant effect as well as bed material and fluidization conditions. In general, the effect of particle size is not clear and must be judged with respect to all mentioned facts.

The bed material can also influence NO_X emissions by enhancing NO formation or reduction. In such case the bed height and particle size will have effect. Sand was observed to increase the NO_X emissions. On the other hand, changing the bed height in all cases influences the residence time in the bed and freeboard which affects the reduction of NO_X making this effect difficult to judge.

Increasing the sorbent (CaO) feed and Ca/S ratio leads to increased NO_X emissions for CFBC. Unreacted sorbent CaO catalyse NO formation under the oxygen rich conditions in the freeboard. The BFBC are either not influenced by sorbent or even small NO_X decrease can be observed in some cases. Unreacted sorbent stays in the low oxygen concentration bed and does not enhance NO formation. Some sorbent is sulphated to CaS that catalyses the NO heterogeneous reduction.

2.4 Options to decrease the NO_X emissions

There are two principal ways how to reduce the emissions of NO_X emitted by combustors. Primary measures are mostly design and combustion conditions adjustments aimed to either decrease NO_X formation or increase their reduction without treating the flue gas. Secondary measures present post-combustion flue gas treatment methods. Primary measures are sufficient at many Czech power plants to meet the emission limits.

2.4.1 Primary NO_X reduction options

Most of the primary measures´ purpose is to lower the combustion temperature and temperature gradient in the combustor or to reduce the residence time of flue gas in high temperature zone, thus lowering the thermal NO (used in PCC). Other measures increase the reduction of NO_X by presenting low oxygen concentration zones. The emission of NO_X can be decreased by up to 80 % by combination of primary measures. [14]

Decreasing the overall excess air

Decreasing the excess air brings less oxygen concentration and promotes the NO reduction. This measure is also closely connected to the combustion efficiency and CO emissions and overall excess air cannot be lowered any more than it already is in most of the cases. Excess air decrease also brings increase in combustion temperature but it´s effect in negligible. [14]

Air staging

Air staging creates low oxygen concentration zone before the secondary air inlet, where the reduction of NO takes place. Positioning the secondary air inlet higher provides higher reduction zone, longer residence time and further decreases the NO_X emissions. Lower gas velocity also increases the residence time in the reduction zone. [14] [25] [30]

Reburning, co-combustion and fuel staging

Staging of the fuel leads to the decrease of combustion temperature and temperature gradient. Co-combusting the mixture of coal and biomass can in some cases decrease the NO_X emissions much more than can be attributed to the dilution. Reburning of natural gas causes NO reduction by equation (48). [11] [14] [25]

Flue gas recirculation

Recirculation of flue gas increases the heat capacity by increasing the concentration of CO_2 on the account of N_2 and also increases the water content. This leads to decreased combustion temperature which in most cases decreases NO emissions. CO_2 and H_2O react with char to produce CO and H_2 which increase the NO reduction. The residence time in the reduction zone is increased as well, which has especially significant effect in case of FBC. The flue gas recirculation also decreases the oxygen concentration in the gas entering the combustion chamber. [30]

2.4.2 Secondary DENO$_X$ options

Secondary DENO$_X$ mechanisms represent the pollution control by flue gas treatment after combustion. These are not of main interest of this work; however, short summary will be presented. Most widely used methods are selective non-catalytic reduction (SNCR) and selective catalytic reduction (SCR). Other methods are not standard and are in the phase of research and development. [14]

SNCR

SNCR is a very simple mechanism that uses ammonia (or urea) injection in the flue gas at a temperature between 1100 – 1400 K. NO is reduced to N_2 in presence of oxygen (excess air is necessary). The mechanism is virtually identical to the reduction mechanism described in NH_3 combustion. Oxygen is needed to convert NH_3 to NH_2 which is the first step as presented in reactions (16) and (18) followed by reactions (24), (25) and (26) which represents direct and indirect reduction to N_2. NO_X reduction of 30 % to 70 % can be achieved. [6] [14]

SCR

SCR is a very effective method that can achieve 80 – 90 % NO_X reduction with use of lower amount of ammonia than SNCR. Temperature range of 520 – 680 K is mostly used. The only difference to SNCR is that the ammonia is chemisorbed on catalyst before reacting with NO. As catalyst mostly noble metals, metal oxides and zeolites are used. [14]

Non- selective catalytic reduction

Non- selective catalytic reduction can achieve up to 95 % of NO_X reduction by using three-way catalyst. Specific conditions near to stoichiometric are needed for optimal performance decreasing its usefulness for power engineering and making it more suitable for combustion engines and transport industry. [14]

Pulsed corona discharge

Treating flue gases by pulsed corona induced plasma can decrease the emissions of NO_X by 60 %. High energy consumption and formation of undesirable by-products makes this method not practical so far. [14]

Electron beam flue gas treatment

Flue gas irradiation by fast electrons creates O and OH radicals which react with NO_X and SO_2 to form acids. NH_3 is also introduced into flue gas to form ammonium nitrate and sulphate. The reduction of emissions can achieve 80 % for NO_X and 70 % for SO_2. [14]

Cyanuric acid method

This method uses cyanuric acid that is injected in the flue gas and decomposes either in gas phase or on particle surface according to reaction (56).

$$(HOCN)_3 \rightarrow 3HNCO \quad (56)$$

Further decomposition of HNCO follows to form NCO, NH_i and CO_i mainly by reactions (57) and (58).

$$HNCO(+H\cdot) \rightarrow NH\cdot(NH_2\cdot) + CO \quad (57)$$

$$HNCO + OH\cdot(NH_i) \rightarrow H_2O(NH_{i+1}) + NCO \quad (58)$$

NH_i reduces NO as was described earlier by reactions (16), (18) and (24) – (26) ; however, main source of NO reduction is equation (59)

$$NCO + NO \rightarrow CO + N_2O \quad (59)$$

Ideal temperature interval for NO removal is 1000 – 1200 K and as can be seen NO reduction is mostly balanced by increasing by N_2O emissions. [6]

2.5 Oxy-fuel FBC

Oxy-fuel combustion is in the centre of attention of many research teams all over the world. It has a big potential as a CCS technology but presents a lot of advantages for combustion process as well. One of its positive effects is the reduction of NO_X emissions. Combustion with pure oxygen eliminates the air originating nitrogen from the combustion process. The flue gas consists mostly of CO_2 and water. Recycling the flue gas is necessary to lower the combustion temperature. The recirculation rate is kept usually between 60 – 80 %. The advantages of oxy-fuel combustion for lowering NO_X emissions are:

1) Higher heat capacity of CO_2 compared to N_2 leads to overall higher heat capacity of flue gas. As a result, the combustion temperature is lowered leading to reduction of NO_X emissions in most of the cases.
2) High rate of flue gas recycle is increasing the residence time in the reduction zone leading to more homogeneous and heterogeneous reduction and reburning.
3) Low N_2 concentration in flue gas eliminates thermal and prompt NO formation. The low N_2 concentration will even cause the thermal Zeldovich mechanism to reverse and convert NO to N_2. Low oxygen concentration can increase the reduction by this mechanism.
4) High concentration of CO_2 leads to an increase in NO formation from volatiles at sub-stoichiometric conditions and to decrease at stoichiometric and fuel lean conditions.
5) High concentration of CO_2 leads to increased CO production through dissociation of CO_2 (reaction (60)), carbon gasification (reaction (61) and (62)) and reaction with H radicals reaction (63).

$$CO_2 \rightarrow CO + \frac{1}{2}O_2 \quad (60)$$

$$C\cdot + CO_2 \rightarrow 2CO \quad (61)$$

$$C\cdot + H_2O \rightarrow CO + H_2 \quad (62)$$

$$H \cdot + CO_2 \rightarrow CO + OH \cdot \quad (63)$$

Increased CO concentration leads to more intense homogeneous reduction.

Oxy-fuel combustion has also other advantages. Elevating the concentration of O_2 can reduce the volume of flue gas and decrease the size of the boiler. The temperature increase is compensated by flue gas recycling. Combining oxy-fuel technology with FBC can bring some advantages over standard pulverized coal boilers.

1) Better temperature control – FBC provides a good convection heat transfer inside the bed as well as high heat capacity to absorb the deviations and create almost constant temperature in the bed. According to Alstom the oxy-fuel FBC can reduce the boiler area by 50 % and cost by 32 % compared to air fired.
2) Fuel flexibility.
3) Low quality fuel combustion is possible.
4) Low NO_X emissions.
5) In-situ desulphurization.

[30] [33] [34]

2.6 NO_X prediction models

Emissions of NO_X are influenced by coal properties, combustion conditions and combustor design. Accurate prediction methods could provide useful information for boiler design and fuel selection. Authors of NO prediction models for FBC usually combine kinetic modelling approach with FBC hydrodynamic models. However, all existing models suffer from inaccuracy, over – complexity or both. Much simpler approach can be found at PCC, where using empirical models leads to very simple correlations and can achieve good agreement with experiments. However, these correlations are used exclusively for PCC, no reference is available for modification of these models for FBC conditions. [35]

Approaches other than kinetic or empirical models can be also found in the literature. Such attempts are rare and are not the focus of this work; however, they are noteworthy. The attempts usually utilize neural networks and self-organizing maps, see e. g. [65].

2.6.1 Kinetic models

Kinetic models of nitrogen chemistry are of two types. First type is very simple and uses just a few overall reactions with experimentally measured overall rate constants – this can be considered a hybrid kinetic-empirical model since it uses both kinetic reaction and empirical constants.

The second type of kinetic model is using detailed chemistry consisting of large number of equations to cover the homogenous and heterogeneous nitrogen oxidation as well as reduction. In this case the reaction kinetic rate constants from literature are used. The simplified method was mostly used before detailed nitrogen chemistry was known. Recently, most of the authors include detailed chemistry into their models which improves accuracy but increases demands on computing capacity. Inclusion of freeboard reactions, that is necessary for relevant predictions of stack emissions, increases complexity even more.

Kinetic models cannot work on a stand-alone basis but must be combined with detailed hydrodynamics model of the fluidized bed. Authors usually consider two phase model of the bubbling fluidized bed with bubble phase and emulsion phase as was suggested by Toomey and Johnstone [4]. The assumption is that all the gas excessing the flow rate given by u_{mf} is passing through the bed in form of bubbles. The assumption is that emulsion phase stays at

minimum fluidization conditions. Bubbles are considered completely void, although it is known that they contain a small amount of solids. The bed flow pattern is strongly dependent on the type of bubbles. Slowly ascending bubbles are not surrounded by any drift and the fluidization air can pass through them upwards. On the other hand, fast bubbles are surrounded by circulating cloud of gas which causes downward flow of solids in the vicinity. Moreover, part of the emulsion phase, that is located in the wake of the bubbles, is ascending with bubbles with a different velocity than the rest of the emulsion phase. These facts are considered in the K-L model which presents an alternative to the simple two-phase model and incorporates not just bubble and emulsion phase (divided to the cloud phase and the rest) but also the wake phase.

Modelling the type of flow in emulsion phase has also several approaches and levels of complexity:

1) 1 D premixed laminar reactor
2) Perfectly stirred reactor
3) Homogeneous plug-flow reactor

The freeboard flow model is necessary to include also freeboard reactions. The solid hold-up of the freeboard is decreasing with height and the voidage is increasing. Downfall of solids can be observed near the wall similar to the lean phase of CFBC.

Circulating fluidized bed model is usually horizontally divided into two parts. The upper part has a typical two-phase flow with upwards flowing core and downwards flowing annulus near the wall. The lower part of circulating fluidized bed has the behaviour of a bubbling or turbulent bed so usually the bubbling bed model is appropriate.

The prediction of nitrogen oxides concentration is based on conservation equations for each phase, which are complemented by interphase transfer coefficients. Different fluidization regimes and conditions can bring change in aplicability of the selected model, which could reduce the prediction accuracy. For maximizing the accuracy it should be also considered that different control volumes can have different hydrodynamic conditions. [3] [6] [36]

2.6.1.1 Review of kinetic models

Horio et al. [37] made a mathematical FBC model for coal combustion which considered simplified NO_X formation and reduction kinetics in the bed. Reduction reactions occurring in the freeboard were not considered which makes this model not suitable for stack emission prediction. The model considered the size distribution and elutriation of the coal. The concentrations of NO in emulsion and bubble phase were derived from mass balance. Constants needed to solve these equations must be obtained experimentally or via correlations from literature.

Rajan et al. [38] developed a similar model with more complex reaction kinetics and FBC hydrodynamics. The model also included freeboard reactions. Nitrogen release during devolatilization and char combustion as well as FBC hydrodynamics was based on empirical correlations. Concentration of NO in each phase (freeboard, bubble and emulsion phase) is given by mass balances. Formation, reduction and interphase exchange are considered.

Beér et al. [39] developed a mechanistic model which divided the bed into two parts. Part 1 near the distributor is supposed to have plug flow behaviour with unimportant bubble phase corresponding to slow bubble regime. Part 2 (the upper region) corresponds to a fast bubble regime of the two-phase fluidized bed. Reaction kinetics is covering not only all homogenous and heterogeneous reactions including reduction but also devolatilization, char combustion and temperature inhomogeneity around the char particles (temperature

overshoot). Volatile nitrogen is supposed to be in form of NH_3. Mass balance equations for bubble phase, emulsion phase and distributor region were derived. Freeboard reactions are not considered.

Lin et al. [40] used a simplified kinetics model with perfectly stirred hydrodynamics of slow bubble regime FBC to predict the NO_X emissions and SOX retention as well as NO_X/SOX interaction. The model incorporates heterogeneous NO reduction on the char surface but neglects homogeneous reduction in the freeboard. Concentration of NO is derived from nitrogen mass balance. The model is in relatively good agreement with experimental results. No influence of sorbent addition on NO emissions can be observed for a BFBC; however, increased NO emissions are observed for CFBC.

Goel et al. [41] created a detailed kinetic model of CFBC using complex fluidized hydrodynamics and nitrogen chemistry. The bed is divided into three parts. The bottom zone has the hydrodynamics of a bubbling bed and is followed by transient and dilute zone with standard core – annulus flow. Chemistry is covered by 348 reversible reactions which include both homogeneous and heterogeneous formation and reduction of NO_X. Model predictions are in a fairly good agreement with experimental results.

Skreiberg et al. [28] made a kinetic FBC model for combustion of wood particles considering two hydrodynamics regimes: plug flow regime and perfectly stirred regime. The kinetics of homogeneous and heterogeneous phase was with 371 reversible reactions. Batch combustion tests were performed in an electrically heated bed with reasonable agreement.

Jensen et al. [42] included the influence of elevated pressure, bed material and sorbent catalytic activity on nitrogen chemistry in their model and identified the combustion and hydrodynamics parameters with largest influence. The bed hydrodynamics is accounting for a two-phase bed (dense and bubble phase) and a freeboard. Air staging, load, mass of bed material, temperature, fuel and bed particle diameter were identified to influence NO emissions. Load and mass of bed material determine the bed specific thermal load. The diameter of bed and fuel particles can change the Geldart classification of particles and influence the division of air between bubble and dense phase leading to overall change in the bed hydrodynamics. Fuel diameter also influences the devolatilization and content of char in the bed.

Löffler et al. [43] presented a kinetic model for combustion of single particle of bituminous coal. The model consisted of 426 reversible homogeneous and heterogeneous reactions including water release from fuel, devolatilization, combustion of volatiles and char and subsequent reduction reactions. The bed was divided into several parts thus respecting temperature inhomogeneity with standard two-phase flow kinetics of bed and freeboard. Experimental results showed good agreement with model predictions.

Gungor [36] made a prediction model for CFBC of low quality coal. The bed hydrodynamics is divided into two parts. The bottom zone is described by a two phase BFBC model; however, it is not certain if the bottom zone of the CFBC is behaving as a bubbling bed or rather the turbulent bed. The upper zone has a core-annulus structure and both zones are divided into control volumes in radial and axial directions. Change of particle size due to attrition, fragmentation and fuel particle combustion is taken into account. Nitrogen kinetics is using just 12 overall reactions and reaction rates devolatilization, combustion of volatiles and char as well as homogeneous and heterogeneous reduction of NO. Fluidized bed heat transfer and dispersion are also included in the model. The predictions were tested on data from three small scale pilot units and show relatively good agreement.

Wei et al. [66] attempted to simplify a previously developed kinetic model containing 504 reactions. The developed skeletal mechanism containing 242 reactions was derived by

eliminating unimportant reaction steps through sensitivity analysis, partial equilibrium analysis and integral reaction flow analysis. As the last step the global mechanism was proposed containing 10 independent reactions describing the production rates of relevant species based on stoichiometry of the skeletal mechanism. The prediction was integrated into the CFD code and the model was validated by experiments with very good agreement for exiting gas concentrations.

Krzywanski et al. [60] developed a kinetic model for CFB co-combustion of biomass with coal. The basic model containing 44 reactions was adjusted for the conditions of co-combustion by modifying reaction rates of 9 selected reactions. The kinetic model is accompanied by hydrodynamic model of the fluidized bed dividing the combustion chamber in 84 elements, considering the dense zone and the dilute zone. The dense zone model considers 3 phases – emulsion, bubbles and clouds. The dense zone model is following Kuni and Levenspiel [3]. During the model validation the difference between NO_X predictions and measured values were ± 20 %.

Selcuk et al. [67] developed a kinetic CFB model for lignite combustion in 0,3 MW_{th} experimental unit. The hydrodynamic part of the model is divided into 2 parts - dense and dilute zone. The dense zone is represented by a two-phase model with emulsion phase, bubble phase and plug flow regime. Dilute zone is represented by a plug flow model based on Kuni and Levenspiel [3]. The kinetic model considers particle temperature and size distribution during devolatilization and char combustion. NO formation includes volatile/char nitrogen distribution and reaction paths. Heterogeneous reactions are considered only in the emulsion phase. The model was validated on a test CFB combustor unit, only the exit concentration of NO could be validated. The prediction accuracy for exit gas NO concentration was very good.

Kilpinen et al. [68] developed a kinetic CFB model containing over 300 reaction steps. The hydrodynamic part consists of 3 regions – dense bubbling bed (represented by a bubbling bed model), splash zone and transport zone, the two later regions are horizontally split into core (upward flow of both gas and solids) and annular zone (gas flows upward, solids flow downward). The kinetic part of the model contains homogeneous and heterogeneous reactions as well as catalytic reactions on solid particle surfaces covering the process of devolatilization, volatile combustion and fixed carbon combustion. Detailed nitrogen chemistry following the paths of volatile and char nitrogen are present. The model was validated by experiment with very bad agreement for NO concentrations. The model is being developed.

Winter et al. [69] developed a kinetic CFBC model of petroleum coke combustion based on laboratory and pilot scale experimental measurements for NO and N_2O prediction. The model is based on single particle combustion. The fluidized bed is modeled as a plug flow reactor, divided into 10 sections with constant parameters. The model is using various sub-models from literature for both the hydrodynamic and kinetic part. The prediction accuracy was satisfactory for both NO and N_2O.

Afacan et al. [70] modified a previously developed model to incorporate combustion of lignites with a high volatile content. The model was validated on a 0,3 MW_{th} experimental unit. The authors identify the most important parameters - the partitioning of volatile nitrogen and char nitrogen, char combustion rate and volatile nitrogen release along the combustor. The model accounts for bed and freeboard hydrodynamics (well mixed and plug-flow two phase model), volatiles release and combustion, char particles combustion and char distribution, heat transfer, elutriation, entrainment, char attrition, sulfur retention and NO_X formation and reduction. The model predictions of NO emissions were in reasonable agreement with the measured data.

2.6.2 Empirical models

The main advantage of empirical models is their simplicity. The data required are usually easy to obtain - proximate and ultimate analysis of the fuel or combustion parameters - and thus the models are convenient to use in industrial praxis. Unlike the kinetic models there is no need for extensive equation system solving and computing capacity. The prediction is based on experimental data and the emission dependency on influencing parameters. The parameters that were identified to have the largest influence, and are used in empirical models, can be divided into three groups:

- Fuel related (nitrogen content, volatile matter content...)
- Boiler design related (staged/un-staged combustion, fuel – air mixing extent...)
- Boiler operation related (excess air, combustion temperature...)

Influence of individual parameters can be observed experimentally by holding the other parameters constant. However, this approach presumes independent effects of parameters which is not necessarily valid for all fuels and combustion conditions.

The main downfall of empirical models is the uncertainty originating from lack of input data e.g. ash composition can promote NO reduction under certain conditions, petrographic composition can significantly influence the devolatilization and char formation process. Another aspect is the extent of mixing of fuel and combustion air. To minimize the uncertainty, correct parameters must be used in the model to cover all important aspects and on the other side not to increase the complexity.

Influencing parameters not included in the input data are considered via constants, their applicability is determining the model limitations. Input parameter and constants selection should be carefully considered. Nevertheless, deviations up to 50 ppm can be measured in the flue gas stream due to inhomogeneity so the prediction reliability of 50 ppm can be considered acceptable. Following chapters are describing empirical models found in literature. [35] [44]

2.6.2.1 Simplified chemistry method

Simplified nitrogen chemistry in Figure 13 could bring some success in achieving generally usable correlation for fuel NO_X prediction; however, this approach is quite outdated and was not pursued in recent years. (Some symbols were changed to conform to the unified style of this work.) The overall fuel nitrogen conversion can be expressed by equation (64) where Greek letters represent partial conversion rates. Partial conversion rates can be investigated and determined separately by experiment or taken from literature.

$$\frac{NO}{NO_{MAX}}[-] = \kappa[\beta_1 \cdot (1-\varphi_1) + (\beta_2 + \beta_1 \cdot \varphi_1) \cdot (1-\varphi_2) + \varphi_3 \cdot (\beta_3 + \beta_1 \cdot \varphi_1 \cdot \varphi_2 \cdot \beta_2 \cdot \varphi_2)] + [(1-\kappa) \cdot \gamma \cdot \mu_2] \quad (64)$$

Tar conversion HCN conversion NH_3 conversion

Char conversion

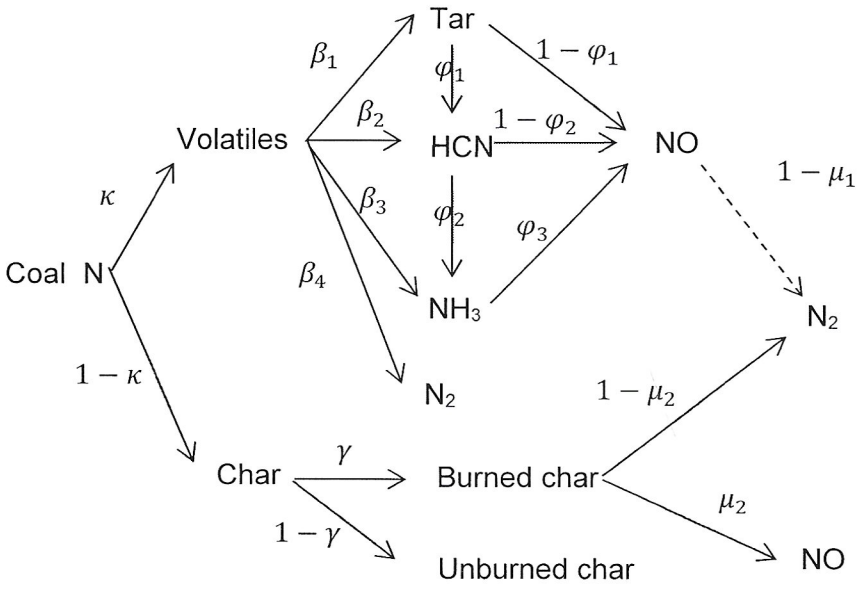

Figure 13: Nitrogen release from fuel [35]

Assuming all volatile nitrogen-containing compounds have the same conversion rate, equation **Chyba! Nenalezen zdroj odkazů.** 64) can be simplified to equation **Chyba! Nenalezen zdroj odkazů.** 65). Applicable correlation can be achieved by expressing the partial conversion rates as functions of various parameters. Fenimore correlated the expression with concentration of H_2O and H_2 in equation (66) and later modified to equation (**Chyba! Nenalezen zdroj odkazů.**67). These correlations do not include any consideration for heterogeneous reduction reactions (dashed lines in Figure 13) which reduces its applicability for FBC.

$$\frac{NO}{NO_{MAX}}[-] = \kappa \cdot \mu_1 + (1-\kappa) \cdot \mu_2 \qquad (65)$$

$$\frac{NO}{NO_{MAX}} = 0{,}56 \cdot \frac{H_2O}{H_2} \cdot EXP\left(\frac{-83{,}763\ kJ}{RT}\right) \qquad (66)$$

$$\frac{NO}{NO_{MAX}} = 700 \cdot H_2O \cdot EXP\left(\frac{-209{,}34\ kJ}{RT}\right) \qquad (67)$$

[35] [44] [45]

2.6.2.2 Pohl´s method

Simple empirical correlations have been developed by Pohl et al. [35] to estimate NO emissions for controlled mixing conditions (different types of PCC flames). Nitrogen content of the fuel is the most important parameter in the correlations followed by volatile content. High temperature volatile content ranging from 1 to 3-fold of a standard volatile content is sometimes used, because PCC furnace temperatures are higher than temperatures used at the thermo-gravimetric analysis. The influence of volatile matter content and fixed carbon content is changing with implementation of air staging. Other parameters are not incorporated in these models directly but through four constants for each firing method. The firing method is determining mixing conditions (flame type) which defines correlation to be used. The prediction

accuracy for PCC boilers was tested by many authors and found to be strongly dependent on flame type.

In case of premixed flame, the agreement with measurements had the determination coefficient $R^2 = 0,9$ for 20 coals and $R^2 = 0,75$ for another 46 coals. Inaccuracy was lower than 50 ppm for all coals except few cases when volatile content was difficult to measure. Relatively accurate predictions were found for radial diffusion flames. The accuracy was tested on 20 coals with $R^2 = 0,9$ and maximum inaccuracy of 70 ppm. In case of axial diffusion flames the agreement was quite low $R^2 = 0,55$. Pohl´s method is widely used and considered sufficiently proven for PCC, modification of Pohl´s method was even incorporated into commercial software for NO_X prediction.

The correlation for NO concentration *NO* [ppm] is given by equation (68), where N^{daf} [%] is nitrogen content of the combustible, *VM* [%] is volatile matter content (daf), *FC* [%] is fixed carbon and NO_{eq} [ppm] is the equivalent flue gas concentration of NO for complete fuel nitrogen conversion, 0 % O_2 and dry basis, see equation (69). Where A^r [-] and W^r [-] represent the ash and water content of the fuel and V_{fd} [m_n^3/kg] is the volume of dry flue gas.

$$NO[ppm] = k_1 + k_2 \cdot \frac{N^{daf}}{1,5} + k_3 \cdot \frac{VM}{40} \cdot \frac{NO_{eq}}{3200} + k_4 \cdot \frac{FC}{60} \cdot \frac{NO_{eq}}{3200} \qquad (68)$$

$$NO_{eq} = \frac{2,1422 \cdot N_{daf} \cdot (1 - A^r - W^r)}{V_{fd}} \cdot 10^6 \qquad (69)$$

Constants k_1 to k_4 that are suitable for different flame types and their values are given in Table 1. The prediction for diffusion flame is recommended for NO prediction at wall fired PCC without staged combustion. Emission of NO is usually lower compared to premixed flame because of lower volatile nitrogen conversion to NO. Axial diffusion flames have relatively long ignition delay (depending on coal type) leading to considerable mixing of fuel and oxygen before ignition which causes lower accuracy that was mentioned earlier.

Table 1: Constants for Pohl´s prediction model

	Premixed flame	Diffusion flame	Staged combustion
k_1	285	340	150
k_2	1280	835	80
k_3	180	20	-30
k_4	-840	-395	100

Staged combustion prediction is suitable for NO prediction for wall fired PCC with staged combustion and represents the minimal value that can be achieved. Staged combustion can reduce NO emissions of PCC by up to 70 %. In this expression the volatile content and fixed carbon influence changed signs. The reason might be the fact that volatile combustibles are causing increased NO reduction under sub stoichiometric conditions.

Pohl´s correlations for all mixing conditions have four terms. The first term represents the fixed emission that is not dependent on fuel nitrogen. This value is higher for un-staged flames, lower for staged flames and can be understood as a measure of fuel – air mixing extent. The second term represents the contribution of fuel nitrogen. The third one is the contribution of volatile matter and the fourth term accounts for fixed carbon content. For un-staged flames

the volatile matter contribution adds to the total NO emissions and the fixed carbon substrates. The explanation can lie in different conversion of volatile nitrogen and char nitrogen into NO. Studies point out that the volatile nitrogen conversion is much higher than conversion of fuel nitrogen.

Pohl´s model cannot be directly applied to FBC since the NO_X formation mechanisms have different weight in FBC conditions. However, a modified version of Pohl´s method could reach similar level of reliability. No mention about such modification was found in literature so far. [9] [35] [46] [47]

2.6.2.3 The method of CRC

The method described by Cooperative Research Centre for Black Coal Utilisation (shortened as CRC) used correlation from equation (70) to fit their plant data for PCC of different coals.

$$NOX[ppm] = a \cdot VM \cdot N^{daf} + b \cdot EXP(\frac{c}{VM}) \qquad (70)$$

The most important parameters are nitrogen content N^{daf} [%] and volatile matter content VM [%], similar to Pohl´s model. Notice that both N_{daf} and VM are expressed in [%] instead of [-]. Constants a, b and c are expected to be unique for each boiler and vary with boiler design. The reliability of prediction was relatively high for coals included in the fitting. For coals not included in the fitting the prediction accuracy was found reasonable with a few exceptions. Very low accuracy was achieved in case of coal blends. It seems that for most of the coal blends the resulting NO_X emissions are not equal to the sum of NO_X emissions of particular coals. Applicability of CRC method to FBC is similar to Pohl´s method. [47]

2.6.2.4 Makino´s method

The correlation proposed by Makino for PCC is predicting the fuel nitrogen conversion based on fuel ratio FR [-] and nitrogen content on the dry basis N^d [-], see equation (71). (Some symbols were changed to conform to unified style of this work.)

$$\frac{NO}{NO_{eq}}[-] = a \cdot \frac{FR}{N^d} + b \qquad (71)$$

Parameters a and b must be fitted based on experimental results measured for a given boiler. The NO [ppm] can be calculated by multiplying the fuel conversion with NO_{eq} from equation **Chyba! Nenalezen zdroj odkazů.** 69). Validation of this method was not found in literature and the applicability to FBC boilers is similar to Pohl´s method. [47]

2.6.2.5 Ibler´s method no.1

Ibler et al. [48] proposed the correlation in equation (72) for prediction of fuel nitrogen conversion to NO in PCC. Where K [-] is fuel related constant (Ibler recommended using values of constant K between 4 and 6 for Czech coals), $O2$ [%vol] is flue gas oxygen concentration and T [K] is combustion temperature. The NO [ppm] can be calculated by multiplying the fuel nitrogen conversion with NO_{eq} from equation **Chyba! Nenalezen zdroj odkazů.** 69).

$$\frac{NO}{NO_{MAX}}[-] = 7 \cdot 10^{-5} \cdot K \cdot O_2 \cdot \sqrt[3]{T - 1025} \qquad (72)$$

The constant $7 \cdot 10^{-5}$ in the equation (72) represents the PCC conditions and a presumably different constant would be needed for FBC conditions. As can be seen from equation (72), Ibler's model is concentrated more on combustion conditions than fuel properties, which are characterized by a constant *K* only.

2.6.2.6 *Ibler´s method no.2*

Another method proposed by Ibler et al. [49] for prediction of *NOX* [g/MJ] for PCC has a separated formula for NO_X formed by thermal and fuel mechanism. The thermal *NOX* [g/MJ] is given by equation (73) and is applicable for temperatures above 1800 K.

$$NOX[g/MJ] = A \cdot \frac{\sqrt{\frac{\lambda_{comb} - 1}{\lambda_{comb}}}}{\sqrt{T_{comb}}} \cdot EXP\left(\frac{-6700}{T_{comb}}\right) \qquad (73)$$

Where λ_{comb} (symbol changed to conform to unified style of this work) and T_{comb} represent excess air and temperature in the combustion zone. Coefficient *A* [$g.MJ^{-1}.K^{0,5}$] is dependent on temperature, oxygen concentration and residence time in the combustion zone.

The fuel nitrogen is given by equation (74), where coefficients k_1 to k_5 represent the influence of excess air in primary mixture, excess air in burner zone, flue-gas recirculation, flue-gas temperature above the combustion zone, and mixing of fuel with primary and secondary air.

$$NOX[g/MJ] = 0{,}7 \cdot N^{daf} \cdot k_1 \cdot k_2 \cdot k_3 \cdot k_4 \cdot k_5 \qquad (74)$$

The values of coefficients k_1 to k_5 differ with burner type and other parameter values, see in more detail in [49]. Applicability to FBC boilers is very limited. Note that the units are [g/MJ] in this case.

2.6.2.7 *The method alleged in [50]*

The method alleged in [50] uses equation (75) to predict the NO_X formation rate.

$$M_{NOX}[g/s] = 0{,}34 \cdot 10^{-7} \cdot M_F \cdot \left(1 - \frac{\xi_c}{100}\right) \cdot Q_i^r \cdot K_{NO2} \cdot \varepsilon_1 \cdot \varepsilon_2 \cdot \varepsilon_3 \cdot (1 - k_1 \cdot r) \cdot k_2 \qquad (75)$$

Where M_F [kg/s] is fuel mass flow, ξ_c [%] is loss by unburned carbon, Q_i^r [MJ/kg] is lower heating value, K_{NO2} [-] is a parameter depending on boiler power output, boiler load and combustion temperature. Following equations are valid for low combustion temperatures (under 1500 °C) for boiler steam output under 70 t/h (equation (76)) and over 70 t/h (equation (77), where $M_{steam,nom}$ [t/h] is nominal steam output.

$$K_{NO2}[g/MJ] = \frac{M_{steam,nom}}{20} \qquad (76)$$

$$K_{NO2}[g/MJ] = \frac{12 \cdot M_{steam,nom}}{200 + M_{steam,nom}} \quad (77)$$

Other coefficients from equation(75) represent the influence of:

ε_1 – fuel, see equation (78) for solid fuels

ε_2 – burners (e.g. $\varepsilon_2 = 1$ for swirl burners, $\varepsilon_2 = 0{,}85$ for stream burners)

ε_3 – combustion chamber temperature ($\varepsilon_3 = 1{,}3$ for smelting boilers, $\varepsilon_2 = 1$ for standard non-smelting boilers)

k_1 – recirculation flue gas input ($k_1 = 0{,}001$ for in primary mixture, $k_1 = 0{,}05$ for input in secondary mixture)

k_2 – air input outside the main burners ($k_2 = 1 - 0{,}025 \cdot \alpha$ for solid fuels)

$$\varepsilon_1 = 0{,}178 + 0{,}47 \cdot N^{daf} \quad (78)$$

Validation of this method was not found in literature and the applicability to FBC is similar to Pohl´s method.

2.6.2.8 *Method of Čarnogurská 1*

Čarnogurská et al. [71] proposed following correlation based on dimensional analysis that is applicable to all types of boilers combusting all types of fuels:

$$NO_X[kg/m^3] = C \cdot \left(\frac{P_k}{Q_{vz}}\right)^m \cdot \left(\frac{p_p}{Q_u}\right)^n$$

Where P_k [kg/s] is a capacity (steam production) of the boiler, Q_{vz} [m^3/s] is the flow rate of combustion air, p_p [Pa] is a combustion pressure and Q_u [J/kg] is the calorific value of the fuel. The constants *C*, *m* and *n* need to be experimentally determined for each boiler and fuel type.

The correlation was validated for one household boiler Verner V140 combusting biomass and for one heating plant boiler combusting black coal.

2.6.2.9 *Method of Čarnogurská 2*

Čarnogurská et al. [72] proposed following correlation for small scale combustors based on dimensional analysis:

$$NO_X[kg/m^3] = C \cdot \left(\frac{P_k}{Q_{vz} \cdot Q_u}\right)^m \cdot \left(\frac{T_{sk}}{T_{vz}}\right)^n$$

Where P_k [W = kg·m^2/s^3] is a performance of the boiler, Q_{vz} [m^3/s] is the flow rate of combustion air, Q_u [J/kg = m^2·s^2] is the calorific value of the fuel, T_{sk} [K] is the flue gas temperature at the end of the boiler and T_{vz} [K] is the combustion temperature. The constants *C*, *m* and *n* need to be experimentally determined for each boiler and fuel type – for a low power output boilers combusting biomass the following constants were proposed: $C = 63236 \cdot 10^{-8}$, $m = 1$ and $n = 3{,}4190$. The model was developed on boiler Verner V210 and verified on Verner V140 with reasonable accuracy.

2.6.3 Empirical model corrections

Parameter studies have been made by Pohl et al. [28] [47] that can be used to evaluate the influence of parameters that are not included in correlations. These studies can be used to implement some of the parameters and increase the prediction accuracy – designated by Pohl XAC and HRS. Fuel nitrogen conversion to NO was observed to linearly increase with increasing primary stoichiometry and primary air velocity. Although the slope is changeable in

each case, due to change of the mixing extent (swirl number for PCC) and residence time, the excess air correction was approximated by equation (79), where *O2* [%] is the flue gas concentration of oxygen.

$$XAC = 0{,}6 + 0{,}135 \cdot O_2 \qquad (79)$$

The change in a power output – heat release per burner zone area *HRBZA* [MW/m^3] – has influence on residence time in high temperature region. Exponential dependency of fuel nitrogen conversion on *HRBZA* was observed and can be expressed by equation (80).

$$HRC = 0{,}34 \cdot EXP(0{,}003 \cdot HRBZA) + 0{,}076 \cdot EXP(0{,}008 \cdot HRBZA) \qquad (80)$$

Flame temperature is affecting the devolatilization process as well as combustion of char in the bed. Higher temperature leads to more complete devolatilization and lesser char content in the bed. The overall effect is strongly depending on fuel type; however, a slight increase of *NO* with increasing temperature is observed in most cases. For some fuels and temperature ranges a maximum is found followed by slight decrease or stagnation. The temperature dependence is included in the heat release correction, so no temperature correction was proposed.

The final *NOX* [ppm], after correction for heat release and excess air, are given by multiplying the prediction by correction coefficients as shown in equation (81).

$$total\ NOX = NO \cdot XAC \cdot HRC \qquad (81)$$

Another correction was developed by CRC [48]. It is claimed by authors that the results are better if the corrections are added to the prediction instead of multiplying as was done by Pohl. The CRC correlation correcting the influence of excess air and heat release are shown in equation (82).

$$correction\ NOX = a \cdot \log(O2) + d \cdot HRBZA \qquad (82)$$

The correction for oxygen concentration as a logarithmic dependency is supposed to bring slightly better results than Pohl´s linear correction. *HRBZA* [MW/m^3] used for heat release correction is defined as thermal load divided by flame volume. [47]

3 Definition of goals

1) Detailed analysis of NO_X formation models for fluidized bed combustors including the dimensional analysis.
2) Contributing to designing and building a newly structured experimental FBC apparatus, that can be operated under wide range of combustion conditions, with the emphasis on conditions insufficiently covered in relevant literature. Obtaining and interpreting an extensive set of experimental data for NO_X emission dependency on combustion conditions for FBC.
3) Selection of the suitable prediction model of NOX for the fluidized bed combustors and its development based on experimental results.

3.1 Applicability

Providing supplies of energy – mostly electricity and heat – to its citizens and industry is one of the most important priorities of every country. Energy supplies should be realized as economically, effectively and ecologically as possible. The reliability is also an important issue. Czech Republic depends in this aspect mostly on fossil fuels and nuclear power as can be seen on Figure 14. Shown values represent average electricity power output in power grid in 2017 (these values do not include the electricity produced and consumed outside the grid). In 2017 the nuclear reactors were undergoing planned reactor shut-downs, hence the production of nuclear energy in Figure 14 was lower than normal. The lowered production of nuclear power plants was compensated by increased electricity production in thermal power plants.

Realistically, the thermal power plants would produce slightly under 50 % of electrical power and nuclear power plants slightly under 40 %.

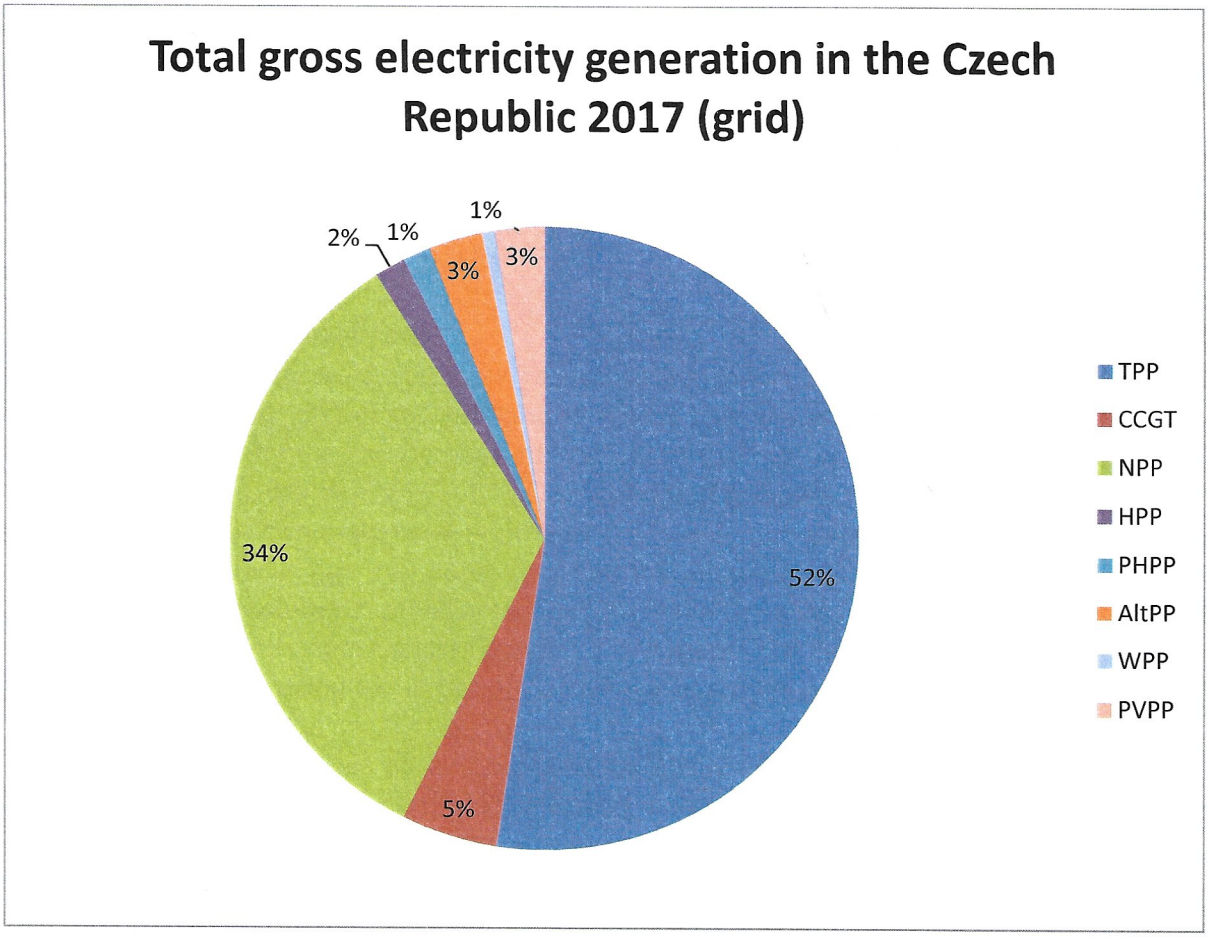

Figure 14: Electricity generation in the Czech Republic 2017 (grid); TPP- thermal power plant, CCGT- combined cycle gas turbine, NPP- nuclear power plant, HPP- hydro power plant, PHPP- pumping hydro power plant, AltPP- alternative power plant, WPP- wind power plant, PVPP- photovoltaic power plant [51]

The dependence on domestic coal could present a problem in near future due to depletion of reserves. It is expected that the coal production of Czech mines will dramatically decrease in next 20 - 25 years. The most significant decrease will come in case of brown/lignite coal. The question is how to supplement these missing resources to generate enough electricity and heat. One of the options that is already being exploited (and is getting more significant) is combustion of low heating value coals, waste, biomass and also co-combustion of coal and biomass. Another problem is the transition between different types of fuel which will magnify as the mines will decrease production. Even replacing one type of brown coal with another can prove to be very difficult and sometimes even impossible. A solution of the energy problem in the near future cannot be expected from renewable sources due to their instability and high costs. Nuclear energy on the other hand has issues with radioactive waste disposal and power output regulation. Moreover, the public opinion is shifting against nuclear power in many countries since the Fukushima accident. With these problems in mind, fluidized bed boilers could present an interesting option for power engineering of Czech Republic thanks to many advantages including ability to combust low quality fuels and relatively high fuel insensitivity.

This work aims to investigate the formation mechanisms of one of the most important pollutants – NO_X – in the fluidized bed boilers to provide useful information for boiler design, fuel selection and combustion parameter selection of the fluidized bed boilers and combustors. [52]

4 New contributions

The methods and tools that were used to reach the goals of this work were following:

1) Dimensional analysis was used to identify the influential combustion and fuel parameters for NO_X formation.
2) An attempt was made to modify existing PCC empirical NO_X prediction models for FBC conditions.
3) Experimental measurements in the research unit Mini-fluid were conducted to investigate the influence of selected parameters on the NO_X emissions (described separately in chapters 5 and 6).

4.1 Dimensional analysis

Dimensional analysis is closely related to the theory of similarity of processes. The theory of similarity of processes recognizes that if two physical processes are similar the observations made for the first process can be concluded for the second process as well.

To evaluate the similarity of two processes the dimensionless criteria (also called similarity criteria or dimensionless numbers) are used. The determination of the important dimensionless criteria can be done through the dimensional analysis. For any similar processes all the important dimensionless criteria have the same value. This also means that the functionalities and dependencies observed in a model can be made relatable to the large-scale applications by using the important dimensionless criteria instead of physical quantities. [54]

The empirical models so far proposed have very limited theoretical background since the dependence on chosen parameters is based mostly on experience. Theoretical approach to selection of parameters is very rare. An attempt utilizing dimensional analysis was used in [71] and [72]. The results were quite promising; however, the proposed correlation is very simple and not suitable for achieving goals of this work (first reference requires experimental determination of several constants for each boiler and fuel type, second reference is intended for small scale boilers combusting biomass).

Although some of the models give reasonably reliable results it is only within certain boundaries. Applying the models on data outside the original data set is usually accompanied with decrease of reliability. Another issue is the applicability of empirical models on different combustion conditions – e.g. PCC and FBC. The theoretical approach to model´s parameter selection could improve general applicability of the models and make them less reliant on primary fitting data. Also, better prediction accuracy can be expected if the models are based on simplified theoretical dependencies.

The findings presented in this chapter and subsequent sub-chapters were published in [I.].

4.1.1 Buckingham´s π-theorem

Dimensional analysis based on Buckingham´s π-theorem can be a very useful tool for investigating phenomena that are either not fully understood or their analytical solution is too complex and does not bring satisfactory results. When dealing with such complex problems we must rely mainly on experiment and empirical correlations. Dimensional analysis can help us not only to investigate which quantities governing the investigated phenomenon are functionally connected but also to better organize and prepare the experiment as well as process the experiment results. Dimensional analysis is quite complex and flexible process. It is possible to reach multiple results that are all correct. However, some results are more clear

and helpful than others. Suitable characterization of the process was done by Matsen [53] who claimed dimensional analysis to be "the mix of physics, mathematics, witchcraft, history and common sense that we call engineering".

The result of dimensional analysis will give us the list of dimensionless complexes, simplexes and parameters connected by a general functionality to investigated phenomenon. Specific form of dependency must be obtained by experiment. Only parameters which are observed to have significant influence should be included in the prediction model. [54]

4.1.2 Dimensional analysis in general

The first step and the largest weakness of every dimensional analysis is the identification of relevant physical quantities. If a relevant physical quantity is omitted the solution will regard this quantity as not relevant to the phenomenon and the results will be flawed. If a non-relevant quantity is added to the relevant quantity list, the effect is difficult to predict. In some cases, this quantity is sorted out and the result of dimensional analysis is applicable, in other cases the quantity is not sorted out and the result is flawed. As we can see the relevant physical quantities must be chosen carefully.

Another important aspect of a dimensional analysis is the choice of fundamental units. This step might seem elementary and in fact it cannot affect the actual correctness of the result – given the choice of physical quantities is correct, the result will be correct despite the choice of units. However, certain choices of units can bring more clear and understandable results than others. In many cases only three fundamental units are chosen: meter *m*, second *s* and kilogram *kg*. In some special cases other units are added as it was observed the dimensional analysis brings better results. E.g. in thermo-mechanics two other units are added: Kelvin *K* and Joule *J*. It is worth pointing out that these units could be expressed as the combination of *m*, *s* and *kg*. *J* is expressed in equation (83).

$$[J] = [kg \cdot m^2/s^2] \qquad (83)$$

Kelvin can be defined in terms of kinetic theory of gases by equation (84). If we would regard Kelvin as a unit derived from the three fundamental units and consider Boltzmann constant to be dimensionless, Kelvin would be equivalent to (85). On this example we can see that most physical units are to certain extent arbitrary.

$$\frac{1}{2} \cdot m \cdot v^2 = \frac{3}{2} \cdot k \cdot T \qquad (84)$$

$$[K] = [kg \cdot m^2/s^2] \qquad (85)$$

After the relevant quantities and their fundamental units are listed, the main part of the dimensional analysis can proceed. Let the investigated phenomenon be influenced by m dimensionally different physical quantities labeled a (a_1 to a_m) which have l fundamental dimensions labeled b (b_1 to b_l). The functionality of m dimensional quantities in equation (86) is replaced by functionality of $m - l$ dimensionless complexes labeled π (π_1 to π_{m-l}) in equation (87). The $m - l$ dimensionless complexes π are linearly independent and are formed from dimensional quantities a and exponents x in equation (88).

$$f(a_1, a_2, \dots, a_m) = 0 \qquad (86)$$

$$f(\pi_1, \pi_2, \dots, \pi_{m-l}) = 0 \qquad (87)$$

$$\begin{aligned} \pi_1 &= a_1^{x_{11}} \cdot a_2^{x_{12}} \dots \cdot a_m^{x_{1m}} \\ &\vdots \\ \pi_{m-l} &= a_1^{x_{m-l\,1}} \cdot a_2^{x_{m-l\,2}} \dots \cdot a_m^{x_{m-l\,m}} \end{aligned} \qquad (88)$$

The dimensionless complexes can be obtained as follows. We arrange the physical quantities into the dimension matrix **A** = ($l \times m$) formed from exponents of fundamental units α_{11} to $\alpha_{m\,l}$ according to equation (89), where columns represent physical quantities and rows represent respective powers of fundamental dimensions.

$$\boldsymbol{A} = \begin{matrix} \\ b_1 \\ \vdots \\ b_l \end{matrix} \begin{matrix} \begin{matrix} a_1 & \cdots & a_m \end{matrix} \\ \begin{bmatrix} \alpha_{11} & \cdots & \alpha_{1\,m} \\ \vdots & \ddots & \vdots \\ \alpha_{l\,1} & \cdots & \alpha_{l\,m} \end{bmatrix} \end{matrix} \qquad (89)$$

Now we must solve the matrix equation **A·x = 0** (see equation (90)), while rank(**A**) < m. This means the number of unknown quantities is higher than the number of equations and the equation system is not complete. To solve this equation system, m dimensionally independent quantities must be chosen as the basic and the remaining k quantities as redundant. The dimension matrix is divided according to equation (91) into a square sub-matrix of basic quantities $\mathbf{A_B}$ and a sub-matrix of redundant quantities $\mathbf{A_R}$. We make sure that det $\mathbf{A_R} \neq 0$

$$\begin{bmatrix} \alpha_{11} & \cdots & \alpha_{1\,m} \\ \vdots & \ddots & \vdots \\ \alpha_{l1} & \cdots & \alpha_{l\,m} \end{bmatrix} \cdot \begin{bmatrix} x_1 \\ \vdots \\ x_m \end{bmatrix} = 0 \qquad (90)$$

$$\boldsymbol{A} = \begin{matrix} \begin{matrix} \mathbf{A_B} & & & \mathbf{A_R} & & \end{matrix} \\ \left[\begin{matrix} \alpha_{11} & \cdots & \alpha_{1l} \\ \vdots & \ddots & \vdots \\ \alpha_{l\,1} & \cdots & \alpha_{l\,l} \end{matrix}\middle|\begin{matrix} \alpha_{1\,l+1} & \cdots & \alpha_{1\,m} \\ \vdots & \ddots & \vdots \\ \alpha_{l\,l+1} & \cdots & \alpha_{l\,m} \end{matrix}\right] \end{matrix} \qquad (91)$$

Now the modified equation system $\mathbf{A_B \cdot x_1 = -A_R \cdot x_2}$ according to equation (92) is solved. Values of redundant physical quantities exponents $(\mathbf{x_{l+1}, \dots, x_m})$ must be chosen. For the matter of simplicity, it is viable to set one redundant exponent equal to unity and the rest equal to zero. The vector $(\mathbf{x_1, \dots, x_l})$ is obtained as a solution of equation (91) as a combination of exponents for π_1. This procedure must be repeated m-l times to obtain the solution matrix **B**, see equation (93).

$$\begin{bmatrix} \alpha_{11} & \cdots & \alpha_{1\,l} \\ \vdots & \ddots & \vdots \\ \alpha_{l\,1} & \cdots & \alpha_{l\,l} \end{bmatrix} \cdot \begin{bmatrix} x_1 \\ \vdots \\ x_l \end{bmatrix} = (-1) \begin{bmatrix} \alpha_{1\,l+1} & \cdots & \alpha_{1\,m} \\ \vdots & \ddots & \vdots \\ \alpha_{l\,l+1} & \cdots & \alpha_{l\,m} \end{bmatrix} \cdot \begin{bmatrix} x_{l+1} \\ \vdots \\ x_m \end{bmatrix} \qquad (92)$$

$$\boldsymbol{B} = \begin{matrix} \\ \pi_1 \\ \vdots \\ \pi_{m-l} \end{matrix} \begin{matrix} \begin{matrix} a_1 & \cdots & a_m \end{matrix} \\ \begin{bmatrix} x_{11} & \cdots & x_{1\,m} \\ \vdots & \ddots & \vdots \\ x_{m-l\,1} & \cdots & x_{m-l\,m} \end{bmatrix} \end{matrix} \qquad (93)$$

The above described procedure can be applied for dimensional quantities with different dimensions only. If the phenomenon is influenced by some dimensionless quantities, these quantities are added to the dimensionless complexes directly. If the phenomenon is influenced by some quantities with the same dimension, only one quantity is included in the dimensional analysis. Other quantities form dimensionless simplexes in relation to the chosen quantity and are added to the dimensionless complexes (e.g. *length/diameter* in Darcy-Weissbach equation). As a result, a list of dimensionless complexes, simplexes and dimensionless parameters is obtained. [54]

4.1.3 Application of dimensional analysis on NO_X emissions prediction

As previous investigation suggests the formation of NO_X is a very complex phenomenon with a lot of influencing parameters. To decrease the complexity, the phenomenon as a whole can be divided into several sub-phenomena that can be investigated separately. After reaching the functionalities and dimensionless complexes for all sub-phenomena the resulting functionality can be obtained as their combination. The investigated sub-phenomena are:

- Nitrogen chemistry and kinetics related processes
- Mass transfer and fluidized bed hydrodynamics processes
- Heat transfer processes
- Dimensionless combustion-related parameters

4.1.3.1 Nitrogen chemistry kinetics related processes

Emissions of NO_X are strongly influenced by nitrogen chemistry, as can be seen in chapter 2.2. Reaction kinetics is studying the velocity which drives the system to equilibrium state. The dimensional analysis was not done by the author of this work, as it was already done by other authors for various reaction types (homogeneous, heterogeneous, catalyzed, competitive or consequential) of first, second and higher orders. The results are surprisingly consistent. No matter the reaction order, complexity and type the dimensionless complexes were in all cases determined to be:

$$c \cdot t \text{ and } \frac{E_a}{R \cdot T}$$

Where c [%/s] is reactant concentration change in time, t [s] is the residence time, E_a [J/kg] is activation energy, R [J/kg·K] is universal gas constant and T [K] is thermodynamic temperature. The dependence on $\frac{E_a}{R \cdot T}$ is presumed to follow Arrhenius law $xp\left(-\frac{E_a}{R \cdot T}\right)$. [54]

4.1.3.2 Mass transfer and fluidized bed hydrodynamics related processes

Fluidized bed hydrodynamics is determining the mixing and fluidized bed mass transfer which is closely related to NO_X formation. To carry on with the dimensional analysis three fundamental dimensions (*m*, *kg*, *s*) are sufficient without additional modifications. Following quantities were selected for the analysis based on information from chapters 2.2.1 and 2.3: superficial velocity u [m/s], minimal fluidization velocity u_{mf} [m/s], dynamic viscosity μ [kg/m·s], gas density ρ_g [kg/m^3], solid density ρ_s [kg/m^3], gravitational acceleration g [m/s^2], sphericity ϕ [-] and geometry represented by particle diameter d [m], bed diameter D [m] and bed height H [m]. After the dimensionless parameter ϕ is separated and simplexes u/u_{mf}, ρ_f/ρ_s, d/D and d/H are formed the remaining quantities are arranged into the dimension matrix **A**, see equation (94).

$$\boldsymbol{A} = \begin{matrix} \\ m \\ kg \\ s \end{matrix} \begin{matrix} \begin{matrix} u & \mu & d & g & \rho_s \end{matrix} \\ \begin{bmatrix} 1 & -1 & 1 & 1 & -3 \\ 0 & 1 & 0 & 0 & 1 \\ -1 & -1 & 0 & -2 & 0 \end{bmatrix} \end{matrix} \qquad (94)$$

Where u, μ and d are chosen as basic quantities and g and ρ_s are redundant. The resulting matrix equations are (95) and (96).

$$\begin{bmatrix} 1 & -1 & 1 \\ 0 & 1 & 0 \\ -1 & -1 & 0 \end{bmatrix} \cdot \begin{bmatrix} x_{11} \\ x_{12} \\ x_{13} \end{bmatrix} = (-1) \begin{bmatrix} 1 & -3 \\ 0 & 1 \\ -2 & 0 \end{bmatrix} \cdot \begin{bmatrix} 1 \\ 0 \end{bmatrix} \qquad (95)$$

$$\begin{bmatrix} 1 & -1 & 1 \\ 0 & 1 & 0 \\ -1 & -1 & 0 \end{bmatrix} \cdot \begin{bmatrix} x_{21} \\ x_{22} \\ x_{23} \end{bmatrix} = (-1) \begin{bmatrix} 1 & -3 \\ 0 & 1 \\ -2 & 0 \end{bmatrix} \cdot \begin{bmatrix} 0 \\ 1 \end{bmatrix} \qquad (96)$$

The solution matrix **B** is shown in equation (97) and the complete list of complexes and simplexes in (98), where Froude number $Fr_p = \frac{u^2}{g \cdot d} = \frac{1}{\pi_1}$ and Reynolds number of particles $Re_p = \frac{u \cdot d \cdot \rho_s}{\mu} = \pi_2$ are related to the particle dimension. As a matter of fact, if another dimension was chosen, results would be analogical, and the dimensionless numbers would be related to different dimension. This result is in accordance with results of other authors, e.g. [55].

$$\boldsymbol{B} = \begin{matrix} \\ \pi_1 \\ \pi_2 \end{matrix} \begin{matrix} \begin{matrix} u & \mu & d & g & \rho_s \end{matrix} \\ \begin{bmatrix} -2 & 0 & 1 & 1 & 0 \\ 1 & -1 & 1 & 0 & 1 \end{bmatrix} \end{matrix} \qquad (97)$$

$$NOX = f\left(Fr_p, Re_p, \Phi, \frac{u}{u_{mf}}, \frac{\rho_f}{\rho_s}, \frac{d}{D}, \frac{d}{H}\right) \qquad (98)$$

4.1.3.3 Heat transfer related processes

Heat transfer is strongly influencing NO_X formation. Fuel particle heating rate and residence time are deciding factor for the devolatilization extent. For the dimensional analysis five fundamental dimensions are needed (*m, kg, s, K, J*) and following quantities were selected: combustor power output P_{th} [W_{th}], combustor maximum power output $P_{MAX,\,th}$ [Wth], fuel particle residence time t [s], fuel particle diameter d [m], specific heat capacity of the fuel c_p [J/kg·K], thermal conductivity of the fuel λ [W/m·K], density of the fuel ρ_f [kg/m^3], convective heat transfer coefficient α [W/m^2·K], bed diameter *D [m]* and bed height *H [m]*. After the simplex $P_{th}/P_{MAX,\,th}$ is formed the dimension matrix can be formed in equation (99).

$$\boldsymbol{A} = \begin{matrix} \\ m \\ kg \\ s \\ K \\ J \end{matrix} \begin{matrix} \begin{matrix} P_{MAX} & t & d & \rho_f & c_p & \lambda & \alpha \end{matrix} \\ \begin{bmatrix} 0 & 0 & 1 & -3 & 0 & -1 & -2 \\ 0 & 0 & 0 & 1 & -1 & 0 & 0 \\ -1 & 1 & 0 & 0 & 0 & -1 & -1 \\ 0 & 0 & 0 & 0 & -1 & -1 & -1 \\ 1 & 0 & 0 & 0 & 1 & 1 & 1 \end{bmatrix} \end{matrix} \qquad (99)$$

Where $P_{MAX,\,th}$, t, d, ρ_f and α are chosen as basic quantities, c_p and λ are redundant. The resulting matrix equations are (100) and (101).

$$\begin{bmatrix} 0 & 0 & 1 & -3 & -2 \\ 0 & 0 & 0 & 1 & 0 \\ -1 & 1 & 0 & 0 & -1 \\ 0 & 0 & 0 & 0 & -1 \\ 1 & 0 & 0 & 0 & 1 \end{bmatrix} \cdot \begin{bmatrix} x_{11} \\ x_{12} \\ x_{13} \\ x_{14} \\ x_{15} \end{bmatrix} = (-1) \begin{bmatrix} 0 & -1 \\ -1 & 0 \\ 0 & -1 \\ -1 & -1 \\ 1 & 1 \end{bmatrix} \cdot \begin{bmatrix} 1 \\ 0 \end{bmatrix} \qquad (100)$$

$$\begin{bmatrix} 0 & 0 & 1 & -3 & -2 \\ 0 & 0 & 0 & 1 & 0 \\ -1 & 1 & 0 & 0 & -1 \\ 0 & 0 & 0 & 0 & -1 \\ 1 & 0 & 0 & 0 & 1 \end{bmatrix} \cdot \begin{bmatrix} x_{21} \\ x_{22} \\ x_{23} \\ x_{24} \\ x_{25} \end{bmatrix} = (-1) \begin{bmatrix} 0 & -1 \\ -1 & 0 \\ 0 & -1 \\ -1 & -1 \\ 1 & 1 \end{bmatrix} \cdot \begin{bmatrix} 0 \\ 1 \end{bmatrix} \qquad (101)$$

The solution matrix **B** is shown in equation (102). The complete list of complexes and simplexes is shown in equation (103), $\pi_1 = \frac{c_p \cdot \rho_f \cdot d}{t \cdot \alpha}$ and $Nu = \frac{1}{\pi_2} = \frac{d \cdot \alpha}{\lambda}$ are related to d. Analogically to the previous case the dimensionless complexes could be also related to other dimension if the analysis is conducted differently.

$$\boldsymbol{B} = \begin{matrix} \\ \pi_1 \\ \pi_2 \end{matrix} \begin{matrix} \begin{matrix} P_{MAX} & t & d & \rho_f & c_p & \lambda & \alpha \end{matrix} \\ \begin{bmatrix} 0 & -1 & 1 & 1 & 1 & 0 & -1 \\ 0 & 0 & -1 & 0 & 0 & 1 & -1 \end{bmatrix} \end{matrix} \qquad (102)$$

$$NOX = f\left(\frac{c_p \cdot \rho_f \cdot d}{t \cdot \alpha}, Nu, \frac{P_{th}}{P_{MAX,th}}, \frac{d_f}{D}, \frac{d}{H}\right) \qquad (103)$$

4.1.3.4 Dimensionless combustion-related parameters

The formation of NO_X is also influenced by some combustion parameters that are dimensionless and can be directly added to the previously formed complexes. These parameters were selected based on chapters 2.2.1 and 2.3: primary oxygen concentration $O2$ [%], total oxygen concentration $O2_{total}$, fuel nitrogen content N^{daf} [-] and volatile matter content V^{daf} [-].

4.1.4 Summary

It can be concluded that dimensional analysis gives logical and satisfactory results with physical meaning. Based on the dimensional analysis in previous chapters, dimensionless complexes, simplexes and parameters governing the NO_X formation from different viewpoints were derived. The overall general functionality is in equation (104).

$$NOX = f\left(\begin{matrix} \frac{E_a}{R \cdot T}, Fr_p, Re_p, \frac{c_p \cdot \rho_f \cdot d}{t \cdot \alpha}, Nu, c \cdot t, \Phi, \frac{u}{u_{mf}}, \frac{\rho_f}{\rho_s} \\ , \frac{d}{D}, \frac{d}{H} \frac{P_{th}}{P_{MAX,th}}, O2, O2_{total}, N^{daf}, V^{daf} \end{matrix}\right) \qquad (104)$$

Specific functionality must be verified by experiment. Only parameters with significant functionality within the limits of standard combustion parameters would be included in the

prediction model. Similarity, criteria Fr_p, Re_p and Nu seem as a good candidate for the significant parameters, as well as Arrhenius term $\frac{E_a}{R \cdot T}$.

4.2 Empirical models proposition for FBC

The kinetic NO_X prediction models described in chapter 2.6.1 can provide very good accuracy. To do that they need to include detailed nitrogen chemistry (hundreds of equations), hydrodynamic model of the fluidized bed and freeboard. They need to account for distributor region, emulsion phase, bubble phase as well as the possibility of different hydrodynamic regimes in different parts of the bed and mass interchange between phases. This approach increases the model complexity beyond acceptable limits and requires an extensive amount of computation time. Kinetic models also provide information that is unnecessarily detailed – concentration profiles of all types of nitrogen oxides through the whole bed and freeboard – while only a single value is needed: *NOX* [ppm] at the exhaust of the smoke stack.

Empirical models can provide the same level of accuracy if used correctly, meaning within their application limits. Application limits are set by the model constants that are compensating for the combustion, fuel and boiler parameters not included in the model input data.

In the chapters 4.2.4 and 4.2.5 the modifications of two empirical models for FBC are proposed – Pohl´s model and Ibler´s model. The data used for models´ modification originates from Czech FBC power plant units – namely Komořany, Mladá Boleslav and Poříčí – and a laboratory unit – Golem. The boilers are described in detail in chapter 4.2.2.

The data used for proposing the prediction models were not measured by author of this work and were obtained on a non-disclosure basis, thus the raw data will not be included in this work.

The findings in chapters 4.2.4 and 4.2.5 were already published in greater detail in [II.] and [III.].

4.2.1 Rationale for model selection and proposed modification

In chapters 2.2 and 2.3 the important influential parameters for NO_X emissions were reviewed and discussed. In chapter 4.1 new parameters were proposed and some of them are later experimentally investigated in chapter 5.

Pohl´s model was chosen as the first representative of empirical models as it is the most widespread and generally used model. It is basing the NO_X prediction on the fuel related parameters – N^{daf} [wt%], *VM* [-] and *FC* [-] – and the combustion parameters – constants k_1 to k_4. Coefficients for staged combustion model were adopted in this work as a basis for *NOX* [ppm] prediction by Pohl´s model (however, a new set of coefficients might be more suitable for FBC). The model modification for O_2 [%vol] influence was included to account for the most influential combustion parameter.

As a second example Ibler´s model was used because it uses a completely different approach. The prediction is based upon combustion parameters – O_2 [%vol] and T [K]. The fuel parameters are considered through fuel specific constant K (different for every fuel). Using a fuel specific constant might be more suitable for the NO_X prediction in FBC due to the complexity of fuel related phenomena (see chapter 2.2 and 2.3) – which simply cannot be fully considered by fuel parameters used in Pohl´s model.

4.2.2 Boiler description and combustion parameter range

The summary of boiler parameters and combustion conditions is shown in Table 2. The steam values for the CTU in Prague pilot scale unit "Golem" are not presented since the boiler

does not produce any steam or utilizable energy and all heat is removed by a water cooling cycle.

The FBC designated K3 with bubbling bed from combined power plant Komořany was used as a first reference. Lower part of the combustion chamber containing the bed is lined and contains in – bed evaporator. The upper part contains wall and grid parts of the evaporator. Convection part, that follows the combustion chamber, contains superheaters (primary, secondary and output) and economizer. Tube – type air heater with a separate part for fluidization and secondary air is the last heat transfer surface of the boiler. The boiler is equipped with bed material recirculation system as well as bed height control. Combustion process is controlled by fluidization air flow rate and fuel input. The steam quality is adjusted by feed water injection before the last superheater.

The FBC designated K90 with circulating bed from Mladá Boleslav combined heat and power plant was used as the second reference. The boiler is designed for hard coal combustion; however, the recently used fuel is a mixture of hard and lignite coal with addition of biomass. The combustion chamber with lined lower part contains the membrane-wall type evaporator. After the combustion chamber a cyclone for coarse particle separation follows. The second duct containing membrane-wall, tube and wall type superheaters and economizer followed by hopper. The third duct contains the tube-type air heater, which is the last heat transfer surface of the boiler. The steam quality is controlled by feed water injection before the second and last superheater.

The boiler from combined heat and power plant Poříčí is a CFBC with natural water circulation and a single drum. The combustion chamber walls constitute a membrane wall evaporator. The lower part of the combustion chamber is protected by lining (4,7 m). Walls also contain secondary air input nozzles and limestone chutes. The second tract contains three convection superheaters regulated by feed water injection.

The FBC "Golem", situated on the premises of CTU in Prague, is a BFBC with thermal power output ca. 500 kW. The first pass is lined and has water cooled double wall on the outer side. Combustion chamber can be considered adiabatic due to very low heat removal. The secondary pass is equipped with fire tube heat exchanger. Fluidization air is supplied by primary air fan with controllable frequency. Primary air is introduced via a V-shaped trough type distributor, equipped with 36 nozzles, at the bottom of the primary pass. Secondary air is supplied by separate fan and distributed at 4 height levels. At each level 4 entry points are situated on the circumference of the primary tract. Each of these 16 entry points is equipped with a control flap. The boiler allows flue gas recirculation from the cyclone exit to the primary air duct. Fuel is introduced to the boiler by a screw conveyor, the entry point is on the bed surface at the wall.

Table 2: Boiler parameters (oxygen concentration is measure after economiser)

	Komořany	Mladá Boleslav	Poříčí	Golem
$M_{steam.nom}$ [t/h]	125	140	250	-
T_{steam} [°C]	490	535	520	-
p_{steam} [MPa]	7,3	12,5	10	-
$O2$ [%]	3,8 – 4,7	4 - 5	3,3 – 6,3	8 – 12,4
T_{bed} [°C]	815 - 866	873	850	800 - 850
Fuel mixture [wt%] LC/B/HC	100/0/0	40 – 85/0 – 25/0 - 50	8 – 100/0 – 92/0	100/0/0

The summary of fuel parameters is shown in Table 3. Fuels combusted are lignite coal (LC), hard coal (HC) and biomass (B) or their mixtures. The subscripts in Table 3 represent the boiler in which the fuel is combusted.

Komořany CHPP is combusting lignite coal (LC_K) only. Mladá Boleslav CHPP is combusting a mixture of hard (HC_{MB}) and lignite coal (LC_{MB}) with addition of biomass (B_{MB}) pellets. Poříčí CHPP is combusting a mixture of lignite coal (LC_P) with biomass (B_P) - wood chips. The combustion tests of the pilot plant boiler Golem were conducted with two types of lignite coal (LC_G and LC_{G2})

Table 3: Fuel parameters

	LC_K	HC_{MB}	LC_{MB}	B_{MB}	LC_P	B_P	LC_G	LC_{G2}
Q_i^r [MJ/kg]	13	24,3	18,8	15,2	17	9	10,1	10,1
W^r [-]	0,28	0,132	0,282	0,137	0,285	0,45	0,30	0,436
A^r [-]	0,15	0,117	0,064	0,045	0,11	0,02	0,28	0,13
N^{daf} [-]	0,01	0,009	0,014	0,019	0,005	0,002	0,013	0,008

4.2.3 Evaluating model prediction accuracy

Variance R^2 was used to evaluate the models´ prediction accuracy in chapters 4.2.4 and 4.2.5.

4.2.4 Pohl´s model modification

At first the original Pohl´s model as was proposed by equation (68) was used. As expected the reliability was very low, see Figure 15. The prediction is almost constant and independent on the actual measured value.

The modification from equation (79) was used to compensate the influence of oxygen concentration and the O_2 coefficient k was optimized by least square method for better fit with the x = y line. The best fit with determination index R^2 = 0,11 was found for k = 19,69, see Figure 16. Some improvement can be seen; however, the reliability is still very low.

It can be observed that the prediction trend of modified Pohl´s model for FBC is virtually non-existent. However, in case of Golem at least a positive trend can be observed. This effect could be caused by the fact that the combustion parameters of large scale boilers are quite stable while the parameters of Golem were varied numerous times during measurement. Also, the measurements on Golem form two discreet groups which represent two different types of lignite coal.

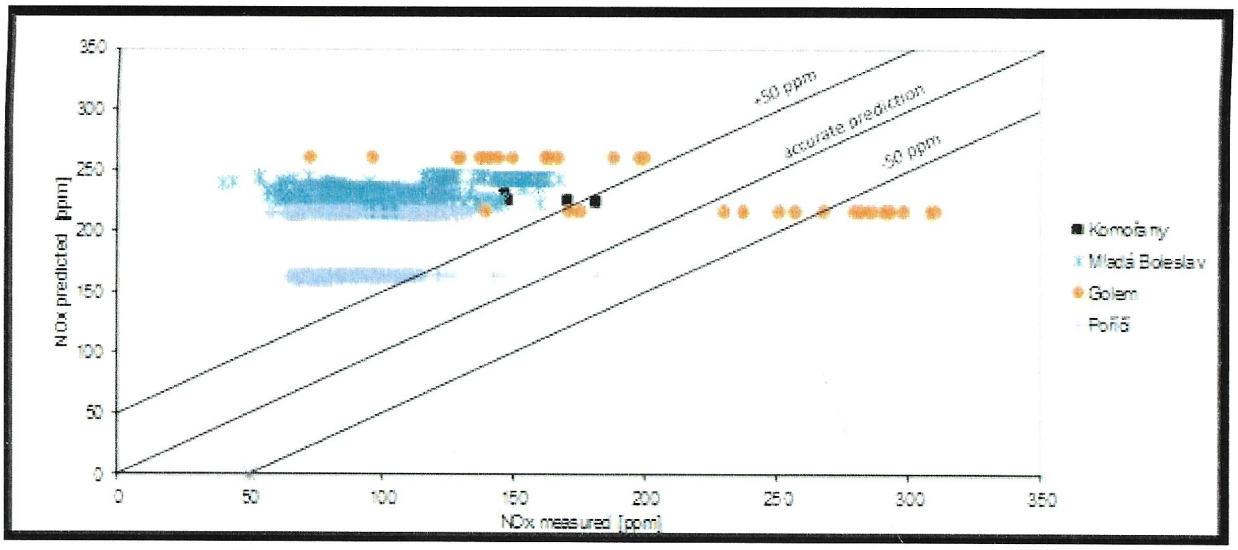

Figure 15: *NOX* [ppm] prediction reliability by original Pohl´s model

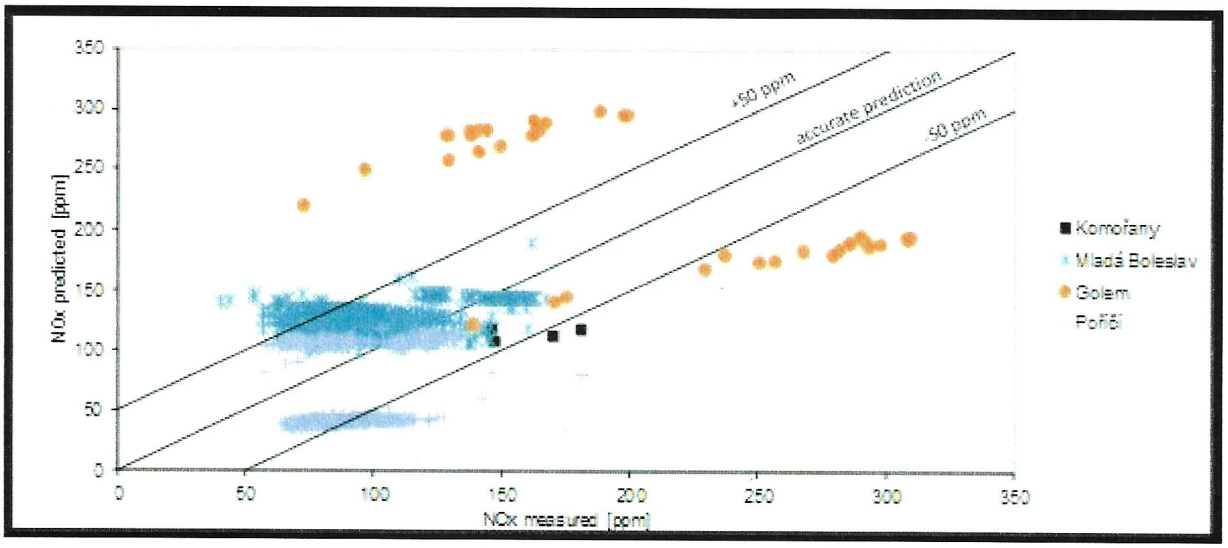

Figure 16: *NOX* [ppm] prediction reliability by Pohl´s model with compensation for oxygen concentration

4.2.5 Ibler´s model modification

Results of original Ibler´s model predictions were not in agreement with measured data, see Figure 17.

To increase the reliability, the combustion constant was modified from $7 \cdot 10^{-5}$ to $2{,}91 \cdot 10^{-4}$ to represent different combustion intensity in FBC and fuel constants K were optimised to values presented in Table 4, both by the least square method fitting the x = y line. See the results in Figure 18 with $R^2 = 0{,}61$.

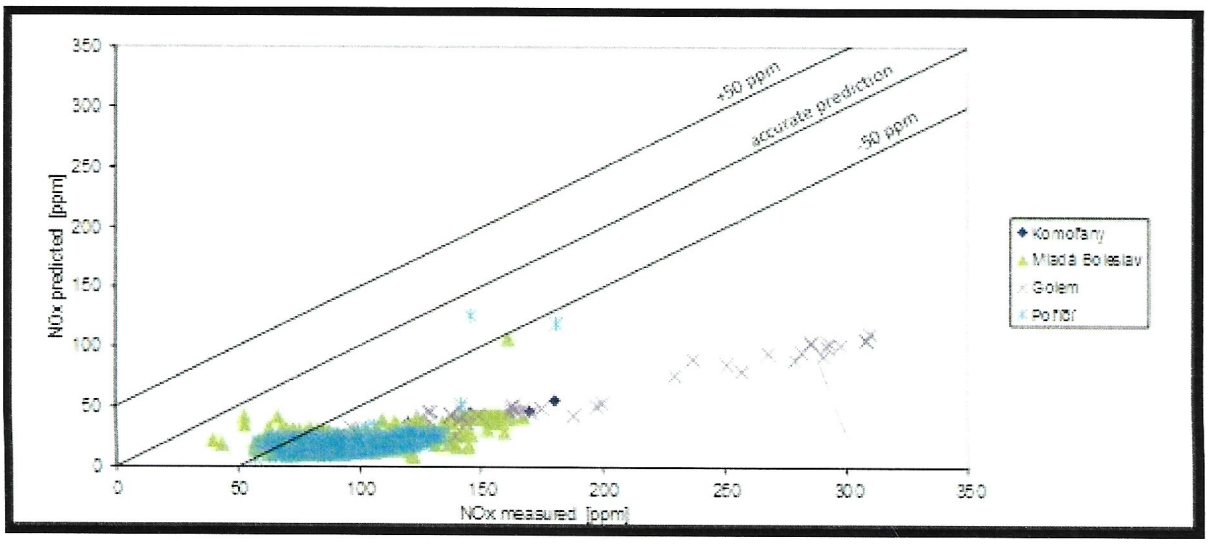

Figure 17: *NOX* [ppm] prediction reliability by original Ibler´s model

Table 4: Values of fuel constant K

	LC_K	HC_{MB}	LC_{MB}	B_{MB}	LC_P	B_P	LC_G	LC_{G2}
K [-]	6,35	4,51	2,84	-3,01	1,41	3,34	0,53	1,90

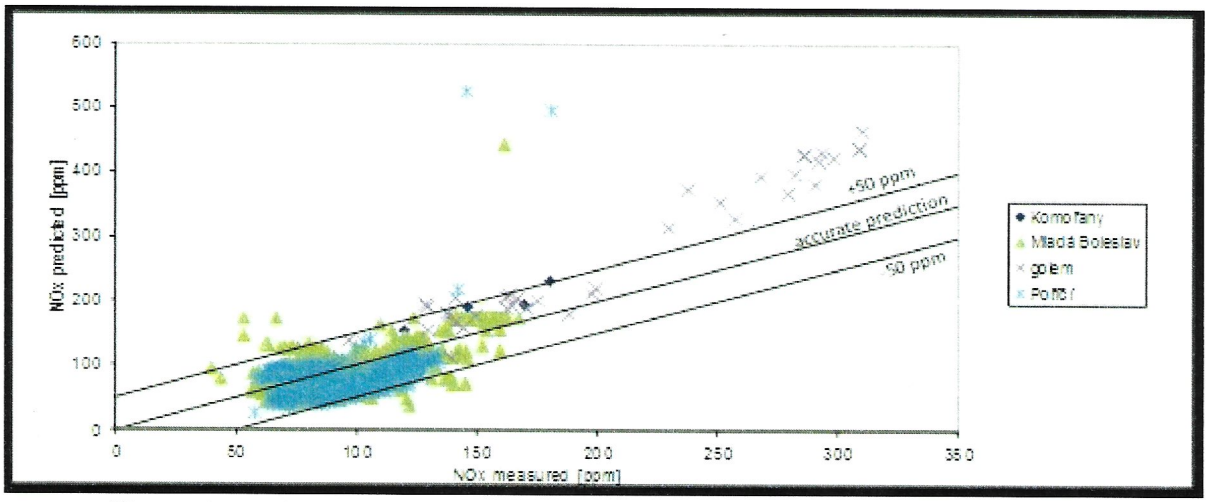

Figure 18: *NOX* [ppm] prediction reliability by Ibler´s model with modified constants

The prediction accuracy significantly increased but the model is not yet satisfactory. It was noted that most of the points that are not in agreement with the prediction can be attributed to fuel mixtures. This observation is in agreement with the literature. Combustion of fuel mixtures shows different *NOX* [ppm] compared to the case of both fuels combusted separately. The conclusion was made that the fuel mixtures are skewing the model, so the new model needs to be applicable exclusively for combustion of single fuels.

If all fuel mixtures are excluded from the prediction and the model is used for single fuel combustion only the determination index rises even higher to $R^2 = 0,81$, see Figure 19. With

the combustion constant $2{,}9 \cdot 10^{-4}$ and fuel constant K from

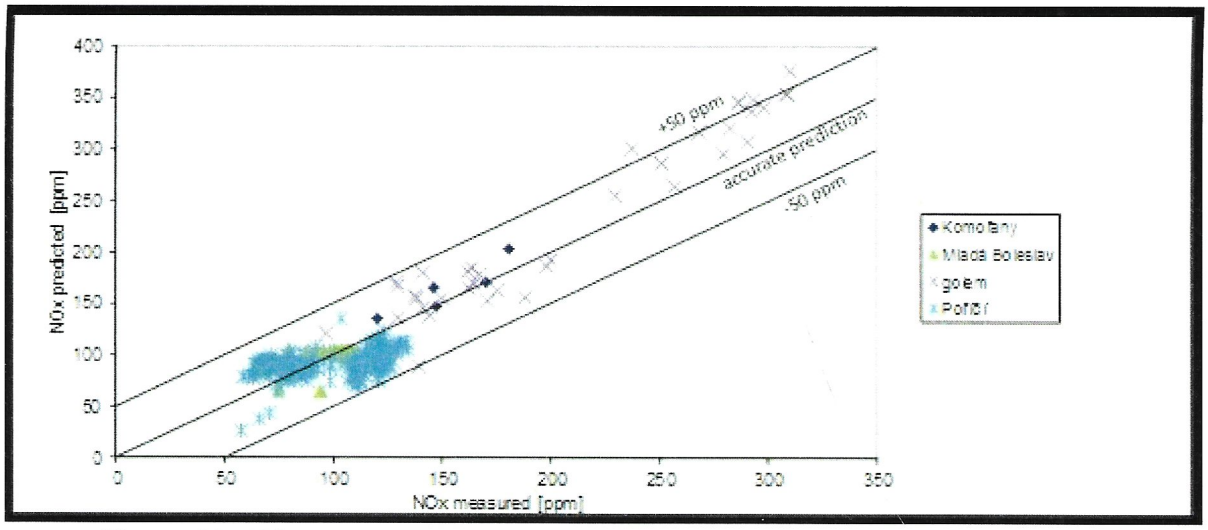

Figure 19: *NOX* [ppm] prediction reliability by Ibler´s model with optimized constants (single fuel combustion only)

Table 5, both optimized by least square method fitting the x = y line.

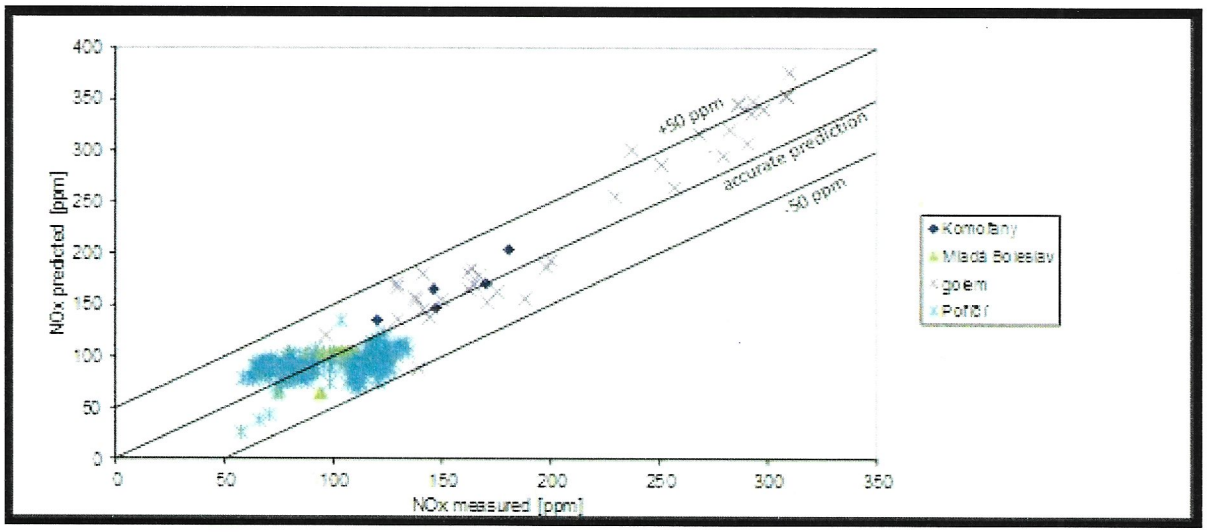

Figure 19: *NOX* [ppm] prediction reliability by Ibler´s model with optimized constants (single fuel combustion only)

Table 5: Values of fuel constant K (single fuel combustion only)

	LC_K	LC_{MB}	LC_P	LC_G	LC_{G2}
K [-]	5,55	2,8	1,43	0,47	1,55

4.2.6 Summary

The modification of existing empirical NO_X prediction models intended PCC for FBC conditions is problematic because the NO_X formation mechanisms in PCC and FBC are different. At FBC the thermal formation mechanism is negligible due to low combustion

temperature and most of the NO_X originates from the fuel. Modifications of two models were proposed – Pohl´s model and Ibler´s model.

Pohl´s model was found to be not suitable for predicting NO_X emissions of FBC even after proposed optimisation. Contradictory to the expectations the constants for staged combustion do not seem to represent the FBC conditions sufficiently. Pohl´s model is too narrowly adapted on PCC boilers and proposed modifications did not bring any positive results. Perhaps different set of combustion constants could bring better results.

Ibler´s model was after modification found to be quite adequate for FBC with $R^2 = 0,61$. Based on the literature it was proposed to include only single fuel combustion regimes of lignite coal in the model. The reason is complex fuel nitrogen behaviour in case of combustion of fuel mixtures. Also, due the vast differences in fuel nitrogen behaviour and conversion when combusting different types of fuel, it seems to be beneficial limiting the empirical model on a single fuel type. Resulting modification brought relatively good model prediction accuracy with $R^2 = 0,81$. Virtually all measured points were predicted within accuracy of ± 50 ppm with exception of a small number of measured states in the laboratory unit.

It needs to be noted that the modified Ibler´s model accuracy was observed just for three units and for lignite coal only. It cannot be considered validated at this point. Also, the prediction accuracy for fuels not included in the original data set was not investigated at all in this work.

5 Experimental part

5.1 Experimental apparatus description

The experimental apparatus used in this work is called Minifluid and is situated on the premises of the CTU laboratory "Hall of turbines" at the address Pod Juliskou 4, Prague 6. The Minifluid is cca 30 kW laboratory BFBC unit that was designed for large flexibility of operating conditions and for wide variety of fuels.

The Minifluid, shown on Figure 20, is insulated with mineral wool and consists of several exchangeable sections – wind box, distributor, bed section, transitional section (cross section increase) and freeboard. Primary air is supplied by the primary air fan. The primary air flow rate is regulated by frequency inverter. Flue gas can be recirculated by flue gas recirculation fan. The recirculated flue gas is extracted after the cyclone and injected into the combustion air just before the wind box. The tract for flue gas recirculation contains a water cooler where partial condensation occurs. The exchangeable distributor is made of perforated plate. The bed height is maintained by a spillway situated 25 cm above the distributor. The spillway leads to a closed vessel where the excess bed material is stored until the end of experiment. Fuel is introduced by a screw feeder at the top of the bed (bubbling bed). Fuel is stored in a hopper sufficient for 30 – 60 minutes of operation. Secondary air is introduced at the lower part of the freeboard through 8 adjustable nozzles. The secondary air is provided by the primary air fan, the secondary tract is parallel with the primary air tract (not shown on Figure 20). Both tracts have a throttle to adjust the primary/secondary air ratio. The electrical air preheater is used for combustion air temperature control and is necessary for the boiler start-up.

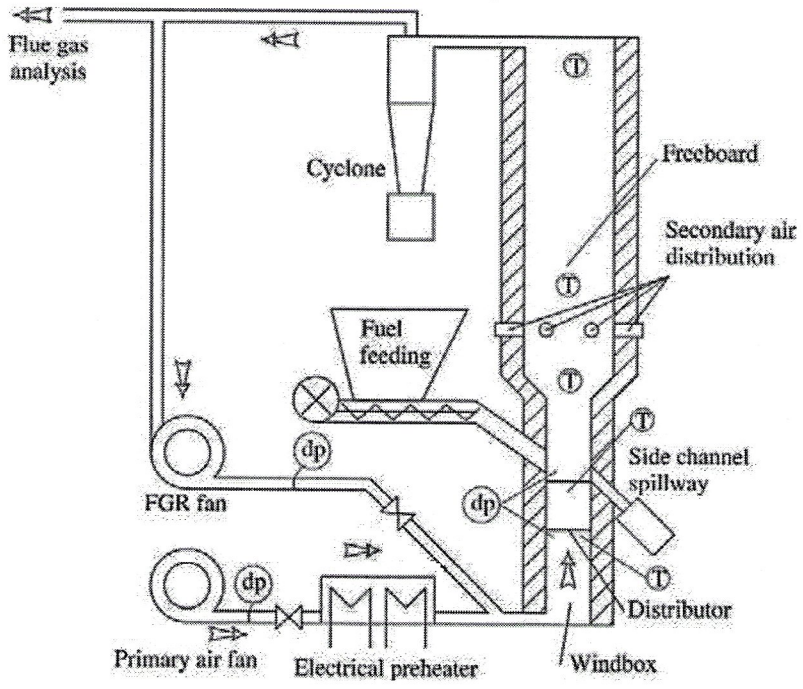

Figure 20: The Minifluid – experimental apparatus scheme [56]

The physical quantities measured during the experiment are the volumetric flow rates – primary, secondary and recirculation (measured by orifice), other quantities are, composition of flue gas at the exit of the combustor (O_2, CO, NOX, SO_2), indicated temperatures (combustion air temperature, bed temperatures – 4 measuring point by 10 cm, freeboard temperatures – 3 measuring point by 45 cm, recirculation temperature) and indicated pressure

drops (see Figure 20). All measured values are automatically saved every 2 seconds (the interval can be changed).

The fluidized bed section has a rectangular shape with dimensions 15 x 22,5 cm and is cca 40 cm high followed by a rectangular freeboard section with dimensions 30 x 40 cm.

For flue gas analysis the Hartman & Braun URAS 10 was used equipped with sensors to measure the concentrations of CO_2, CO, NO_X and O_2. The O_2 concentration was measured using the paramagnetic principle. The concentrations of CO_2, CO and NO_X was measured by infrared spectroscopy. The measured concentration of nitrogen oxides NO_X represents a sum of NO and NO_2 concentrations, as the analyser measures NO_2 while converting all NO to NO_2 (using a catalyst). The flue-gas for analysis was taken at the end of freeboard (before the cyclone). The concentration of all measured gases though the experiments can be seen in the electronic Appendix.

The analyzed gas was dried using Peltier cooling. The calibration of sensors was done at the start of every measurement day using air and a calibration gas.

The experiments were conducted over an extended period of time between 2014 and 2018. The main part of measurements was done between winter 2014 and summer 2016. After the results were evaluated a need for additional conformation measurements arose, these had to be postponed due to the laboratory reconstruction. The last measurements were finished in January 2018. During the extended time of experimentation, the Minifluid was modified. Now both the primary air flow and the recirculation flow are provided by one fan and the adjustment of flow rates ratio is done by throttle. Gas burner was added under the distributor to fix the problem with start-up and fuel ignition. [56] [57]

5.2 Start-up procedure

The sequence of steps performed to start the Minifluid up is shown below:

1) Starting the computer and the control software
2) Starting the primary air fan, opening the inspection window and removing the bed material used in previous experiment
3) Cleaning the distributor and pouring in the new bed material, closing the inspection window
4) Emptying the spillway vessel, cleaning and emptying the cyclone
5) Calibration of the flue gas analyser, setting the analyser sensors input to "air" setting (to avoid measuring the high emission values during the start-up)
6) Disassembling and cleaning the flue gas analyser probe (not required after every measurement, done once per week)
7) Starting the gas burner and the air preheating, warming up the bed
8) After the bed temperature reaches 450 °C or more the primary air flow rate can be increased to the level of fluidization and fuel feeding can start
9) Ignition achieved usually after 20 – 60 minutes of manually adjusting the parameters, turning off the gas burner and the air heating
10) Setting the flue gas analyser to "flue gas" setting, starting the saving of measured data (creating a file YYYY.MM.DD)
11) Setting the parameters of desired measured state

5.3 Shut down procedure

The sequence of steps performed to shut the Minifluid down is shown below:

1) Stopping the fuel feeding, stopping the data saving
2) Setting the analyser sensors input to "air" setting
3) Increasing the primary air flow to speed up the cooling process
4) After all measured temperatures fall below 200 °C the Minifluid can be shut down safely

5.4 Fuels used

Two fuels were used during the experiments – lignite coal and wooden pellets. The characteristics of the fuels are presented in this chapter.

The fluidization velocity during the measurements was 29 – 57 m^3/h_{nom} for wooden pellets and 33 – 57 m^3/h_{nom} for lignite coal. This corresponds to a (2 – 4)·u_{mf} for wooden pellets and (4 – 7)·u_{mf} for lignite coal.

Lignite coal – Bílina

The fuel properties of the lignite coal of the mine Bílina are shown in the Table 6.

Table 6: Lignite coal characteristics

C^{daf} [-]	0,6727
H^{daf} [-]	0,0545
O^{daf} [-]	0,2579
S^{daf} [-]	0,0044
N^{daf} [-]	0,0105
A^r [-]	0,16
W^r [-]	0,21

The lignite coal was combusted in the bed of its own ash. The ash constituting the original bed was sieved to eliminate any larger particles. However, over the course of some experiments larger ash particles started aggregating in the lower part of the bed on top of the distributor plate. The particle diameter d = 0,5 mm was obtained by screen analysis. The bed weight was 3,2 kg.

Wooden pellets

The fuel properties of wooden pellets are shown in the Table 7.

Table 7: Wooden pellets characteristics

C^{daf} [-]	0,4976
H^{daf} [-]	0,06
O^{daf} [-]	0,44
S^{daf} [-]	0,0002
N^{daf} [-]	0,0022
A^r [-]	0,01
W^r [-]	0,08

The VM [-] at biomass can be expected 0,70 – 0,85. From the visual observation of the combustion process the devolatilization occurred above the fluidized bed (in the freeboard). Intensive combustion was observed in the freeboard very time the fuel was fed. This indicates that a large portion of the latent heat was released in the freeboard and only small part of latent heat coming from the devolatilized char was released in the fluidized bed.

The wooden pellets were combusted in the bed of ceramic balls, trademark "Liapor", with the particle size range 0 – 2 mm. The particle diameter d = 1,12 mm was obtained by

screen analysis [58]. Before every measurement day new bed of particles was brought in since the previous bed material was contaminated with ash particles. The bed weight was 3,15 kg.

5.5 Experiments´ methodology

Parameters that influence *NOX* [ppm] can be taken from literature review (chapter 2.3). Some additional parameters were proposed by Dimensional analysis in chapter 4.1. In the experimental part some of the influential parameters were selected and the dependency of *NOX* [ppm] on the selected parameters was examined. Not all proposed parameters could be experimentally examined due to experimental apparatus limitations.

To examine the dependency of *NOX* [ppm] on selected parameters, groups of experiments were carried out. In each experimental group only one parameter is varied while other parameters are kept constant. However, keeping oxygen concentration constant during the experiments showed to be impossible on the current unit. This problem was solved by examining the oxygen concentration influence first and establishing a functional dependency. This dependency was later used to correct the oxygen changes in all other experiments. This approach assumes independent effect of parameters which is realistically not completely valid but is often assumed in the relevant literature during experiments. In each group of experiments several measurement batches were done in attempt to get wider range of measured parameters and in attempt to duplicate some of the measurements.

See the experiment groups´ description below.

1) Primary oxygen concentration in the flue gas O_2 [%]
2) Combustion temperature (of the bed) t_{bed} [°C]
3) Total oxygen concentration in flue gas (with secondary air) O_{2total} [%]
4) Reynolds number of bed particles Re_p [-]
5) Flue gas recirculation coefficient r [-]

The oxygen concentration in the flue gas was investigated first because it was expected to have the strongest influence on *NOX* [ppm] and it was needed to correct the oxygen concentration variations in other groups of experiments. The secondary air tract was closed during the measurements so the *O2* [%] measured was all provided by the primary air tract – for this reason the O_2 concentration is called "primary". The primary oxygen concentration was varied by adjusting the fuel input while keeping the primary air ventilator setting constant (thus keeping the Reynolds number and flow pattern constant). Slight temperature changes were observed but the temperature influence on *NOX* [ppm] is expected to be much lower so the slight changes were neglected.

Combustion temperature t_{bed} [K, °C] was investigated second and it was adjusted by primary air preheating. The change in primary air temperature resulted in the slight changes in air flow rate. These changes were numerically corrected by the dependency obtained in the first group of experiments.

Total oxygen concentration $O2_{total}$ [%] was the third investigated parameter. During this group of experiments the secondary air tract was opened (during all other experiment groups it remained closed) so the *O2* [%] measured was provided by both primary and secondary tract – for this reason the O_2 concentration is called "total". The part of total oxygen concentration provided by primary air was later numerically calculated based on primary air flow rate and fuel input. The flow rate of secondary air was varied by throttle while the fuel and primary air setting was kept constant. Unfortunately, the primary air flow rate did not remain constant – the primary air flow rate dropped significantly when the secondary air tract was opened and later

decreased even further with increasing the secondary flow rate. This effect also resulted in increased bed temperature when the secondary air was increased. The temperature changes were neglected, and the primary air drop was numerically corrected by the dependency obtained in the first group of experiments.

Reynolds number of bed particles Re_p [-] was the fourth investigated parameter. The Re_p [-] was varied by adjusting the primary air flow rate while the fuel setting remained constant. This caused the primary oxygen concentration and temperature to change. The temperature changes were neglected, and the primary air drop was numerically corrected by the dependency obtained in the first group of experiments.

Flue gas recirculation coefficient r [-] was the last investigated parameter. Unfortunately, the recirculation was not functional on the original experimental setup, so modifications had to be made to conduct the experiments, see chapter 5.1. The ventilator setting had to be different for each measured state and the flow rate was adjusted to the original value using the throttle valves. The primary air changes were numerically corrected by the dependency obtained in the first group of experiments.

5.5.1 Determination of bed temperature

The temperature measured at the centre of the bed – t2 – (second measurement point in the bed) was selected to represent the bed temperature. Other options were also considered.

It was observed that the lowest measuring point in the bed – t1 – sometimes shows extremely low temperature which is caused by large bed particles sinking and sedimenting on the bottom of the fluidized bed. The sediment particles were not in the state of fluidization and combustion was not occurring in the region. This phenomenon did not happen during all measurements but the temperature t1 seems unreliable to be included in the determination of the representative temperature.

The measuring point t3 could be observed through the inspection window and it was situated on the edge of the bed or in the splash zone. For this reason, t3 was also not included it in the determination of the representative bed temperature.

5.5.2 Start of experiments and time duration

After the Minifluid was started up it was necessary to achieve stable combustion parameters before the measurement could start. It usually took 15 – 45 minutes for temperature to become relatively stable in the new setting, other parameters adjusted much more rapidly. After the values of all parameters became relatively stable the measurement was started.

To evaluate the time length necessary for a representative measurement a 2-hour experiment was conducted, and the average values over different time periods were compared. See Table 8. It is obvious that the measured values averaged over 10 minutes to 2 hours vary only slightly and even 10 minutes would be representative for one measured state. However, longer time period was used as the standard measurement duration ranging usually from 15 to 30 minutes.

Table 8: Average values over different time period – wooden pellets combustion

	t_{bed} [°C]	*O2* [%]	*NOX** [ppm]	*NOX* St.dev. [ppm]	*CO* [ppm]
2 hours	839	12,56	73,9	11,4	65
1 hour	835	12,64	77,0	11,6	67
30 min	833	12,65	80,7	11,5	72
20 min	830	12,65	83,0	11,1	72
10 min	827	12,67	86,0	11,0	66

5.5.3 NO_X emissions expression

There are several options how to express the emissions of NO_X. The flue gas analyser is measuring and saving the emission value in ppm, this is labelled *NOX* [ppm]. During the first evaluation step in chapter 6, the correction for standard *O2* [%] was made – coal 6 %, biomass 11 %. This value was labelled *NOX** [ppm]. See Electronic appendix 2.

During the final evaluation a correction for *O2* = 0 % was made to compare coal and biomass and the NO_X emissions were expressed as a fraction of maximum equivalent NO emissions. This value was labelled $\frac{NOX}{NO_{eq}}$ [-]. The maximum equivalent NO emissions NO_{eq} [ppm] are the emissions measured if all the fuel nitrogen would leave the combustion process as NO. The NO_{eq} is calculated from equation (105).

$$NO_{eq}[ppm] = \frac{2{,}1422 \cdot N_{daf} \cdot (1 - A^r - W^r)}{V_{fd}} \cdot 10^6 \qquad (105)$$

See Electronic appendix 3.

5.6 Measurement error and uncertainty

The measurements of physical quantities must be repeatable and reproducible regardless of the measurement method and apparatus. However, each measurement of a physical quantity has a certain amount of imprecision. Evaluation of a measured quantity needs to include:

1) determining the representative value of the measured quantity,
2) determining the interval of uncertainty around the measured value where the real value should be found.

Both can be done either by statistical determination or by estimation.
[59]

5.6.1 Types of errors

The difference between the measured value of a physical quantity and its real value is called error. Different types of errors are described in following subchapters. It is obvious that the exact value of error cannot be specified since the real physical value is not known. For this reason, uncertainty is used, see chapter 5.6.2.

Serious error

Serious errors have various exceptional cases. They cause the measured value to be significantly distant from the rest of the measurements. For the correct evaluation these measurements must be discarded.

Random error

The root cause of random error cannot be tracked down. Random error is made up by a large amount of small errors that occur through the measurement process.

Systematic error

Systematic error (also called the measurement bias) has causes that can be to a certain extent identified.

[59]

5.6.2 Uncertainty

The term uncertainty was established on the recommendation of CIMP – The international committee for measures and weights. The guidelines on how to express uncertainty were issued by ISO in 1993.

Uncertainty U comprises of all factors that influence the measured value. It represents a qualified estimation of relation between the measurement and the real value of physical property. It is usually expressed as interval, see equation (106).

$$x = \bar{x} \mp U \qquad (106)$$

Where $\bar{x}$ is an arithmetic mean. It was proposed to use the arithmetic mean to determine the representative value of the large number of measurements (more than 7 measurements). [59]

Standard uncertainty

The standard uncertainty U is used to evaluate the uncertainty of the experiment. Standard uncertainty is based on the standard deviation. Standard deviation is a basic measure to quantify the variation and dispersion of measured values. It is calculated according to the equation (107).

$$U = \sigma = \sqrt{\frac{1}{n-1} \cdot \sum_{n}^{i=1} (\bar{x} - x_i)} \qquad (107)$$

The expression of standard uncertainty is shown in equation (108) and it represents the interval where the real value is with the probability of 68 %.

$$x = \bar{x} \mp \sigma \qquad (108)$$

There are many other possibilities how to express the uncertainty of the measurement. For example:

1) Maximum uncertainty – the interval which contains the real value with the probability of 99,7 % (± 3σ)
2) Probable uncertainty - the interval which contains the real value with the probability of 50 % ($\pm \frac{2}{3}\sigma$)

However, the standard uncertainty was selected as a sufficiently suitable value.

[59]

6 Evaluation of results

Measured values in graphs are displayed with the error bars of ± δ.

6.1 Repeatability of results

From all the measurements that were done, many states were measured more than once. The repeated measurements were done on a different day with a new bed material. It is interesting to point out those measurements and compare the results. The repeatability of the measurements seems to be quite good with exception of several measured states with exceptionally high CO concentration. See Table 9 and Table 10.

Table 9: Wooden pellets – combustion states measured multiple times

Prim. fan [Hz]	*Prim. air flow [m^3/h_n]*	*P_{th} [%]*	*Preheat*	*t_{bed} [°C]*	*O2 [%]*	*NOX* [ppm]*	*CO [ppm]*
12	40,3	44	-	825	12,1	85,19	130
12	42,1	44	-	839	12,6	73,89	65
15	51,5	44	-	776	13,6	88,89	106
15	51,3	44	-	782	12	94,51	150
15	49,9	44	yes	838	13,1	86,38	62
15	50	44	yes	821	12	90,71	131
15	51,1	66	-	858	10,4	83,49	112
15	53,8	66	-	850	11,7	81,3	80
10	33,1	55	-	916	8,1	64,17	63
10	34,6	55	-	951	7,9	70,57	20
12	42,5	55	-	893	9,7	76,58	31
12	42,8	55	-	891	10,3	73,11	42
14	51,3	55	-	869	9,9	80,35	45
14	50,7	55	-	852	11,1	70,61	94
16	58,8	55	-	827	11,5	80,36	102
16	57,7	55	-	761	12,4	67,24	165
14	51,4	77	-	900	9,2	74,63	37
14	50,2	77	-	863	11,3	84,47	79
12	42,9	100	-	1032	4,1	61,76	201
12	41,8	100	-	972	8,1	73,34	16
12	41,4	100	-	1030	8,6	61,43	38
12	44,1	77	-	960	7,3	71,1	18
12	41,8	77	-	923	9,8	79,6	31
10	33,1	44	-	905	8,2	69,74	27
10	32,9	44	-	918	8	65,88	31

Table 10: Lignite coal – combustion states measured multiple times

Prim. fan [Hz]	*Prim. air flow[m^3/h_n]*	*P_{th} [%]*	*Preheat*	*t_{bed} [°C]*	*O2 [%]*	*NOX* [ppm]*	*CO [ppm]*
10	30,8	50	-	962	6,4	276	276
10	31,8	50	-	959	6,8	290	142
10	32,3	50	-	944	5,8	289	290
10	30,9	34	-	786	11	377	335
10	31,3	34	-	783	11,5	413	331
10	32,2	34	-	790	10,5	381	275
12	38	50	-	884	7,8	329	317
12	41,2	50	-	846	8,7	354	269
14	45,9	50	-	844	9,8	393	162
14	49,4	50	-	781	10,4	369	287
15	52,2	66	-	880	9,8	432	410
15	56,2	66	-	1070	7	290	156
15	52,3	80	-	940	7,6	359	384
15	53,2	80	-	976	6,5	326	404
15	54,1	80	-	981	6,1	211	2875
15	56,3	80	-	996	5,6	258	1915
15	51,7	100	-	1076	4,4	289	150
15	50,9	100	-	1064	4	267	587
12	40,7	44	-	755	10,9	379	303
12	42,6	44	-	745	12,8	405	1305
12	37,4	44	yes	860	10,1	379	356
12	37,3	44	yes	843	11,4	419	341
15	47,8	100	-	1091	5,9	243	243
15	56,3	100	-	980	7,2	222	3139

It can be observed that the lignite coal is much more prone to suffer from unstable combustion conditions or incomplete combustion – high CO concentrations. The measurements with too high *CO* [ppm] were later eliminated from the evaluation since the *NOX** [ppm] is skewed.

6.2 Wooden pellets

6.2.1 Primary oxygen concentration

The primary oxygen concentration was varied by adjusting the fuel input while keeping the primary air fan setting constant. Three batches of measurements were done. The first one for primary air fan set to 12 Hz translating to flow rate cca 40 m^3/h_N with P_{th} = 44 – 100 %. The second one for primary air fan set to 14 Hz translating to flow rate cca 50 m^3/h_N with P_{th} = 44 – 100 %. The third one for primary air fan set to 15 Hz translating to flow rate cca 51,5 m^3/h_N with P_{th} = 44 – 66 %. See Appendix 1.

In all three cases a steady linear increase of $\frac{NOX}{NO_{eq}}$ was observed through the whole measured range of *O2* from 4,1 % to 13,6 %. The summary of all 3 measurement batches is shown in Figure 21.

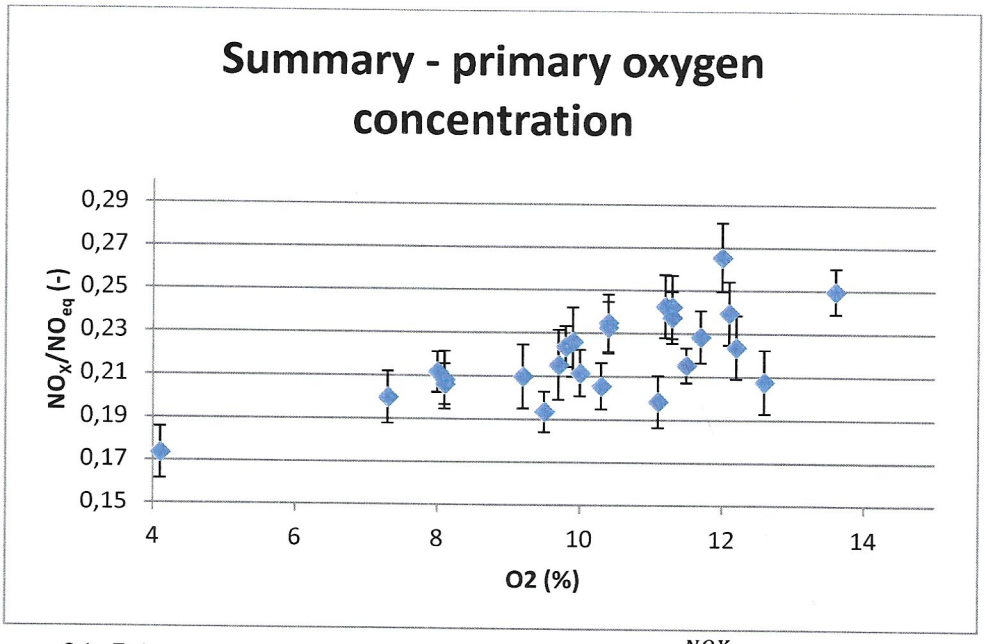

Figure 21: Primary oxygen concentration influence on $\frac{NOX}{NO_{eq}}$ – summary (wooden pellets)

6.2.2 Bed temperature

The bed temperature/combustion temperature was varied by the primary air preheating. The increase of the combustion air temperature caused changes in the primary flow rate and in the primary oxygen concentration. The primary oxygen concentration changes were numerically corrected as was mentioned earlier.

Five batches of measurements were done altogether. The first one and second one for primary air fan set to 12 Hz translating to flow rate cca 40 m^3/h_N with P_{th} = 44 %. The third one and fourth one for primary air fan set to 15 Hz translating to flow rate cca 51,5 m^3/h_N with P_{th} = 44 %. The fifth one was done after the Minifluid modification with primary air set to 19 Hz translating to flow rate 57 m^3/h_N with P_{th} = 66 %. See Appendix 1.

The measurement done on the modified Minifluid (measurement batch 5) is obviously inconsistent with the rest of the data. See the summary on Figure 22. The reason is probably not the changed configuration, after all the hydrodynamic mixing conditions of the fluidized bed remained the same. Before the measurements batch 5 was done, it was noted that the supply of wooden pellets was gone, and a new pack had to be bought. The suspected reason is different composition of the new pack of pellets. The measurement batch 5 is disregarded for obviously different results. The summary of batches 1 – 4 is shown on Figure 23. The measurements batches 1 – 4 are showing a steady linear decrease of $\frac{NOX}{NO_{eq}}$ with increasing combustion temperature in the temperature range 776 – 890 °C.

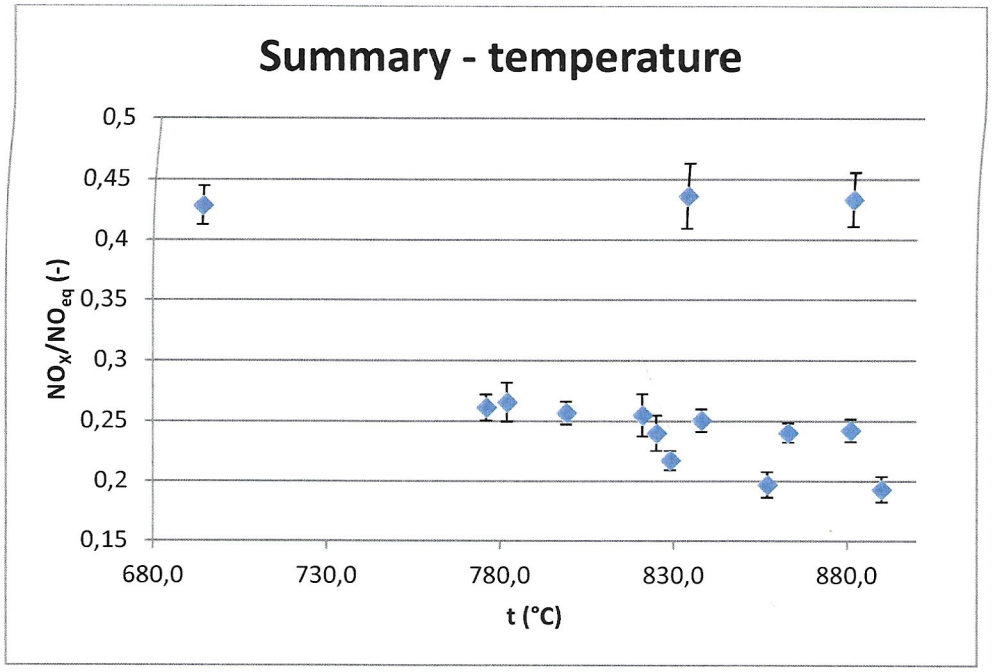

Figure 22: Bed temperature influence on $\frac{NOX}{NO_{eq}}$ – summary (wooden pellets)

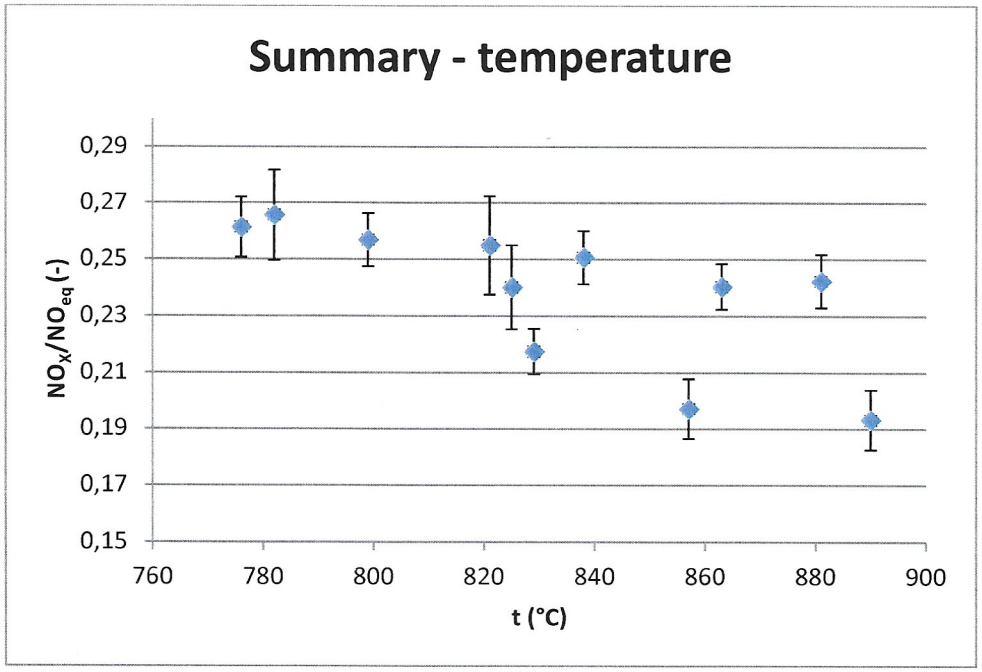

Figure 23: Bed temperature influence on $\frac{NOX}{NO_{eq}}$ – summary of batches 1 – 4 (wooden pellets)

6.2.3 Total oxygen concentration

The total oxygen concentration was varied by adjusting the secondary air flow rate while the fuel and primary air ventilator setting was kept constant. Unfortunately, the primary air flow rate did not remain constant - the primary air flow rate dropped significantly when the secondary air duct was opened and later decreased even further with increasing the secondary flow rate. This effect also resulted in increased bed temperature when the secondary air was

increased. The primary oxygen concentration changes were corrected as was mentioned earlier.

Three batches of measurements were done. The first one for primary air fan set to 10 Hz translating to flow rate cca 32 m^3/h_N with P_{th} = 66 %. The second and third one for primary air fan set to 12 Hz translating to flow rate cca 41,5 m^3/h_N with P_{th} = 100 %. The primary flow rate without secondary air started at indicated values and with introduction of more secondary air decreased to 29,5 m^3/h_N for the first batch and 37 m^3/h_N for the second and third batch. See Appendix 1.

It was observed that the $\frac{NOX}{NO_{eq}}$ is decreasing with introducing more secondary air. See Figure 24. The measured range was $O2_{total}$ = 4,1 – 10,3 % of with $O2$ = 4,1 % in batch 1, $O2_{total}$ = 6,3 – 10,5 % with $O2$ =6,3 % in batch 2 and $O2_{total}$ = 8,1 – 11,4 % with $O2$ = 8,1 % in batch 3.

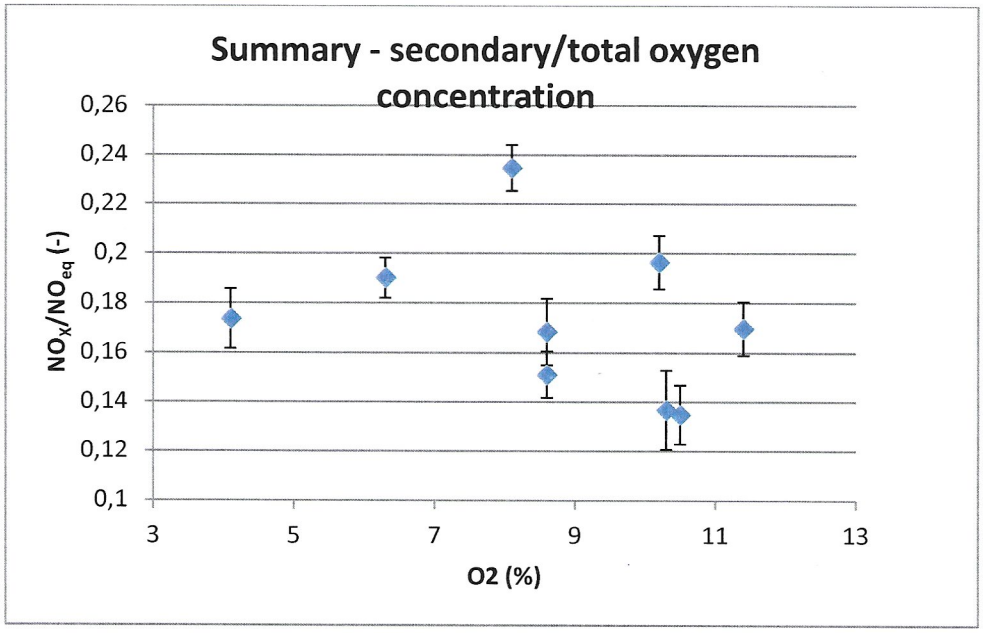

Figure 24: Total oxygen concentration influence on $\frac{NOX}{NO_{eq}}$ – summary (see the primary air flow rate description in text) (wooden pellets)

6.2.4 Reynolds number of particles

The Reynolds number of particles was varied by adjusting the primary air flow rate while the fuel setting remained constant. This caused the primary oxygen concentration and temperature to change. The changes were numerically corrected as previously stated.

Five batches of measurements were done. The first one with primary air fan set to 10 – 15 Hz translating to flow rate cca 33 – 51,5 m^3/h_N with P_{th} = 44 %. The second one with primary air fan set to 10 – 12 Hz translating to flow rate cca 33 – 40 m^3/h_N with P_{th} = 66 %. The third one with primary air fan set to 10 – 17 Hz translating to flow rate cca 33 – 57 m^3/h_N with P_{th} = 55 %. The fourth one with primary air fan set to 12 – 14 Hz translating to flow rate cca 40 – 51,5 m^3/h_N with P_{th} = 77 %. And the fifth one with primary air fan set to 12 – 14 Hz translating to flow rate cca 40 – 51,5 m^3/h_N with P_{th} = 100 %. See Appendix 1.

The summary of batches 1 – 5 is shown on Figure 25. A slight linear increase is observed in the whole measured range of Re_p = 5043 to 14464.

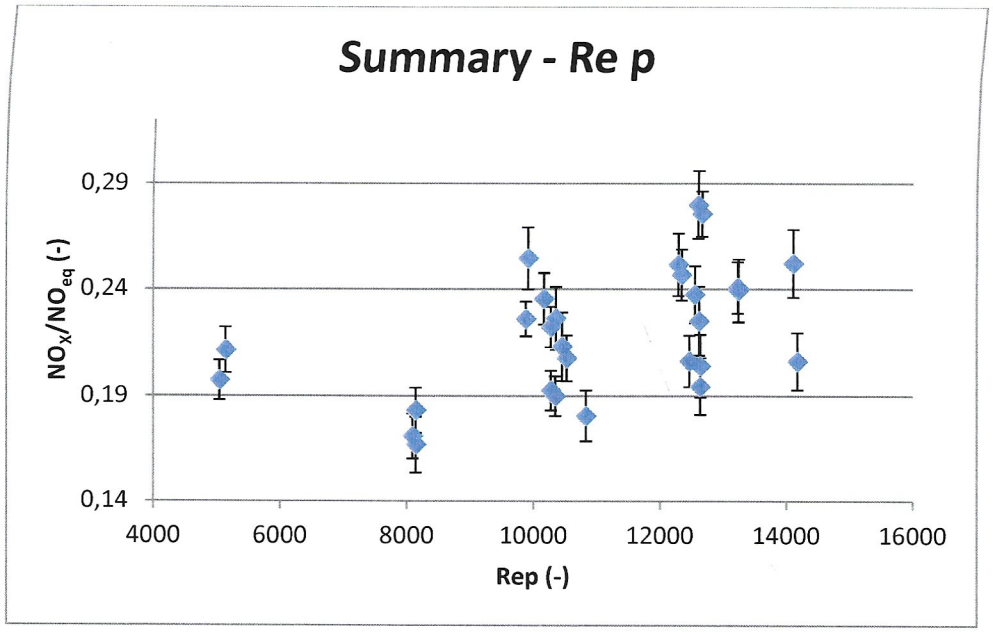

Figure 25: Reynolds number of particles influence on $\frac{NOX}{NO_{eq}}$ – summary (wooden pellets)

6.2.5 Flue gas recirculation

Flue gas recirculation was measured after the Minifluid was modified, see chapter 5.1. The ventilator setting had to be different for each state and the flow rate was adjusted with the valves to same value. Oxygen fluctuations were corrected by using the formula in previous chapters.

Several batches of measurements were done. All measured states with recirculation that were achieved were quite unstable regarding the bed temperature and had very high concentrations of CO. From this reason the results were discarded, and no evaluation was done for wooden pellets.

6.3 Lignite coal

6.3.1 Primary oxygen concentration

The primary oxygen concentration was varied by adjusting the fuel input while keeping the primary air fan setting constant. Three batches of measurements were done. The first one for primary air fan set to 10 Hz translating to flow rate cca 32 m^3/h_N with P_{th} = 33 – 50 %. The second one for primary air fan set to 12 Hz translating to flow rate cca 43 m^3/h_N with P_{th} = 36 – 50 %. The third one for primary air fan set to 15 Hz translating to flow rate cca 52 m^3/h_N with P_{th} = 44 – 66 %. See Appendix 2.

In all three cases a steady linear increase of $\frac{NOX}{NO_{eq}}$ was observed through the whole measured range of *O2* = 4 % - 13,5 %. The summary of all 3 measurement batches is shown in Figure 26. Some other measurement points from different measurement groups were added to the summary.

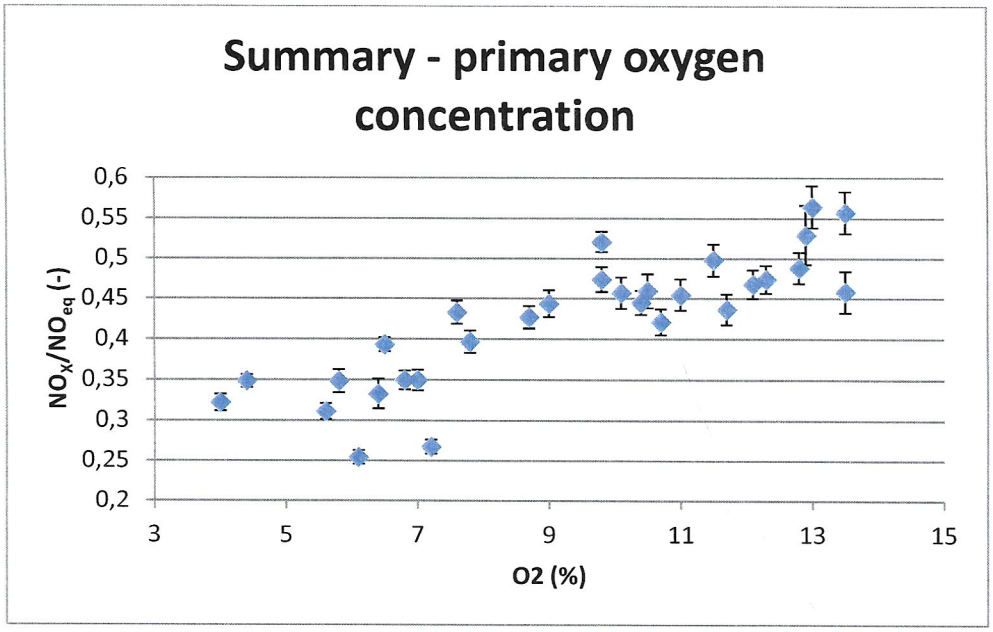

Figure 26: Primary oxygen concentration influence on $\frac{NOX}{NO_{eq}}$ – summary (lignite coal)

6.3.2 Bed temperature

The bed temperature was varied by the primary air preheating. The increase of the combustion air temperature caused changes in the primary flow rate and in the primary oxygen concentration. The primary oxygen concentration changes were numerically corrected as was mentioned earlier.

Three batches of measurements were done altogether. The first one for primary air fan set to 10 Hz translating to flow rate cca 32 m^3/h_N with P_{th} = 33 %. The second one for primary air fan set to 12 Hz translating to flow rate cca 43 m^3/h_N with P_{th} = 44 %. And the third one for primary air fan set to 16 Hz translating to flow rate cca 57 m^3/h_N with P_{th} = 40 %. See Appendix 2.

In batches 1 and 3 a steady linear decrease of $\frac{NOX}{NO_{eq}}$ was observed. In batch 2 no significant trend can be observed. The summary is presented in Figure 27.

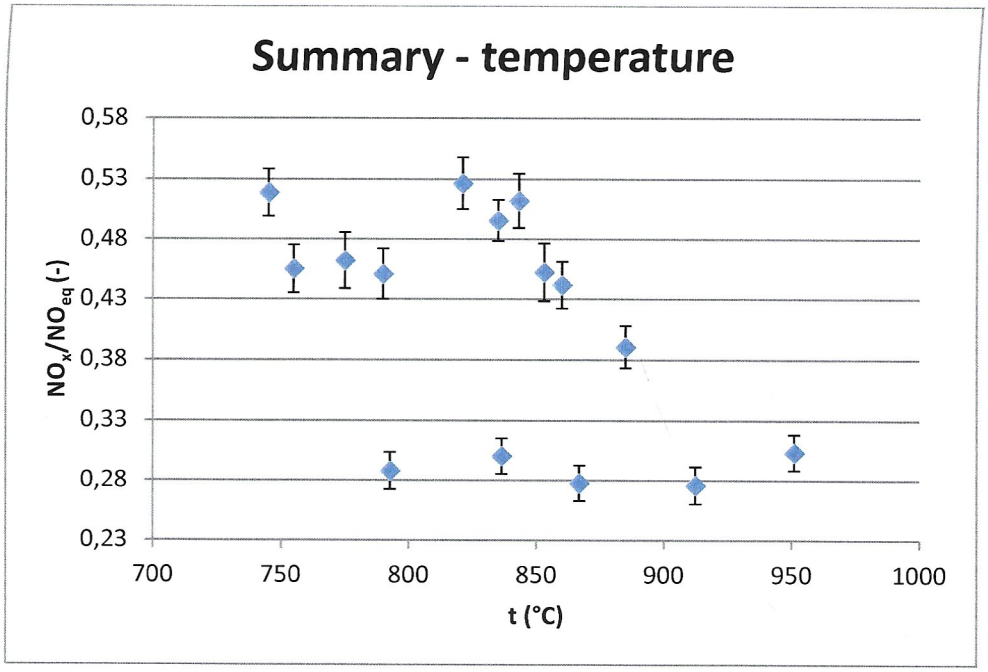

Figure 27: Combustion temperature influence on $\frac{NOX}{NO_{eq}}$ – summary (lignite coal)

6.3.3 Total oxygen concentration

The total oxygen concentration was varied by adjusting the secondary air flow rate while the fuel and primary air ventilator setting was kept constant. Unfortunately, the primary air flow rate did not remain constant - the primary air flow rate dropped significantly when the secondary air duct was opened and later decreased even further with increasing the secondary flow rate. This effect also resulted in increased bed temperature when the secondary air was increased. The primary oxygen concentration changes were corrected as was mentioned earlier.

Three batches of measurements were done. The first one for primary air fan set to 15 Hz translating to flow rate cca 52 m^3/h_N with P_{th} = 100 %. The second one for primary air fan set to 10 Hz translating to flow rate cca 32 m^3/h_N with P_{th} = 50 %. The third one for primary air fan set to 15 Hz translating to flow rate cca 52 m^3/h_N with P_{th} = 80 %. The primary flow rate without secondary air started at indicated values and with introduction of more secondary air decreased to 46,5 m^3/h_N for the first batch, to 28,5 m^3/h_N for the second batch and to 50,5 m^3/h_N for the third batch. See Appendix 2.

The summary of batches 1 – 3 is shown on Figure 28. A slight linear decrease is observed in the whole measured range of total oxygen concentration. The measured range was $O2_{total}$ = 4 – 10,4 % with $O2$ = 4 % in batch 1, $O2_{total}$ = 6,8 – 11,9 % with $O2$ = 6,8 in batch 2 and $O2_{total}$ = 6,5 – 10,5 % with $O2$ = 6,5 % in batch 3.

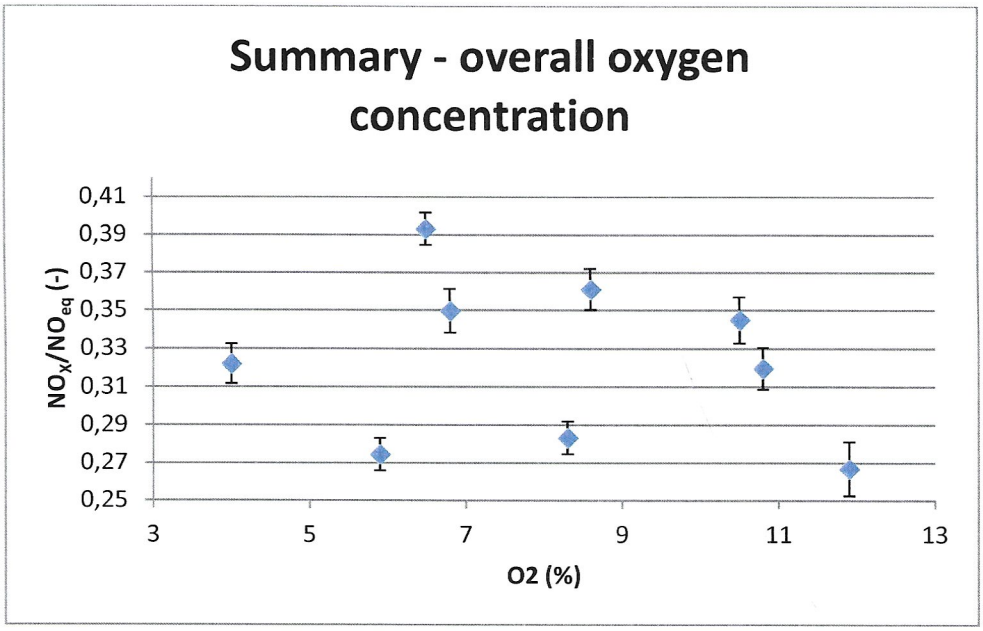

Figure 28: Total oxygen concentration influence on $\frac{NOX}{NO_{eq}}$ – summary (lignite coal)

6.3.4 Reynolds number of particles

The Reynolds number of particles was varied by adjusting the primary air flow rate while the fuel setting remained constant. This caused the primary oxygen concentration and temperature to change. The changes were numerically corrected as previously stated.

Two batches of measurements were done. The first one with primary air fan set to 8 – 14 Hz translating to flow rate cca 26 – 45 m^3/h_N with P_{th} = 33 %. The second one with primary air fan set to 10 – 16 Hz translating to flow rate cca 32 – 57 m^3/h_N with P_{th} = 50 %. See Appendix 2.

The summary of batches 1 and 2 is shown on Figure 29. No trend was observed. The measured range was Re_p = 2897 – 6264.

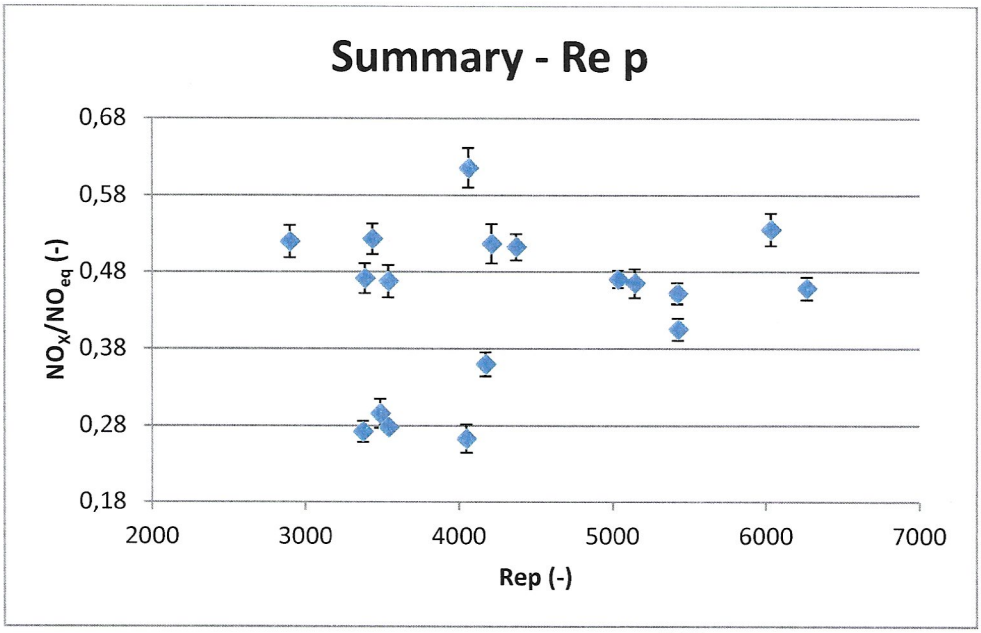

Figure 29: Reynolds number of particles influence on $\frac{NOX}{NO_{eq}}$ – summary (lignite coal)

6.3.5 Flue gas recirculation

Flue gas recirculation was measured after the Minifluid was modified, see chapter 5.1. The ventilator setting had to be different for each state and the flow rate was adjusted with the valves to same value. Oxygen fluctuations were corrected by using the formula in previous chapters.

Two batches of measurements were done with the same parameters. Other parameters were tried but the combustion was not stable. The primary air fan set to 15 Hz translating to flow rate cca 52 m^3/h_N with P_{th} = 80 %. See Appendix 2.

The summary of batches 1 and 2 is shown on Figure 30. A decreasing trend can be observed. The measured range of flue gas recirculation was r = 0 – 0,42.

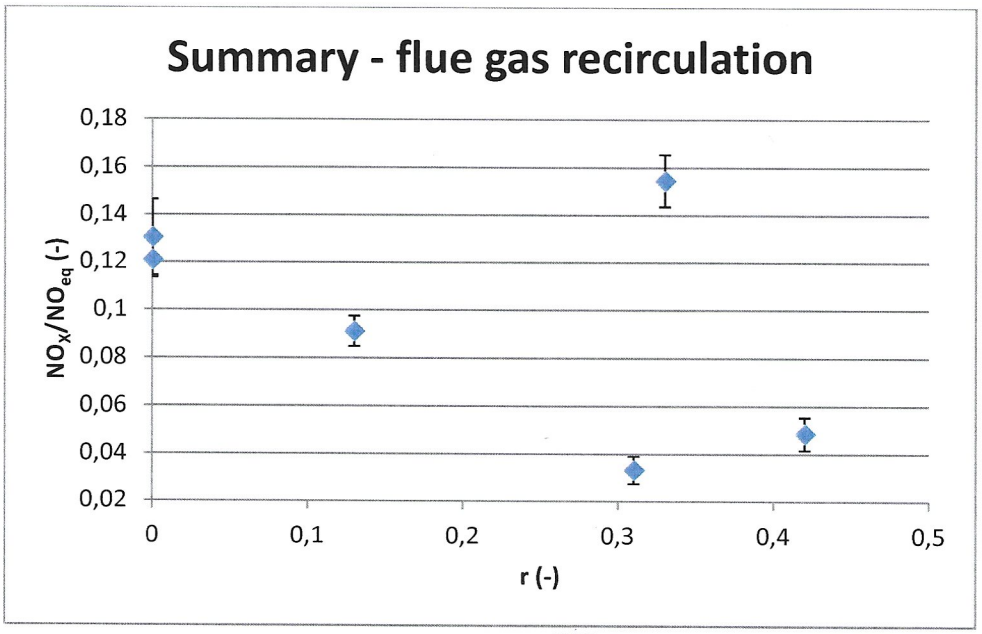

Figure 30: Recirculation influence on $\frac{NOX}{NO_{eq}}$ – summary (lignite coal)

6.4 Other observations during the experiments

Not all measurements that were done are mentioned in chapters 6.2 and 6.3. Some other measurements were done in the beginning of the measurements either before the plan of experiment was developed or just to see how stable the combustion will be under certain conditions. Some interesting observations were made, and they are presented in this chapter.

1) An attempt was made to combust wooden pellets in ceramic balls of different (bigger) average particle size. When the size range 1 – 4 mm was used much higher primary air flow had to be used to bring the bed into the state of fluidization. Also, the large bed particles tended to settle on the distributor plate making the bed highly segregated. This particle size was thus abandoned, and further measurements were done in the ceramic balls with size 0 – 2 mm as mentioned earlier, which was the finest available size.

2) The lignite coal was delivered in big-bags in a state with very wide range of particle sizes. At first several measurements were done using the unmodified coal and

compared with measurements using the coal sieved through to get rid of all particles larger than 5 mm. The measured results were comparable, no significant difference in combustion parameters or emissions was observed. In the end it was decided to use the sieved through coal for the measurements because it reduced the amount of large particles sedimenting on the distributor plate over the course of the experiment. However, this suggest that the influence of fuel particle size on the NO_X conversion is relatively small under the measured conditions.

3) Incomplete combustion (gasification) was occurring during the start-up and also in certain small rate during all measurements – which lead to increased CO emissions. In some cases, the CO emissions increased during the measurements to very high levels (thousands of ppm). These measurements had to be discarded because the incomplete combustion – the presence of CO – is strongly affecting the NO emissions. See chapter 2.2.1. Lignite coal showed to be much more prone to incomplete combustion than wooden pellets due to higher content of fixed carbon.

4) The stability of combustion conditions was satisfactory; however, the level of stability was varying depending on combustion conditions of the measured state. In other words, some measurements were more stable than others. Some states were surprisingly stable and some other had relatively high oscillations (pulsations) of the combustion parameters and emissions. See Figure 31 as an example of the stable measurement. The difference between max. and min. temperature over the whole measurement is cca 30 °C. The measurement has very low standard deviation of NO_X concentration – 4 ppm.
See Figure 32 as an example of the measurement with high oscillations. The temperature differences during the measurement are about 80 °C and constant temperature oscillations can be observed. The measurement has quite high standard deviation of NO_X concentration – 20 ppm.

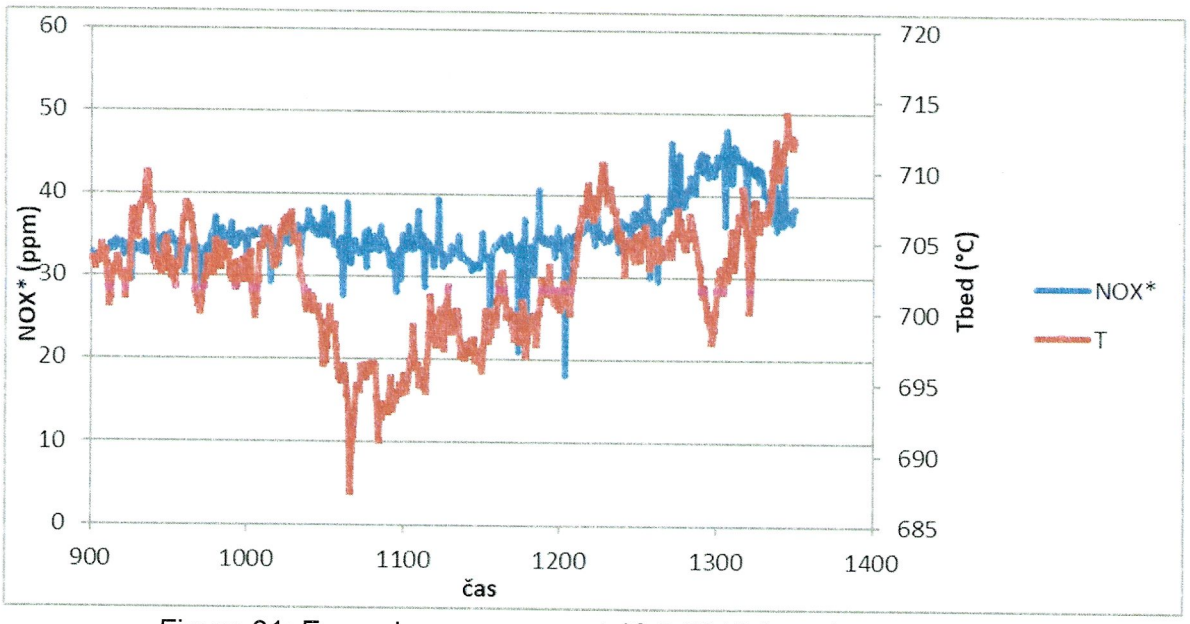

Figure 31: Example measurement 19.5.2016 (wooden pellets)

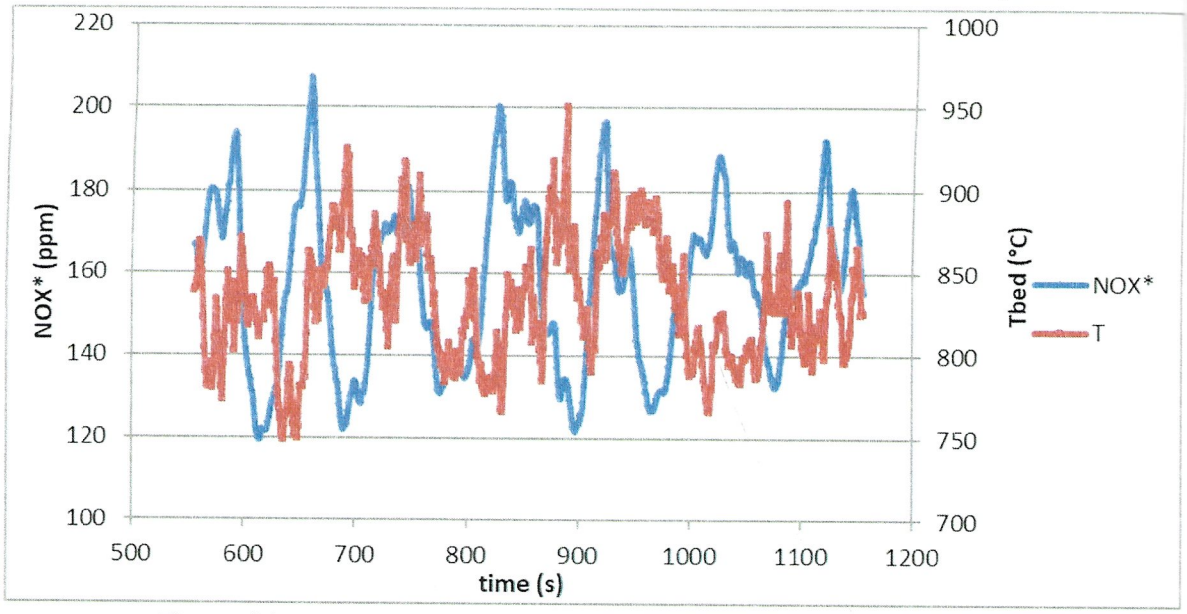

Figure 32: Example measurement 19.1.2018 (wooden pellets)

6.5 Correlation analysis

The dependencies of $\frac{NOX}{NO_{eq}}[-]$ on selected parameters, measured in chapters 6.2 and 6.3, were proposed through correlation analysis. The following functional dependencies were considered and compared:

1) Linear function
2) Power function
3) Logarithmic function (natural)
4) Exponential function

In each case the functional dependency with the highest R^2 was selected and their reliability was evaluated. When the reliability was judged sufficient ($R^2 \geq 0,5$) the dependency was suggested for use. See Table 11 for the summary of suggested dependencies for wooden pellets and Table 12 for dependencies for lignite coal. The discussion on proposed dependencies is below.

Table 11: Proposed functional dependencies – wooden pellets

Parameter	Suggested dependency	R^2 [-]
O2 [%]	$\frac{NOX}{NO_{eq}}[-] = 0{,}0072 \cdot O2[\%] + 0{,}147$	0,51
t_{bed} [°C]	$\frac{NOX}{NO_{eq}}[-] = -0{,}0005 \cdot t[°C] + 0{,}6289$	0,51
$O2_{total}$ [%]	very uncertain correlation – different approach suggested	0,11
Re_p [-]	very uncertain correlation	0,25
r [-]	n/a	n/a

Table 12: Proposed functional dependencies – lignite coal

Parameter	Sugested dependency	R^2 [-]
O2 [%]	$\frac{NOX}{NO_{eq}}[-] = 0{,}0241 \cdot \Delta O2[\%] + 0{,}1991$	0,73
t_{bed} [°C]	very uncertain correlation	0,28
$O2_{total}$ [%]	no correlation	-
Re_p [-]	no correlation	-
r [-]	very uncertain correlation	0,32

It can be noted that the proposed linear functions for primary oxygen concentration O2 [%] have adequate correlation R^2 = 0,51 for wooden pellets and moderately good correlation R^2 = 0,73 for lignite coal. See Figure 33 and Figure 34.

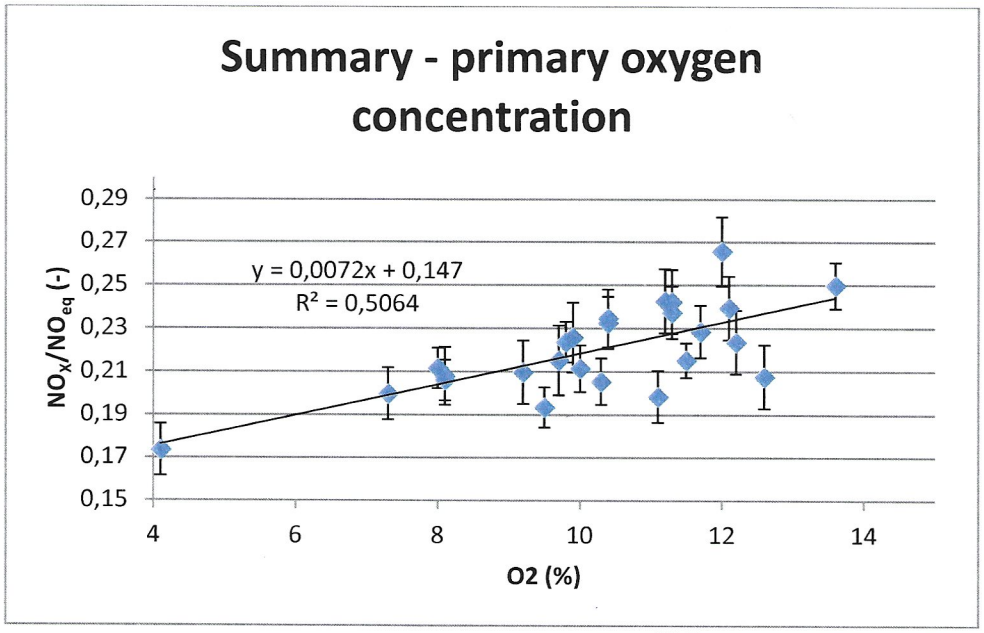

Figure 33: Primary oxygen concentration influence on $\frac{NOX}{NO_{eq}}$ – summary and proposed correlation (wooden pellets)

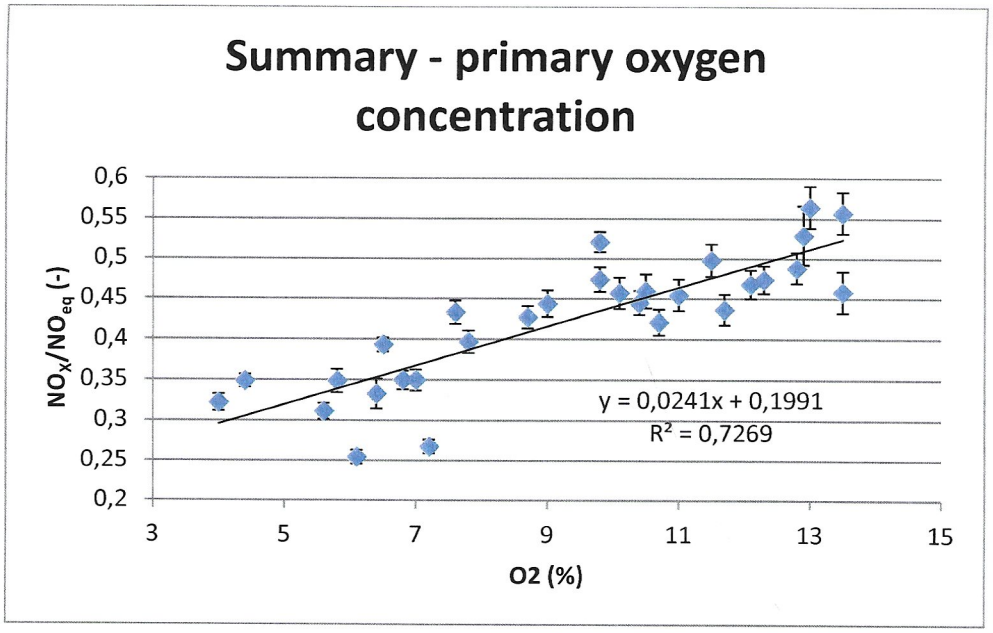

Figure 34: Primary oxygen concentration influence on $\frac{NOX}{NO_{eq}}$ – summary and proposed correlation (lignite coal)

In case of wooden pellets, the proposed linear function for temperature t_{bed} [°C] influence had adequate correlation R^2 = 0,51, probably thanks to:

1) biomass going through complete devolatilization even at lower temperatures and
2) the char structure and amount does not vary significantly with the temperature.

In case of lignite coal, the best cosidered function had very uncertain correlation R^2 = 0,28 probably since the char structure was varying with the temperature (see more detailed discussion in chapter 6.6). See Figure 35 and Figure 36.

It must be noted that the measured dependency is expressing the final stack NO_X emissions, including the processes of devolatilization, fuel/air mixing, NO reduction and others. It should not be confused with the temperature dependency based on stoichiometry.

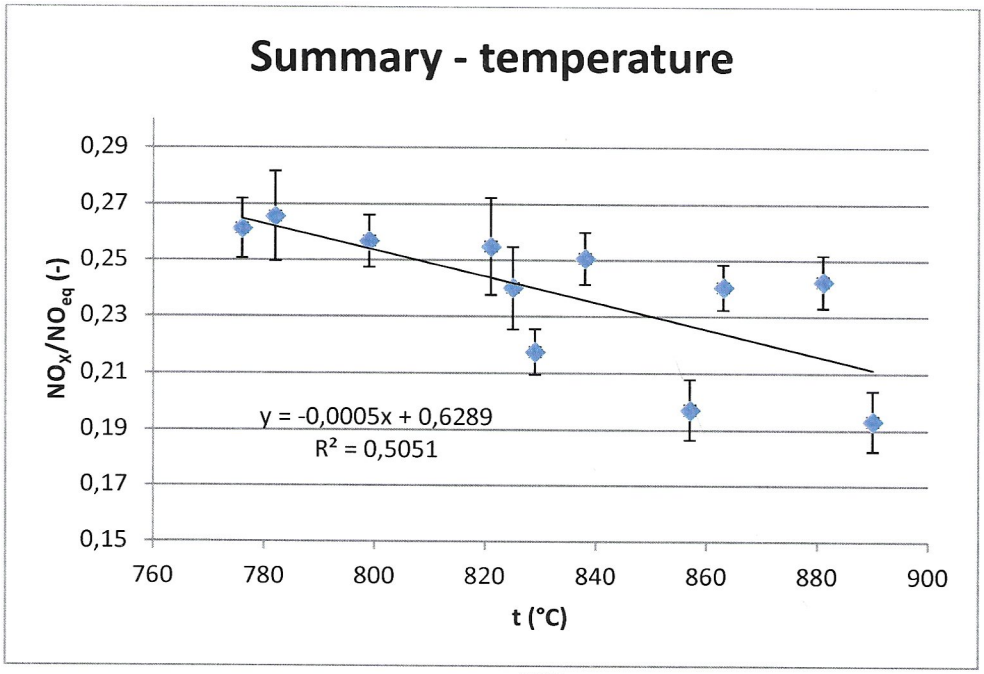

Figure 35: Bed temperature influence on $\frac{NOX}{NO_{eq}}$ – summary of batches 1 – 4 and proposed correlation (wooden pellets)

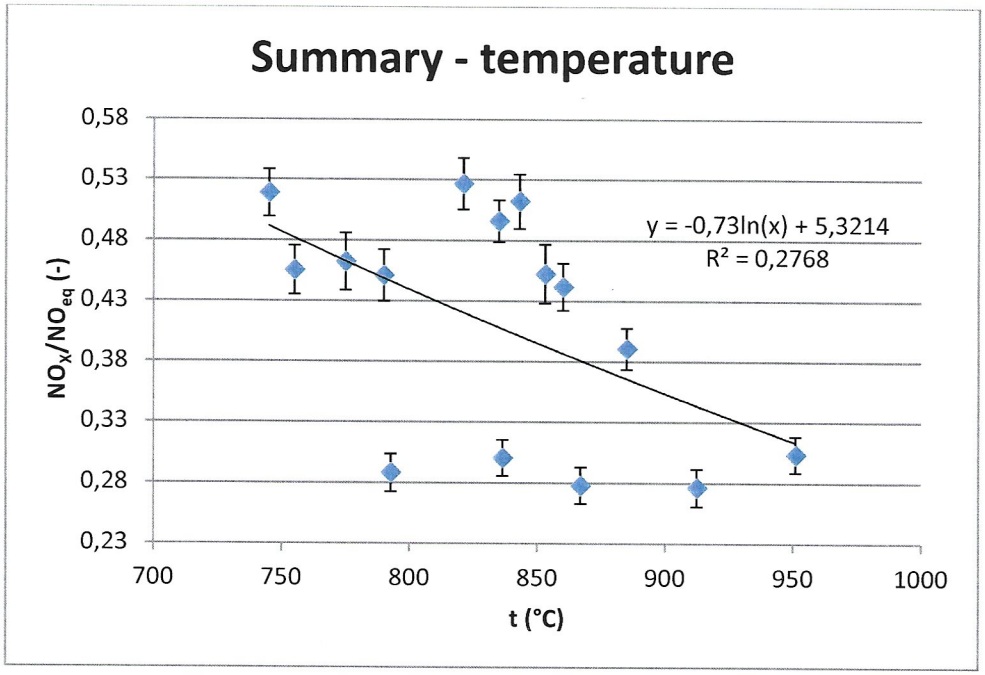

Figure 36: Combustion temperature influence on $\frac{NOX}{NO_{eq}}$ – summary and proposed correlation (lignite coal)

The best obtained functions for total oxygen concentration $O2_{total}$ [%] had very uncertain correlation for wooden pellets R^2 = 0,11 and no correlation for lignite coal R^2 = 0,05. These functions cannot be considered reliable. See Figure 37 and Figure 38.

It is also obvious that the slope of $O2_{total}$ influence on $\frac{NOX}{NO_{eq}}$ was increasing with the $O2$, the concentration of primary oxygen, in case of wooden pellets. See Figure 39. The slope increase is shown in Figure 40. The detailed discussion is provided in chapter 6.6.

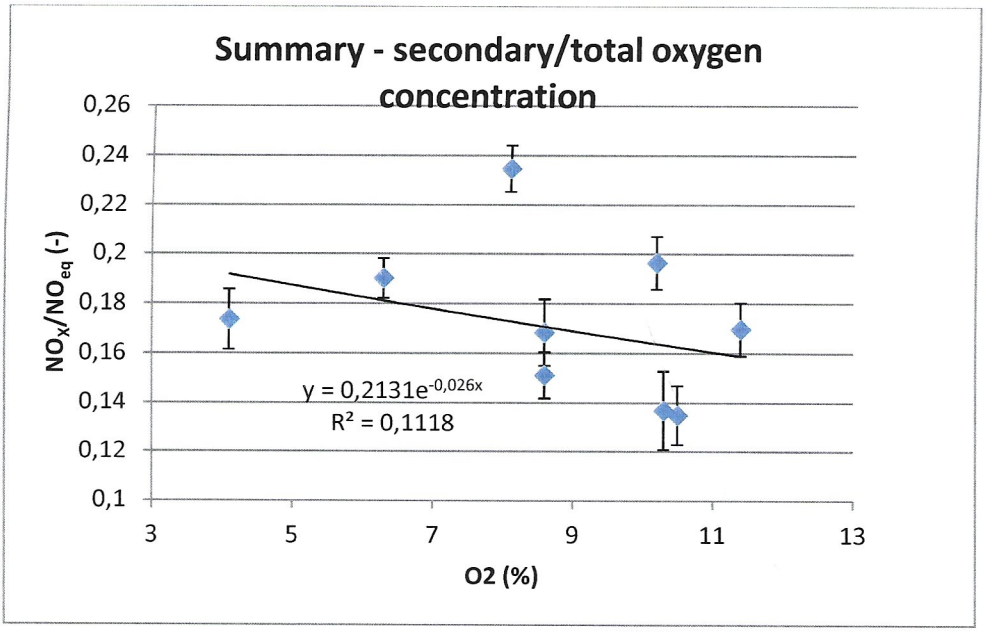

Figure 37: Total oxygen concentration influence on $\frac{NOX}{NO_{eq}}$ – summary and proposed correlation (wooden pellets)

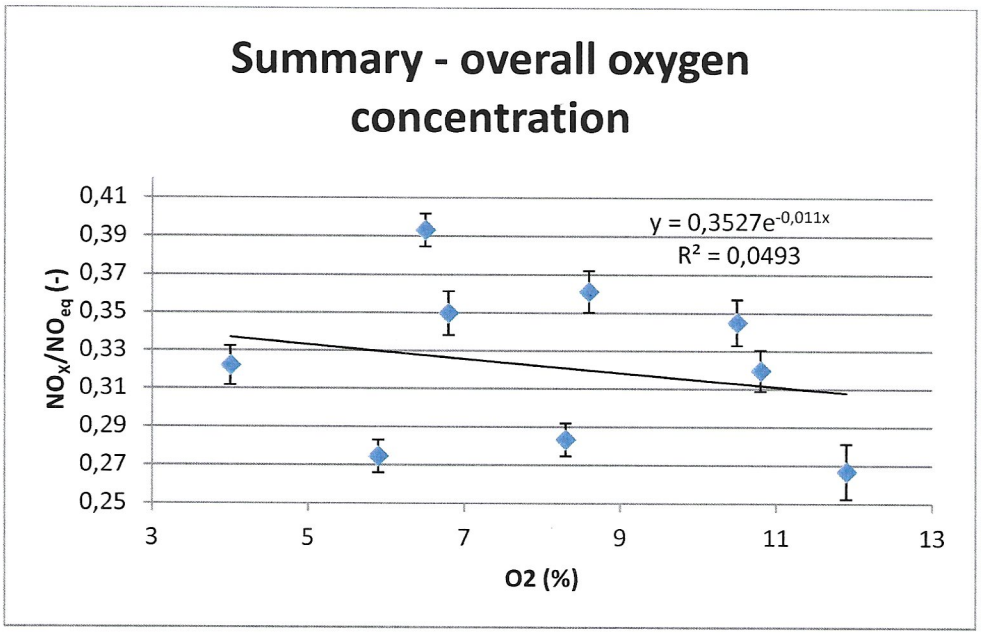

Figure 38: Total oxygen concentration influence on $\frac{NOX}{NO_{eq}}$ – summary and proposed correlation (lignite coal)

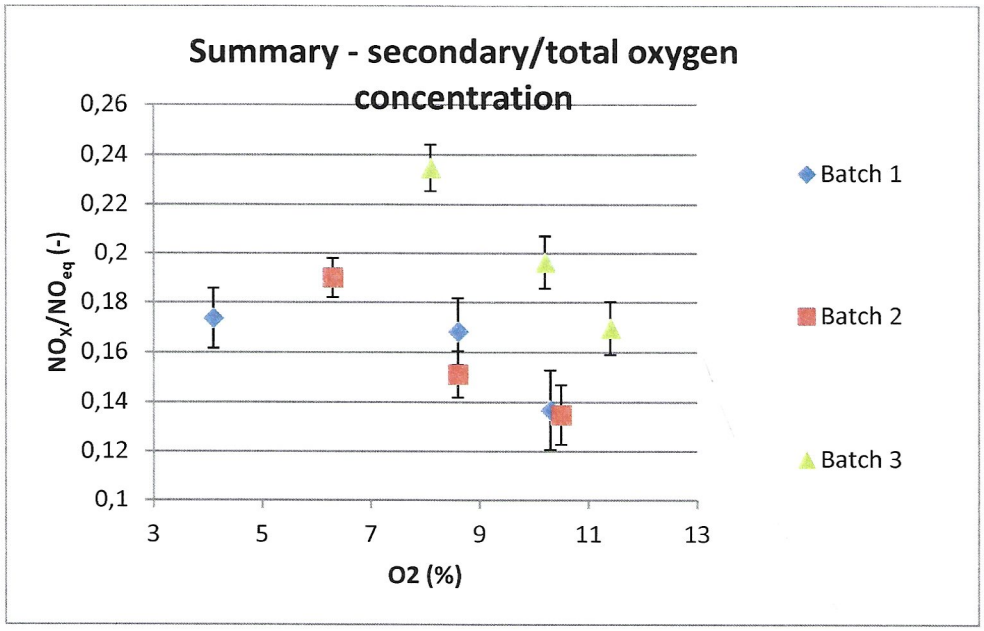

Figure 39: Total oxygen concentration influence on $\frac{NOX}{NO_{eq}}$ – batches 1 - 3 (wooden pellets)

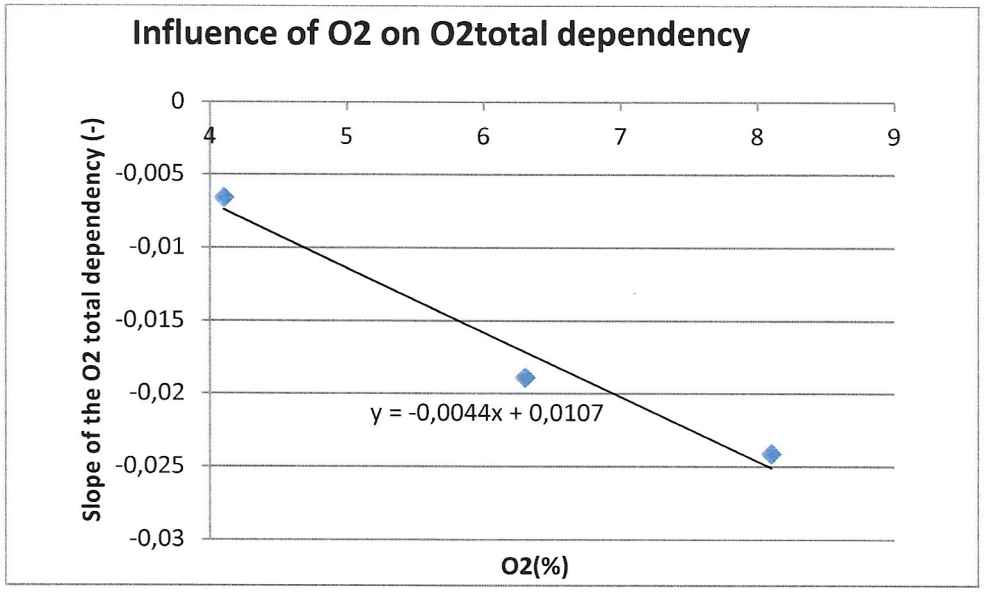

Figure 40: Influence of *O2* on $O2_{total}$ dependency (wooden pellets)

This means that our initial assumption – the independent effect of the parameters – is not valid in case of staged combustion of wooden pellets.

The best obtained function for Re_p [-] show very uncertain correlation in case of wooden pellets R^2 = 0,25, and no correlation in case of lignite coal R^2 = 0,05. See Figure 41 and Figure 42. The reason is the combination of insufficient uniformity of the bed particles and the fact that the influence of Re_p [-] on $\frac{NOX}{NO_{eq}}$ is simply too weak to manifest in a clear way. See discussed in more detail in chapter 6.6.

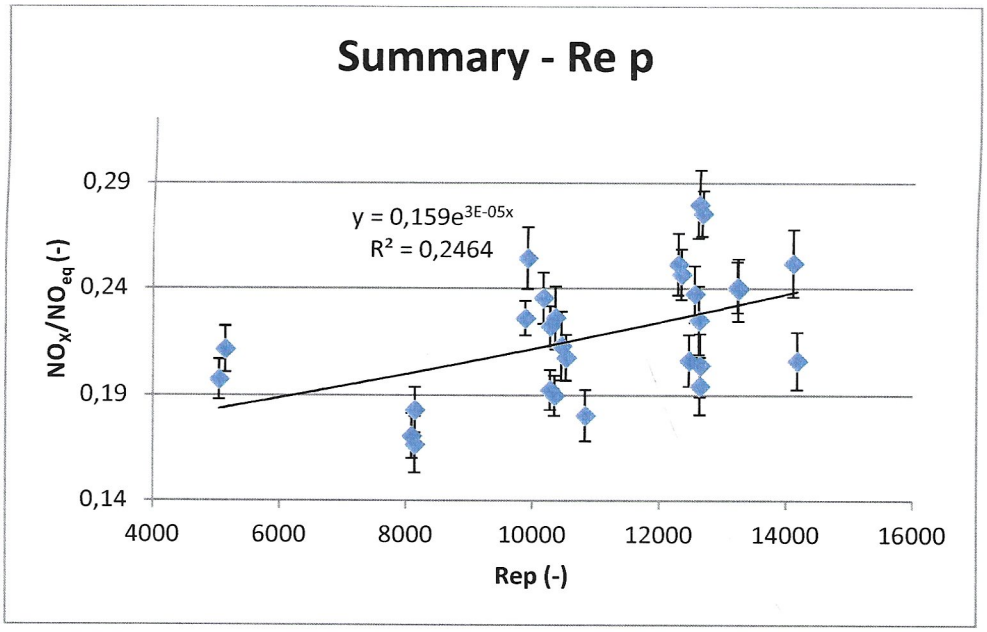

Figure 41: Reynolds number of particles influence on $\frac{NOX}{NO_{eq}}$ – summary and proposed correlation (wooden pellets)

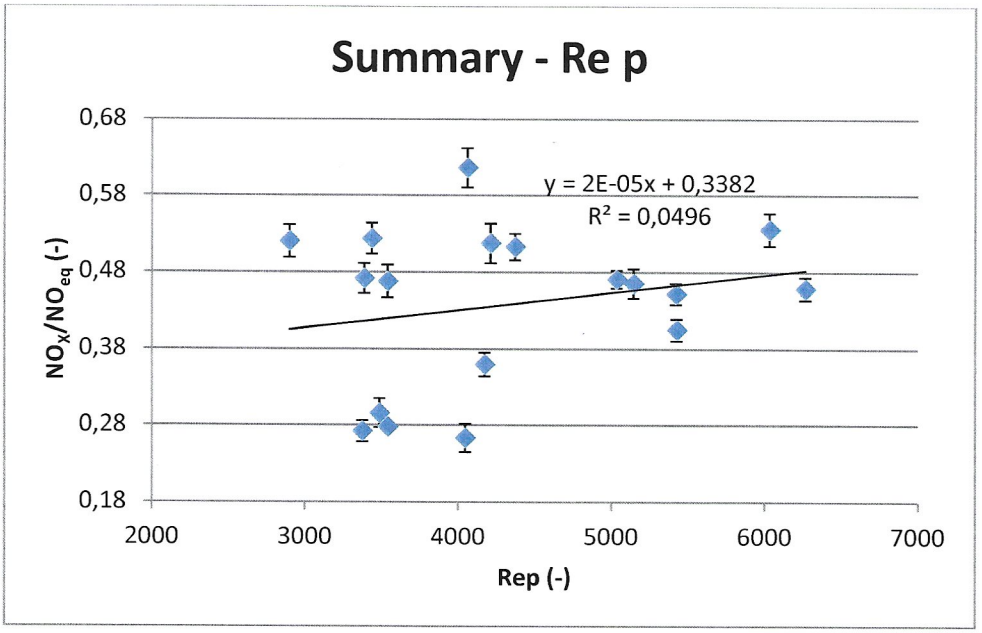

Figure 42: Reynolds number of particles influence on $\frac{NOX}{NO_{eq}}$ – summary and proposed correlation (lignite coal)

The best obtained function for flue gas recirculation coefficient *r* [-] shows very uncertain correlation in case of lignite coal R^2 = 0,32. The reason why the correlation is not higher can be caused by the fact that in this case the primary air flow was varying significantly, and the necessary numerical corrections introduced another uncertainty into the process.

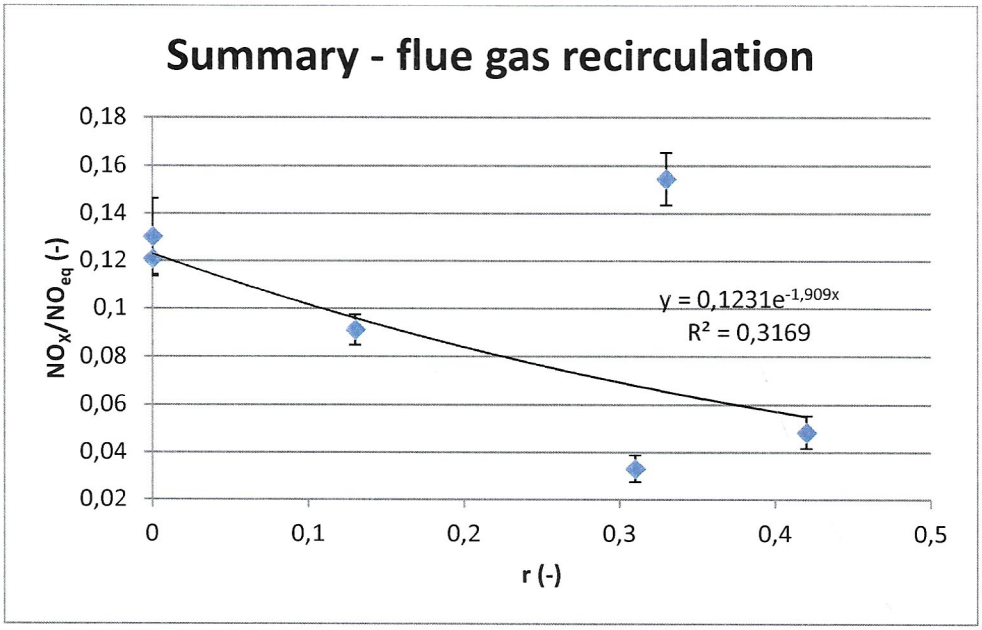

Figure 43: Recirculation influence on $\frac{NOX}{NO_{eq}}$ – summary and proposed correlation (lignite coal)

6.6 Evaluation of results - discussion

After the measurements were done and evaluated, the functional dependencies were proposed. See Table 11 and Table 12 (functional dependencies are limited to the measurement range of combustion parameters that are mentioned in the text).

The maximum equivalent emissions are NO_{eq} = 1046 ppm for wooden pellets and NO_{eq} = 2437 ppm for lignite coal. The measured $\frac{NOX}{NO_{eq}}$ was found in the range of $\frac{NOX}{NO_{eq}}$ = 0,12 – 0,28 for wooden pellets with the higher end being far from optimal combustion conditions. Typical value for combustion conditions close to optimal was $\frac{NOX}{NO_{eq}}$ = 0,12 – 0,15. This was achieved without the flue gas recirculation. With flue gas recirculation even lower number can be expected. This is with accord with the literature review where values $\frac{NOX}{NO_{eq}} \geq 0{,}1$ are considered typical. See chapter 2.3.1.

The measured $\frac{NOX}{NO_{eq}}$ was found in the range of $\frac{NOX}{NO_{eq}}$ = 0,04 – 0,71 for the lignite coal, with the higher end being far from optimal combustion conditions. Typical value for combustion conditions close to optimal was $\frac{NOX}{NO_{eq}}$ = 0,04 – 0,06. Flue gas recirculation had an extremely strong influence - the lowest conversion achieved without flue gas recirculation was $\frac{NOX}{NO_{eq}}$ = 0,28. This is with accord with the literature review where optimized values around $\frac{NOX}{NO_{eq}}$ = 0,05 are considered typical. See chapter 2.3.1.

The value of $\frac{NOX}{NO_{eq}}$ was found linearly increasing with increasing primary air concentration for both fuels with adequate to moderately good correlation with R^2 = 0,51 (wooden pellets) and R^2 = 0,73 (lignite coal). The functional dependency was consistent over several measurements over the whole measurement range, that was $O2$ = 4,1 % - 13,6 % for wooden

pellets and $O2$ = 4 % - 13,5 % for lignite coal. The measurements were done in the temperature range of t_{bed} = 727 – 1032 °C for wooden pellets and t_{bed} =783 – 1076 °C for lignite coal. See Figure 21 and Figure 26 for summary.

This finding is consistent with the literature review where linear increase is also observed, although some authors also proposed logarithmic dependency (the logarithmic dependency was very close to a linear dependency though). See chapter 2.3.1. The slope of linear increase was found to be steeper for lignite coal compared to wooden pellets.

The reason for linear increase of $\frac{NOX}{NO_{eq}}$ with primary oxygen concentration is believed to be the fact that under higher oxygen concentration more complete combustion occurs reducing the CO concentrations. Another effect is faster combustion of fixed carbon in the bed and resulting lowed fixed carbon amount in the fluidized bed. These two effects lead to decrease of NO reduction and thus increase $\frac{NOX}{NO_{eq}}$. This also explains why the slope is steeper for lignite coal compared to wooden pellets – lignite coal has much higher content of fixed carbon.

The value of $\frac{NOX}{NO_{eq}}$ dependency on bed temperature is not as clear and well defined as is the case for oxygen concentration. For wooden pellets $\frac{NOX}{NO_{eq}}$ was found to linearly decrease with adequate consistency with R^2 = 0,51 (if we exclude the measurement done on the different pack of the pellets). See Figure 23 for summary. For lignite coal somewhat more scattered results were obtained over the course of several measurements and a logarithmic function was fitted with R^2 = 0,28. Some measurements indicated decreasing trend while others show no dependency at all over the same measured range. See Figure 27. The measurements were done in the range t_{bed} = 776 – 890 °C for wooden pellets and t_{bed} = 745 – 951 °C for lignite coal. The measurements were done in the oxygen concentration range of $O2$ = 10 – 13,6 % for wooden pellets and $O2$ = 9,8 – 12,4 % for lignite coal and the measurements we numerically corrected to the same oxygen concentration using the previously obtained functional dependencies.

If we look in the literature review the result is not surprising at all. Some authors observed increasing $\frac{NOX}{NO_{eq}}$ with increasing temperature but it was for fuels that were not completely devolatilized under the lower temperatures. This is clearly not the case of biomass or lignite coal. The effect of decreasing $\frac{NOX}{NO_{eq}}$ with increasing combustion temperature can be attributed to two effects – firstly higher active surface of fixed carbon formed under higher temperature (leading to higher NO reduction), and secondly to the catalytic effect the lignite coal ash to NO reduction increase in higher temperatures. The temperature effect on $\frac{NOX}{NO_{eq}}$ is obviously much more complex phenomenon in the case of coal compared to biomass.

The $\frac{NOX}{NO_{eq}}$ was found decreasing with increasing total oxygen concentration for both fuels. Exponential functions were the best fit in both cases with very uncertain correlation (R^2 = 0,11) for wooden pellets and no correlation (R^2 = 0,05) for lignite coal. The dependency was found to be strongly influenced by the primary oxygen concentration in case of wooden pellets. See Figure 39. The slope of the dependency is getting steeper with increasing primary oxygen concentration for wooden pellets. On the other hand, the trend was found independent on primary oxygen concentration for lignite coal. See Figure 28. The measurements were done for primary oxygen concentrations $O2$ = 4,1 – 8,1 % and total oxygen concentration $O2_{total}$ =

4,1 – 11,4 % for wooden pellets. The measurements were done for primary oxygen concentrations $O2$ = 4 – 6,8 % and total oxygen concentration $O2_{total}$ = 4 – 11,9 % for lignite coal. The measurements were done in the temperature range of t_{bed} = 966 – 1032 °C for wooden pellets and t_{bed} = 959 – 1064 °C for lignite coal. The measurements were numerically corrected to the same primary oxygen concentration using the previously obtained functional dependencies.

This observation is quite interesting. In the literature the measurements of secondary air influence on NO_X emissions were done in order to keep the total oxygen concentration constant, in other words increasing secondary oxygen concentration led to decreased primary oxygen concentration. The observed effect of decreased NO_X emissions was then attributed to the decrease in primary air concentration. The conclusion from the literature is that introducing secondary air allows us to decrease primary air thus decreasing the NO_X concentrations. No effect of secondary air alone was observed or even attempted. However, this work was observing the effect of secondary air/oxygen concentration change while the primary air/oxygen concentration was kept stable. Since the secondary air is introduced above the bed the explanation of the NO_X emissions decrease must lie in some other effect. Moreover, the NO_X decreased even though a significant drop of CO was observed after the secondary air introduction. The explanation must lie in the freeboard processes. There are 3 hypotheses suggested, that were taken under consideration:

1) Introducing the secondary air from multiple nozzles causes more intense mixing of the flue gas. This increased mixing is the cause of increased NO reduction despite the CO drop.
2) The reduction on the surface of entrained solids.
3) The independent effect of parameters principle, that was adopted in the beginning, is not true for the case of staged combustion.

The hypotheses 1 and 2 are not very likely since the influence of CO concentration is extremely strong and the freeboard reduction on entrained solids is reported to be negligible in the literature. The most probable cause is the non-applicability of the independent effect of parameters that gives misleading results when the parameter is investigated separately.

It is also important to note that introduction of secondary air in different height above the bed would most likely lead to a different dependency and the proposed dependency is limited to this one single height of secondary air injection – this information is based on literature review and was not tested.

Another observed phenomenon was the sensitivity to primary oxygen in case of wooden pellets, which was not observed in case of lignite coal. The answer to this effect is probably again the non-applicability of the independent effect of parameters in case of primary/secondary air mixtures.

The value of $\frac{NOX}{NO_{eq}}$ was found increasing with increasing Reynolds number of particles for wooden pellets. See Figure 25. Exponential function was fitted; however, the correlation was very uncertain with R^2 = 0,25. The dependency is more consistent compared to lignite coal, where no correlation (R^2 = 0,05) was achieved by a linear function. In case of lignite coal, the measured points are extremely scattered to the point that no reliable correlation can be concluded. The measurements were done for Reynolds number of particles Re_p = 5043 – 14 464 for wooden pellets and Re_p = 2897 – 6264 for lignite coal. The measurements were

done in the temperature range of t_{bed} = 727 – 972 °C for wooden pellets and t_{bed} = 736 – 974 °C for lignite coal and in the oxygen concentration range of $O2$ = 7,3 – 13,6 % for wooden pellets and $O2$ = 5,8 – 13,5 % for lignite coal. The measurements we numerically corrected to the same primary oxygen concentration using the previously obtained functional dependencies.

The reason that the dependency of $\frac{NOX}{NO_{eq}}$ on Re_p was more consistent for wooden pellets and extremely incoherent for lignite coal is the bed material size distribution consistency and the corresponding type of flow.

As was stated earlier the wooden pellets were combusted in the bed of ceramic balls with diameters ranging from 0 – 2 mm. The representative diameter was determined to be d = 1,2 mm and the actual diameter of particles was from very narrow range around the representative diameter. Also, all the particles had more or less spherical shape. The value of Reynolds number of particles was Re_p = 5043 – 14 464. This means in case for wooden pellets combustion virtually all the bed particles were safely in the turbulent flow regime. This leads to more consistent results.

On the other hand, lignite coal was combusted in the bed of its own ash. Even though the largest particles were removed by sieving, the rest of the particles still had very wide range of diameters. Also, the shape of particles was much more non-spherical. The value of Reynolds number of particles was lower, only Re_p = 2897 – 6264. The lower Re_p in combination with wider distribution of particles sizes and shapes probably lead to significant number of particles being in transient or even laminar flow regime. This probably caused the unpredictability of the results and inability to clearly define a trend of the dependency in case of lignite coal.

It is also obvious that the dependency of $\frac{NOX}{NO_{eq}}$ on Re_p is quite weak compared to other investigated dependencies. This fact also contributed to decreasing the correlation of proposed functions.

The value of $\frac{NOX}{NO_{eq}}$ was found decreasing with increasing recirculation for lignite coal. Exponential function was proposed with R^2 = 0,32. In case of wooden pellets, no stable state with recirculation was achieved. The dependency that was observed for lignite coal is quite well defined and clear. The measurements were done for r in range of r = 0 – 0,42. The measurements were done in the temperature range of t_{bed} = 870 – 948 °C and in the oxygen concentration range $O2$ = 3,9 – 7,8 % for lignite coal. The measurements we numerically corrected to the same primary oxygen concentration using the previously obtained functional dependencies.

The reason flue gas recirculation is decreasing the NO emission is well discussed in literature. Many authors often argument that the reduction of NO emissions is due to longer residence time in the bed – where reduction occurs. This is true if the total gas velocity is kept constant. In other word when the recirculation is introduced the primary air flow rate is decreased. In that case also the cumulative influence of lower primary oxygen concentration is observed. This work was observing the effect of flue gas recirculation while the primary air was kept constant. In other words, as the recirculation was introduced the total flow rate through the bed and the gas velocity increased. This means that the residence time of the flue gas in the bed remained constant. The effect observed in this work cannot be contributed to the decrease of primary air or to the increase of residence time on the bed. The observed effect must be attributed to other causes like increased CO_2 concentration and increased concentration of water. They both react with the char contained in the bed. CO_2 forms CO after

the reaction with char and water forms H_2. This increases the NO reduction in the bed significantly.

Viewing the obtained experimental values and proposed correlations from the viewpoint of the dimensional analysis we can conclude that the results are not surprising. Given the large number of parameters influencing the process of NO_X formation (and reduction) and given the complexity of the whole process it is indeed difficult to find some clear dependencies and correlations. The literature review confirms this finding as many publications mentioned in chapter 2.3 reported contradictory results. Yet the dimensional analysis remains a convenient tool for analysing and investigating the potential influencing parameters.

It also needs to be noted that some variations and inconsistencies in the resulting measured trends can be caused by the differences in stability of measured states. There were significant differences in stability of measured states as is noted in chapter 6.4 (Figure 31 and Figure 32). Some states were very stable with very low fluctuations in parameters and very low standard deviation of measured NO_X concentration, while other states showed large fluctuations in combustion parameters and the standard deviation of measured NO_X concentration was high. This phenomenon – the stability of the measured state – could have influenced the evaluation of measured values and introduce additional uncertainty.

7 Conclusion

The issue of NO_X formation during the combustion of solid fuels (coal and biomass) in the fluidized bed combustors and the possibility of NO_X emission prediction are examined in the presented work.

The theoretical approach was made to identify influential parameters for use in empirical models by the means of dimensional analysis. Two previous attempts of theoretical approach to this problematic were found in the literature, see page 52. The dimensional analysis seems as a fitting tool. The process of NO_X formation was separated in three fields – kinetic, hydrodynamic and heat transfer processes – that were investigated separately. Dimensionless parameters were proposed including Reynolds number of particles, Froud number and others. (I.)

Modifications were proposed to the current empirical models, used for NO_X prediction for pulverized coal combustors, to be applicable to fluidized bed combustors. Pohl´s and Ibler´s models were used. The data from commercial fluidized bed combustors used in combined heat and power plants were obtained and used to propose the model modifications. Satisfactory results were obtained for the modified Ibler´s model if limited to single fuel type combustion (lignite coal). The proposed modified model is of course far from being validated given the small sample size. (II.) (III.)

The most extensive part of the work was the experimental investigation of selected influential parameter´s influence on NO_X emissions. Five measurement groups were made to investigate the following parameters – primary oxygen concentration, combustion temperature, total oxygen concentration in case of air staging, Reynolds number of bed particles and flue gas recirculation coefficient. During each measurement group the investigated parameter was varied while other parameters were kept constant if possible.

In case of lignite coal, the optimal conversion of fuel nitrogen was $\frac{NOX}{NO_{eq}} = 0{,}04 - 0{,}06$. The most significant parameter influencing the NO_X emissions was the flue gas recirculation coefficient (power of 10^{-1}), followed by the primary oxygen concentration (power of 10^{-2}). The significance of total oxygen concentration in case of air staging was relatively low (power of 10^{-3}) and almost no influence was observed for bed temperature (power of 10^{-4}) and Reynolds number (power of 10^{-5}).

In case of biomass, the optimal conversion of fuel nitrogen was $\frac{NOX}{NO_{eq}} = 0{,}12 - 0{,}15$ (without recirculation, if the recirculation would be possible the conversion is expected to drop to cca 0,1). The most significant parameter influencing the NO_X emissions was the combination of primary oxygen concentration and total oxygen concentration in case of air staging (power 10^{-2} to 10^{-3}). It was concluded that in this case the principle of independent effect of parameters does not apply and both parameters must be evaluated together. The significance of bed temperature and Reynolds number was extremely low (power 10^{-4}, and 10^{-7}).

Dependencies were proposed, see Table 11 and Table 12, when sufficiently reliable correlation was found.

Further research activities following the publication of this work should be aimed at exploring the parameters proposed by the dimensional analysis that were not experimentally investigated by this work. The proposed empirical models can be validated for the data not included in the original fit. Based on the presented knowledge new empirical models and model corrections for prediction of NO_X emissions in fluidized bed combustors could be proposed.

References

1. Kaltschmitt, M. *Energie aus Biomasse, Grundlagen, Techniken und Verfahren.* ISBN 978-3-662-47437-2 : Springer Berlin Heidelberg, 2009.

2. Černý, V. *Spalovací zařízení a výměníky tepla.* Prague : Edition center CTU, 1986.

3. Kunii, D. a Levenspiel, O. *Fluidization engineering.* ISBN 9780409902334 : Butterworth-Heinemann, 1991.

4. Teyssler, J. *Spalování popelnatých hnědých uhlí.* Praha : Státní nakladatelství technické literatury, 1988.

5. Vyhláška 415/2012 o přípustné úrovni znečišťování a jejím zjišťování a o provedení některých dalších ustanovení zákona o ochraně ovzduší. *Sbírka zákonů ČR.* 2014.

6. Miller, J. A. and Bowman, C. T. Mechanism and modeling of nitrogen chemistry in combustion. *Prog. Energy Combust. Sci.* 1989, Vol. 15, pp. 287 - 338.

7. Thomas, K. M. The release of nitrogen oxides during char combustion. *Fuel 76.* 1997, pp. 457 - 473.

8. Williams, A., et al. A review of NOx formation and reduction mechanisms in combustion systems, with particular reference to coal. *Journal of the institute of energy 70.* 1997, pp. 102 - 113.

9. Winter, F., Wartha, C. a Hofbauer, H. NO and N2O formation during the combustion of wood, straw, malt, waste and peat. *Bioresource Technology 70.* 1999, pp. 39 - 49.

10. Hupa, M. Chemistry of biomass and waste derived fuels - highlights and problems. Fuel quality impacts : conference, 2012.

11. Hayhurst, A. N. a Lawrence, A. D. The amounts of NOx and N2O formed in a fluidized bed combustor during the burning of coal volatiles and also of char. *Combustion and flame 105.* 1996, pp. 341 - 357.

12. Johnson, Jan E. Formation and reduction of nitrogen oxides in fluidized-bed combustion. *Fuel.* 1994, pp. 1398 - 1415.

13. Pereira, F. J., et al. NOx emissions from fluidized-bed coal combustors. *Symposium (International) on combustion.* 1975, Vol. 15, pp. 1149 - 1156.

14. Mahmoudi, Shiva, Baeyens, Jan and Seville, J.P.K. NOx formation and selective non-catalytic reduction (SNCR) in a fluidized bed combustor of biomass. *Biomass and energy 34.* 2010, pp. 1393 - 1409.

15. Åmand, L. E. a Leckner, B. Influence of Fuel on the Emission of Nitrogen Oxides (NO and N2O) From an 8-MW Fluidized Bed Boiler. *Combustion and Flame 84.* 1991, pp. 181 - 196.

16. Hampartsoumian, E. and Gibbs, B. M. NOx formation and reduction in fluidized bed combustors. *Journal of the Institute of energy.* 1984, Vol. 57, pp. 402 - 410.

17. Hayhurst, A. N. a Lawrence, A. D. The effect of solid CaO on the production of NOx and N2O in fluidized bed combustors: studies using pyridine as a prototypical nitrogenous fuel. *Combustion and flame 105.* 1996, pp. 511 - 527 .

18. Lin, Weigang, Valkenburg, J. M. a van den Bleek, Cor M. Prediction of NOx and SOx emissions in FBC of coal using easy to determine coal and sorbent characteristics. *Fuel Processing Technology 24.* 1990, pp. 399 - 405.

29. Rodriguez-Mirasol, J., et al. NO and N2O decomposition over coal char at fluidized-bed combustion conditions. *Combustion and flame 99.* 1994, pp. 499 - 507.

20. Makarytchev, S. V., et al. Catalyzed NOx formation under fluidized-bed combustion conditions. *Chemical engineering science 15.* 1995, pp. 2489 - 2490.

21. Åmand, L. E. a Leckner, B. Influence of air supply on the emissions of NO and N2o from a circulating fluidized bed boiler. *Twenty-Fourth Symposium (International) on Combustion.* 1992, pp. 1407 - 1414.

22. Lin, Weigang, et al. Modelling CO2 and NOx emissions in fluidized bed combustion of coal. *Fuel.* 1993, pp. 299 - 304.

23. Lu, Yong, Hippinen, Ilkka a Jahkola, Antero. Control of NOx and N2o in pressurized fluidized-bed combustion. *Fuel.* 1995, pp. 317 - 322.

24. Findlay, K. a Probert, S. D. Limiting NOx and SOx emissions from industrial-size fluidised-bed combustor. *Applied energy 45.* 1993, pp. 1 - 99.

25. Gulyurtlu, I. K., Bordalo, C. a Cabrita, I. A. The effect of staging of reburning fuel to reduce NOx and N2O levels during fluidised bed coal combustion. *Fluidized bed combustion - Volume 2.* 1995, pp. 1351 - 1357.

26. Winter, F., et al. The NO and N2O formation mechanism during devolatilization and char combustion under fluidized-bed conditions. *Twenty-sixth Symposium (International) on Combustion.* 1996, pp. 3325 - 3334.

27. de Diego, L. F., et al. Influence of operating parameters on NOx and N2O axial profiles in a circulating fluidized bed combustor. *Fuel, Vol 75, No. 8.* 1996, pp.y 971 - 978.

28. Skreiberg, Ø., et al. Kinetic NOx modelling and experimental results from single wood particle combustion. *Fuel 76.* 1997, pp. 671 - 682.

29. Köpsel, R. F. W. a Halang, S. Catalytic influence of ash elements on NOx formation in char under fluidized bed conditions. *Fuel vol. 76, no. 4.* 1997, pp. 345 - 351.

30. Hosoda, H., et al. NOx and N2O emission in bubbling fluidized-bed coal combustion with oxygen and recycled flue gas: Macroscopic characteristics of their formation and reduction. *Energy and Fuels 12.* 1998, pp. 102 - 108.

31. Pilawska, M., et al. The production of nitric oxide during the combustion of methane and air in a fluidized bed. *Combustion and flame 127.* 2001, pp. 2181 - 2193.

32. Valentim, B., et al. Combustion ctudies in a fluidised bed - the link between temperature, NOx and N2O formation, char morphology and coal type. *International Journal of Coal Geology 67.* 2006, pp. 191 - 201.

33. Duan, L., et al. Effects of operation parameters on NO emission in an oxy-fired CFB combustor. *Fuel Processing Technology 92.* 2011, pp. 379 - 384.

34. Toftegaard, M. B., et al. Oxy-fuel combustion of solid fuels. *Progress in energy and combustion science 36.* 2010, pp. 581 - 625.

35. Pohl, J.H., et al. Correlation of NOx emissions with basic physical and chemical characteristics of coal. *Proc. Joint Symposium on Stationary Combustion NOx Control.* 1983.

36. Gungor, A. Prediction of SO2 and NOx emissions for low-grade Turkish lignites in CFB combustors. *Chemical engineering journal 146.* 2009, pp. 388 - 400.

37. Horio, M., Mori, S. a Muchi, I. A model study for the development of low NOx fluidized-bed coal combustors. *The rpoceedings of the fifth international conference on fluidized bed combustion.* 1977, pp. 605 - 623.

38. Rajan, R.R. a Wen, C.Y. A comprehensive model for fluidized bed coal combustors. *AIChE journal (Vol.26, No.4).* 1980, pp. 642 - 655.

39. Beér, J.M. a Lee, Y.Y. No formation and reduction in fluidized bed combustion of coal. *Journal of the institute of energy.* 1981, pp. 38 - 47.

40. Lin, W., Valkenburg, P.J.M. a Van den Bleek, C.M. Prediction of NOx and SOx emissions in FBC of coal using easy to determine coal and sorbent characteristics. *Fuel processing technology 24.* 1990, pp. 399 - 405.

41. Goel, S., et al. Emissions of nitrogen oxides from circulating fluidized-bed combustors: modeling results using detailed chemistry. *Twenty-sixth Symposium (International) on Combustion.* 1996, pp. 3317 - 3324.

42. Jensen, A. a Johnsson, J.E. Modelling of NOx emissions from pressurized fluidized bed combustion - a parameter study. *Chemical engineering science, Vol.52, No. 11.* 1997, pp. 1715-1731.

43. Löffler, G., et al. NOx and N2O formation mechanism - A detailed chemical kinetic modeling study on a single fuel particle in a laboratory-scale fluidized bed. *16th internation conference on FBC.* 2001, pp. 228 - 235.

44. Pohl, J.H., et al. The influence of fuel properties and boiler design and operation on NOx emissions. *Joint symposium on stationary combustion NOx control.* 1987, pp. 24-28.

45. Juniper, L.A. a Pohl, J.H. Techniques to control NOx emissions from australian coal-fired boilers. *1st Australian Flame Days.* 1990.

46. Juniper, L. a Holcombe, D. Formation and control of NOx emissions from coal fired boilers. *AIE seminar on clean use of coal.* 1992.

47. Bennet, P.A. NOx prediction research report 20. *Final report of Cooperative research centre for black coal utilization.* 2001.

48. Ibler, Z. a Karták, J. *Technický průvodce energetika.* Praha : Nakladatelství BEN, 2002.

49. Ibler, Z. Modely výpočtů emisí oxidů dusíku při spalování fosilních paliv. *Energetika 40.* 1990, pp. 344-347.

50. Metodika opredelenija vybrosov okislov azota s dymovymi gazami kotlov. *Sojuztechenergo.* MU 34-70-051-83 1984.

51. ČEPS web site. [Online] 2018. [Cited: 8 march 2018.] http://www.ceps.cz/cs/data#Generation.

52. Štefanica, J. a Hrdlička, J. Charakteristika bublinkové fluidní vrstvy pro kotel na biomasu - master thesis. Prague : CTU in Prague, Faculty of Mechanical Engineering, 2011.

53. Matsen, J.M. Scale-up of fluidized bed processes: Principle and practise. *Powder Technology.* 1996, pp. 237 - 244.

54. Kožešník, J. *Teorie podobnosti a modelování.* Praha : Academia, 1983.

55. Leckner, B., Szentannai, P. a Winter, F. Scale-up of fluidized-bed combustion - A review. *Fuel 90.* 2011, pp.y 2951-2964.

56. Hrdlička, J., Skopec, P., Opatřil, J., Dlouhý, T. Oxyfuel combustion in a bubbling fluidized bed combustor. *Energy Proceedia 116.* 2016, pp. 116 - 123.

57. Skopec, P., Hrdlička, J., Vodička, M., Pilař, L., Opatřil, J. Combustion of Lignite Coal in a Bubbling Fluidized Bed. *Energy proceedia.* 2017, pp. 600 - 607.

58. Opatřil, J., Hrdlička, J. Citlivost součinitele přestupu tepla ve fluidní vrstvě na použitý střední průměr částic. Energie z Biomasy *XVI.* Lednice : ISBN 978-80-214-5286-2, 2015.

59. Vybíral, B. Zpracování dat fyzikálních měření. downloaded 22.3.2018 from: http://fyzikalniolympiada.cz/texty/mereni.pdf.

60. Krzywanski J., Rajczyk R., Nowak W. Model Research of Gas Emissions from Lignite and Biomass Co-combustion in a Large Scale CFB Boiler. *Chemical and Process Engineering 35 (2).* 2014, pp. 217 – 231.

61. Zhou H., Huang Y., Guiyuan M., Liao Z., Cen K. Experimental investigations of the conversion of fuel-N, volatile-N and char-N to NO_X and N_2O during single coal particle fluidized bed combustion. *Journal of the energy institute 90.* 2017, pp. 62 – 72.

62. Xu M., Li S. Experimental study on N_2O emissions in O_2/CO_2 combustion with high oxygen concentration in circulating fluidized bed. *Journal of the Energy Institute 92*. 2019, pp. 128 – 135.

63. Li P.-W., Chyang C.-S. A comprehensive study on NOX emissions and fuel nitrogen conversion of solid biomass in bubbling fluidized beds under staged combustion. *Journal of the energy institute, https://doi.org/10.1016/j.joei.2019.02.007*. Cited 24.7.2019.

64. Li P.-W., Chyang C.-S., Ni H.-W. An experimental study of the effect of nitrogen origin on the formation and reduction of NO_X in a fluidized-bed combustion. *Energy 154*. 2018, pp. 319 – 327.

65. Liukkonen M., Hiltunen T., Halikka E., Hiltunen Y. Modeling of the fluidized bed combustion process and NOX emissions using self-organizing maps: An application to the diagnosis of the process states. *Environmental Modeling and Software 26*. 2011, pp. 605 – 614.

66. Wei X., Guo X., Li S., Han X., Schnell U., Scheffknecht G., Risio B. Detailed Modeling of NOX and SOX Formation in CO-combustion of Coal and Biomass with Reduced Kinetics. *7th symposium on Coal Combustion*. 2011, pp. 3117 – 3124.

67. Selcuk N., Ozkan M. Simulation of circulating fluidized bed combustors firing indigenous lignite. *International Journal of Thermal Sciences 50*. 2011, pp. 1109 – 1115.

68. Kilpinen P., Kallio S., Konttinen J., et al. Towards a quantitative understanding of NO_X and N_2O emission formation in full-scale circulating fluidized bed combustors. *In proceedings of the 16th International Conference on Fluidized Bed Combustion*. 2001.

69. Winter F., Loffler G., Wartha Ch. Hofbauer H., Preto F., Anthony E. J. The NO and N_2O Formation Mechanism under Circulating Fluidized Bed Combustor Conditions: from the Single Particle to the Pilot-Scale. *The Canadian Journal of chemical engineering 77*. 1999, pp. 275 – 283.

70. Afacan O., Gogebakan Y., Selcuk N. Modeling on NOX emissions from fluidized bed combustion of high volatile lignites. *Combustion Ccience and Technology 179*. 2007, pp. 227 – 247.

71. Čangourská M., Příhoda M., Brestovič T. Modeling of nitrogen oxides formation applying dimensional analysis. *Chemical and Process Engineering 32 (3)*. 2011, pp. 175 – 184.

72. Čangourská M., Příhoda M., Koško M. Modeling of Nitrogen Oxides Production during Wood Combustion. *Acta Mechanica Slovaca 16(1)*. 2012, pp. 18 – 25.

Published papers

I. **Štefanica, J., Hrdlička, F., Petr, V.** Využití dimenzionální analýzy pro predikci NO_X ve fluidních kotlích. *Energie z Biomasy XIV.* Lednice : ISBN 978-80-214-4775-2, 2013, pages 79 – 83.

II. **Štefanica, J. a Hrdlička, J.** NO_X PREDICTION FOR FBC BOILERS USING EMPIRICAL MODELS. *Acta Polytechnica 54(1).* 2014, pages 68 - 73.

III. **Štefanica, J., Hrdlička, J., Skopec, P., Opatřil, J., Pilař, L.** PREDICTION OF NO_X EMISSIONS FOR FBC BOILERS BY EMPIRICAL MODELS – THE INFLUENCE OF SCALE-UP. *The Holistic Approach to Environment 6.* 2016, pages 189-199.

The experimental measurements and findings presented in Chapter 6 have not been published yet. Their publication is expected in 2019/2020.

List of appendices:

1) Measurement evaluation of wooden pellets
2) Measurement evaluation of lignite coal

Electronic appendices

1) Dissertation (.pdf)
2) Measurement data (excel)
3) Evaluation of results (excel)

Appendix 1 – Measurement evaluation of wooden pellets

1) *Primary oxygen concentration, Measurements batch 1 – 3*

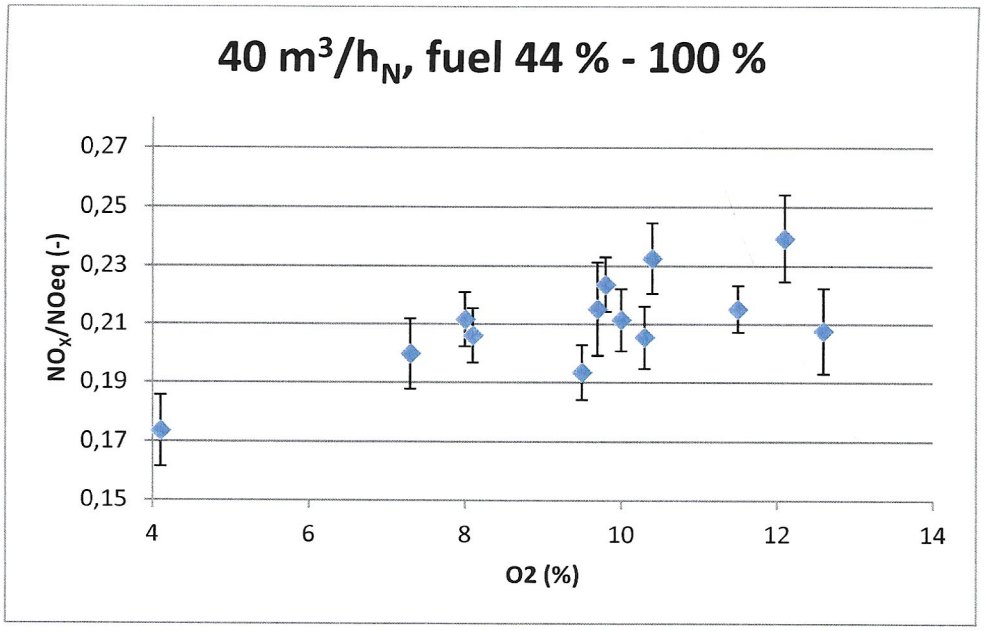

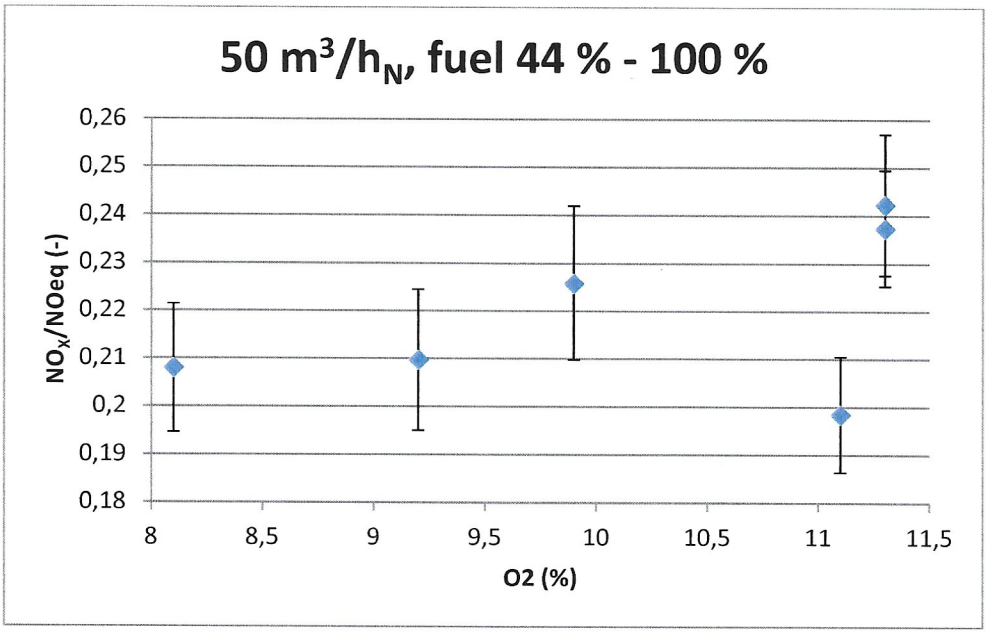

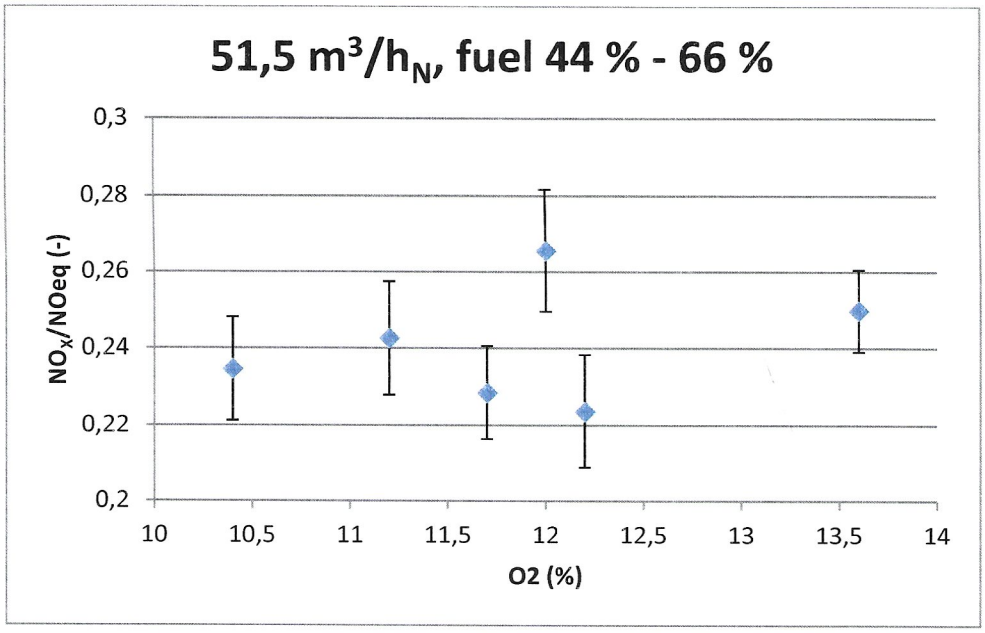

2) Temperature, measurements batch 1 - 3

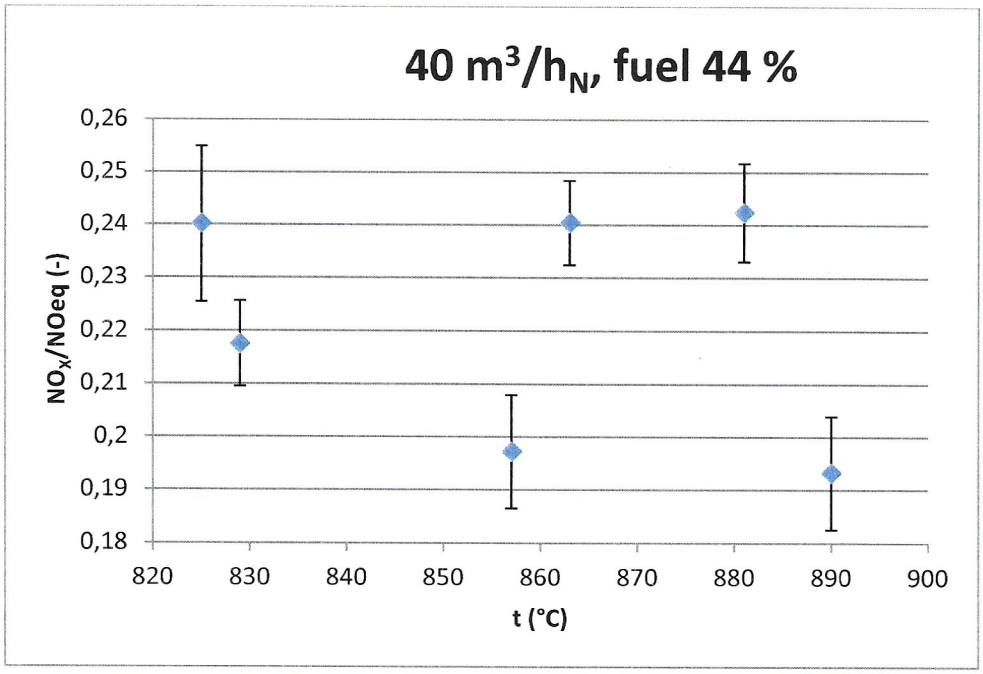

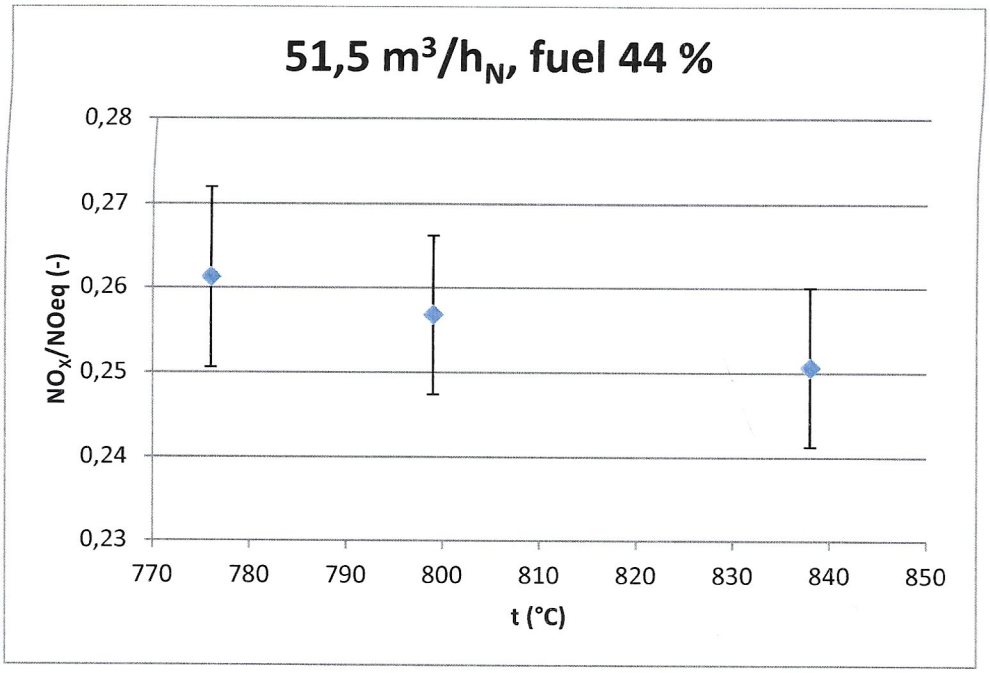
51,5 m³/h_N, fuel 44 %
0,28
0,27
0,26
0,25
0,24
0,23
NO_X/NOeq (-)
770
780
790
800
810
820
830
840
850
t (°C)

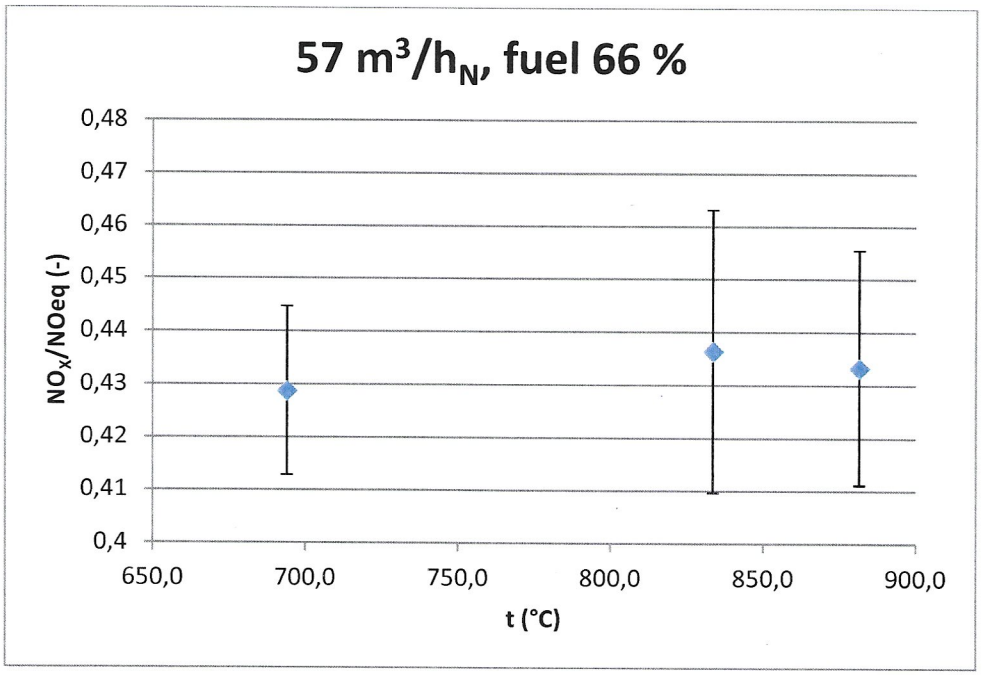
57 m³/h_N, fuel 66 %
0,48
0,47
0,46
0,45
0,44
0,43
0,42
0,41
0,4
NO_X/NOeq (-)
650,0
700,0
750,0
800,0
850,0
900,0
t (°C)

3) Total oxygen concentration (air staging) – measurements batches 1 - 3

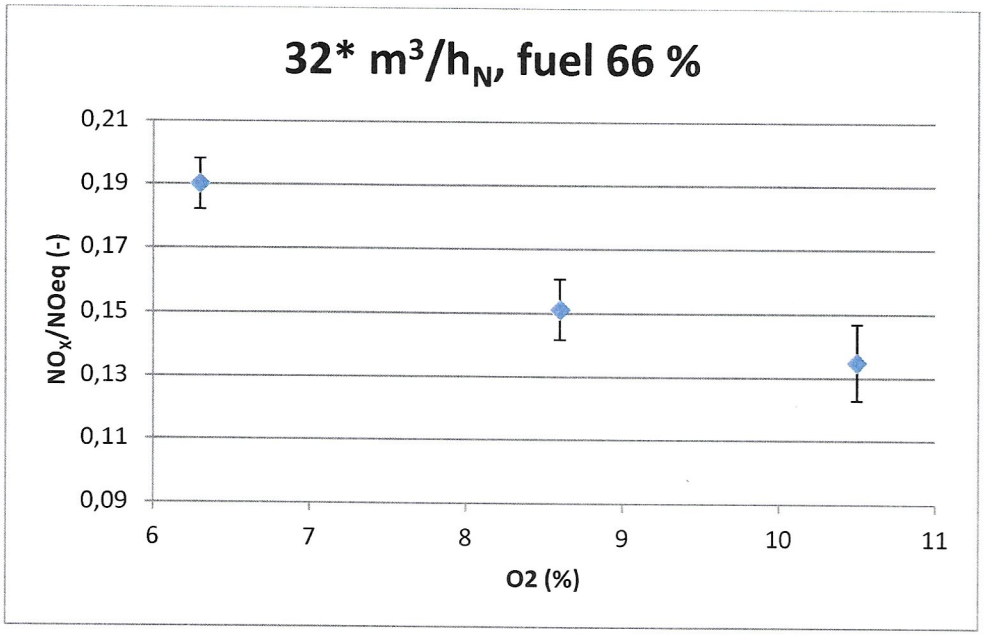

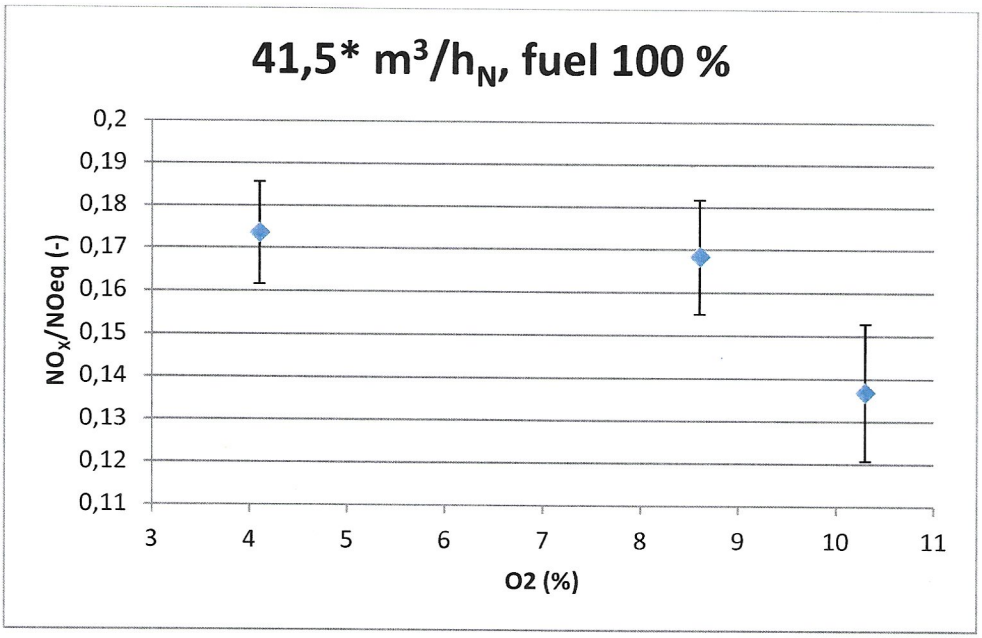

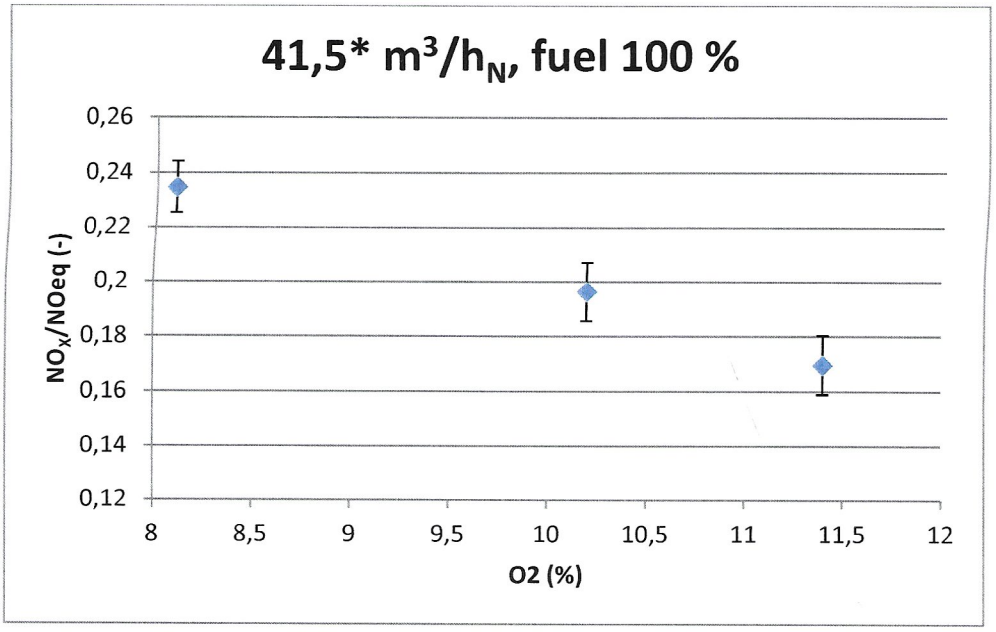

4) Reynolds number of particles, measurements batches 1 - 5

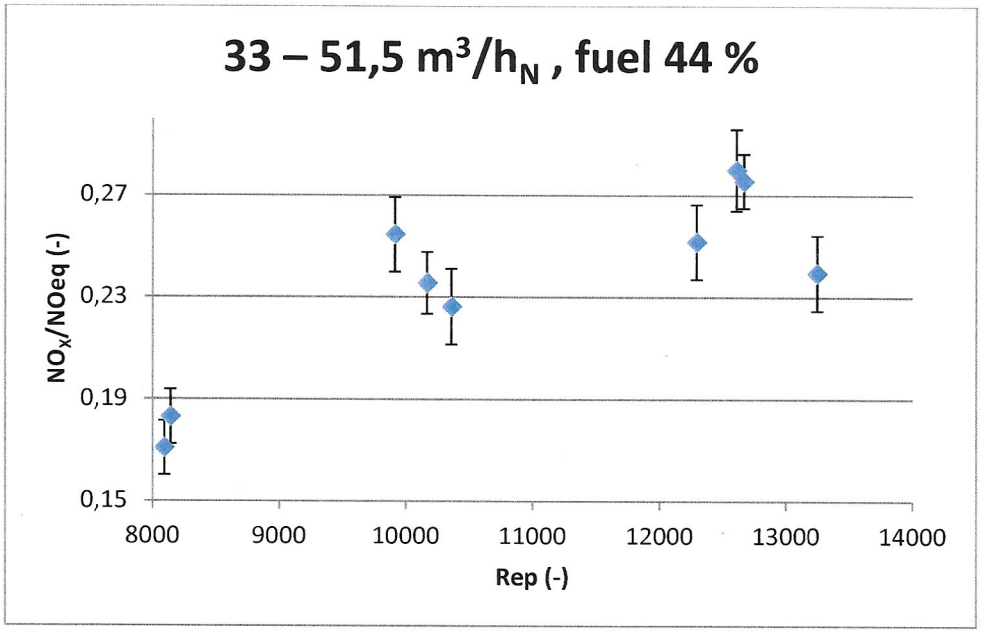

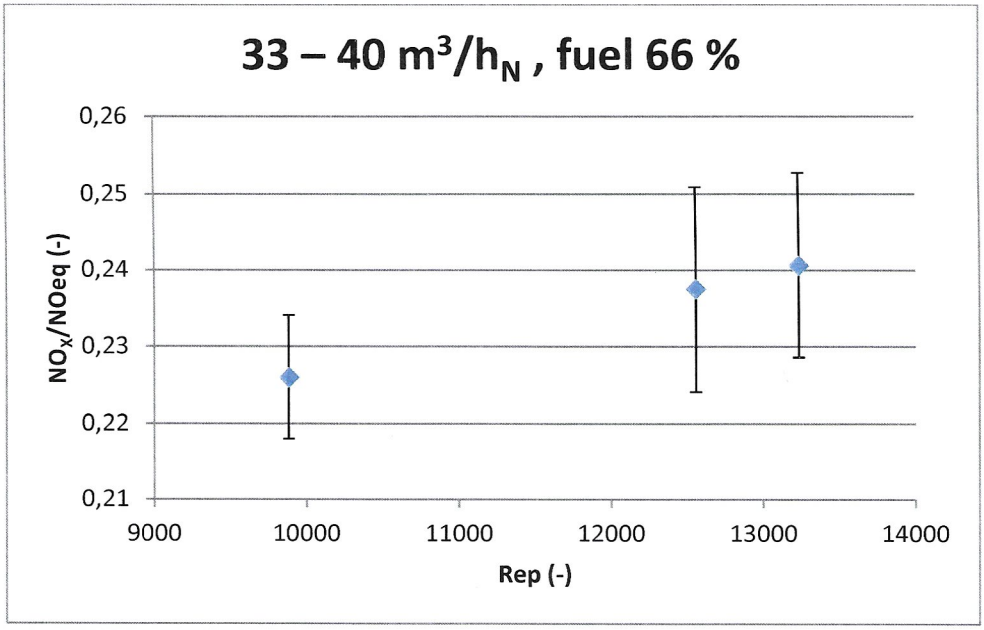
33 – 40 m³/h_N , fuel 66 %
0,26
0,25
0,24
0,23
0,22
0,21
NOx/NOeq (-)
9000
10000
11000
12000
13000
14000
Rep (-)

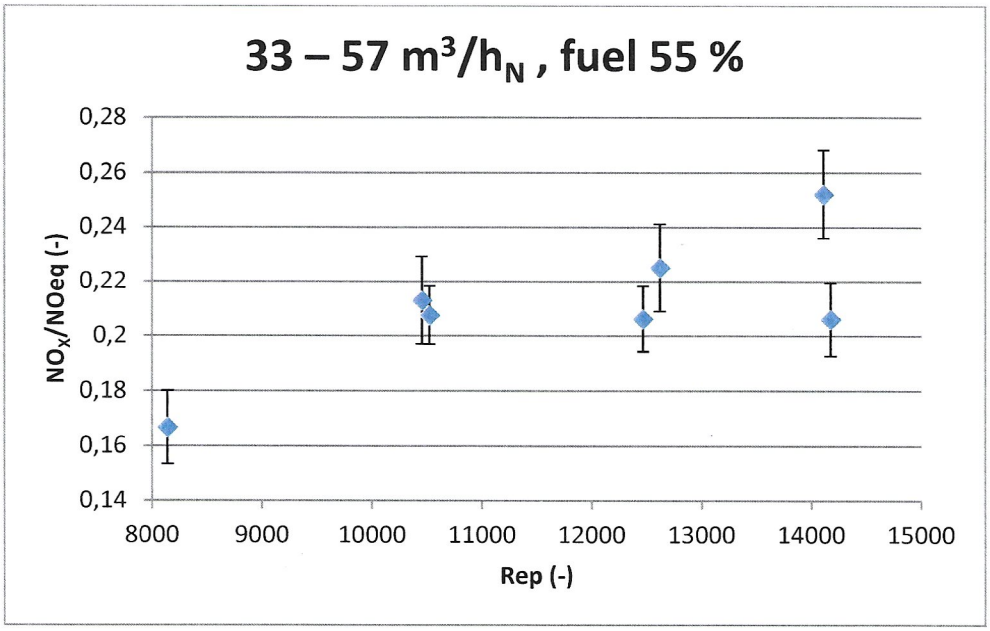
33 – 57 m³/h_N , fuel 55 %
0,28
0,26
0,24
0,22
0,2
0,18
0,16
0,14
NOx/NOeq (-)
8000
9000
10000
11000
12000
13000
14000
15000
Rep (-)

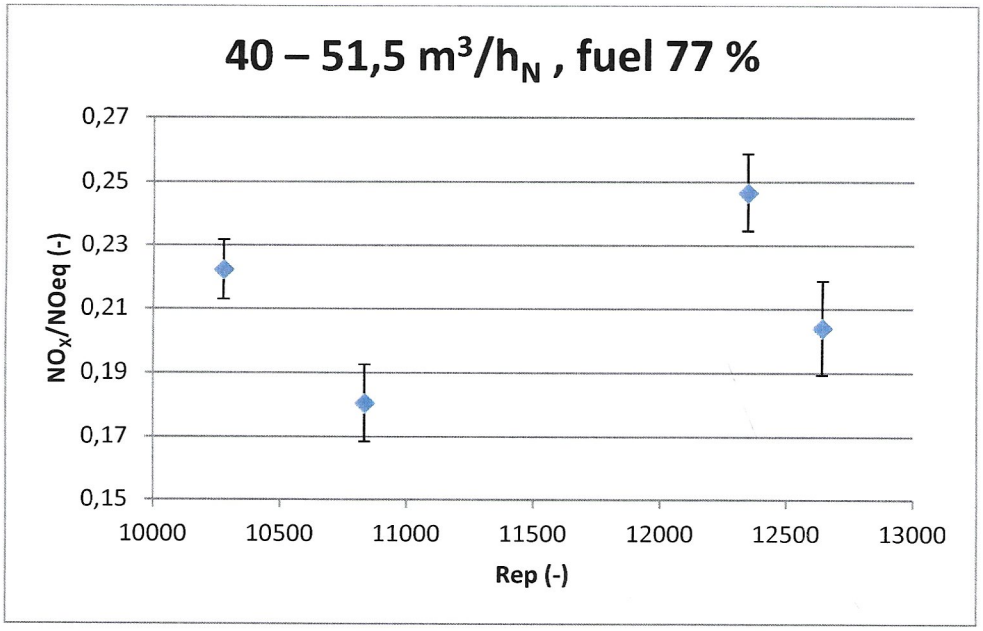
40 – 51,5 m³/h_N , fuel 77 %
0,27
0,25
0,23
0,21
0,19
0,17
0,15
NO_X/NOeq (-)
10000
10500
11000
11500
12000
12500
13000
Rep (-)

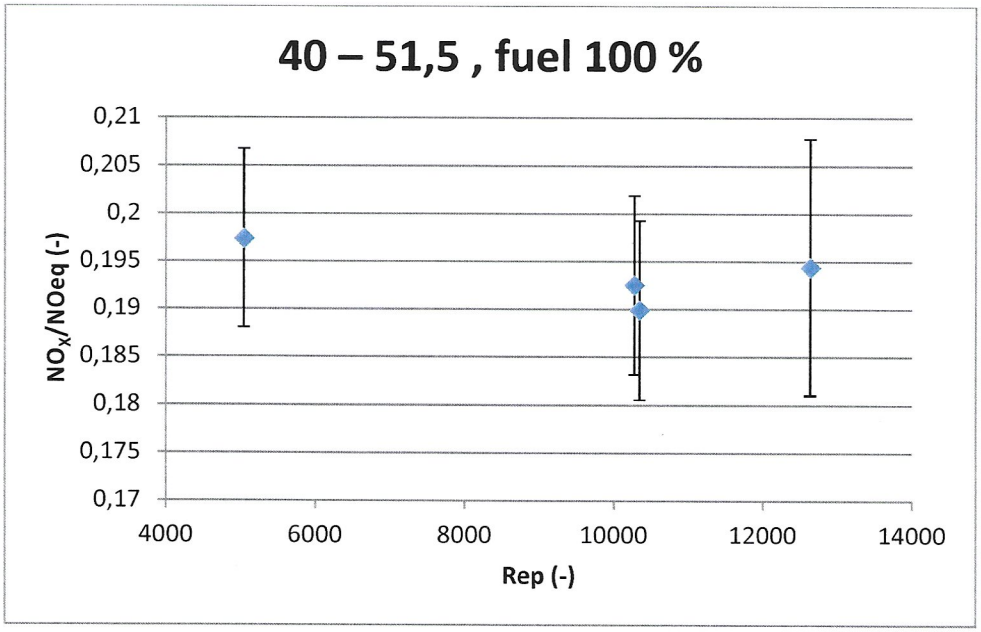
40 – 51,5 , fuel 100 %
0,21
0,205
0,2
0,195
0,19
0,185
0,18
0,175
0,17
NO_X/NOeq (-)
4000
6000
8000
10000
12000
14000
Rep (-)

Appendix 2 – Measurement evaluation of lignite coal

1) Primary oxygen concentration, Measurements batch 1 – 3

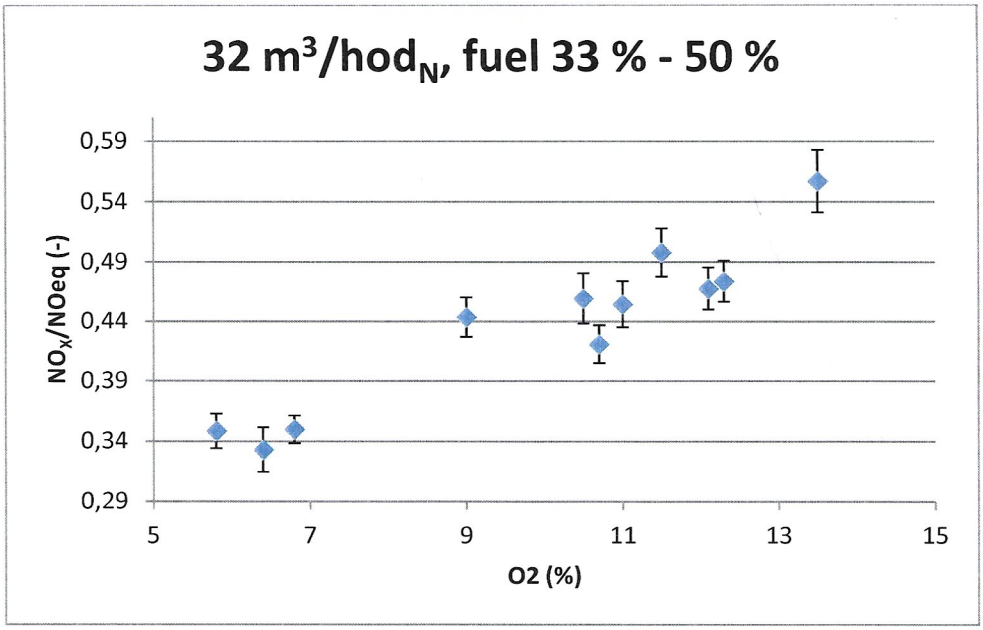

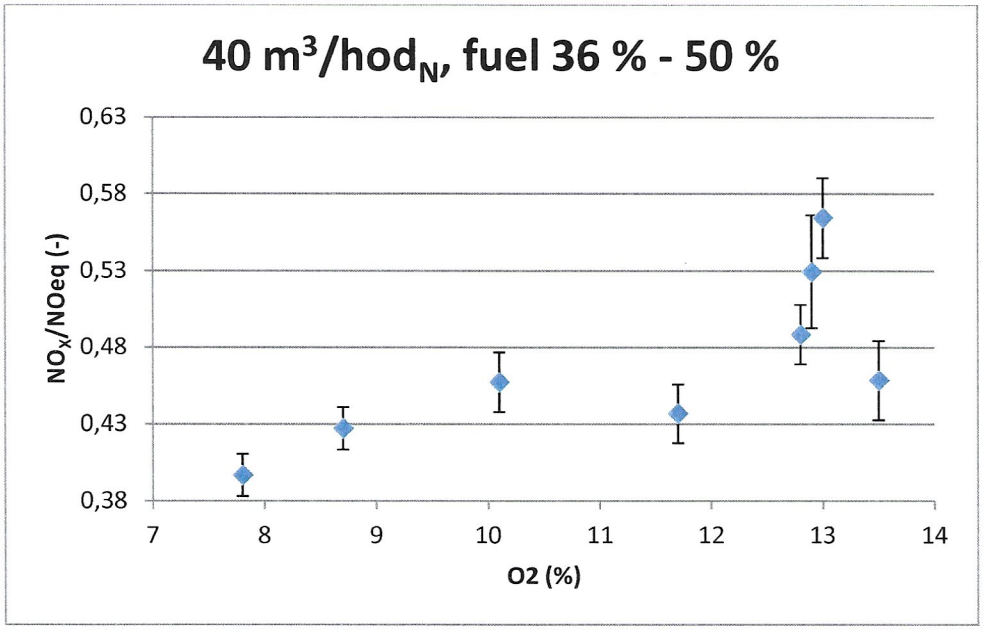

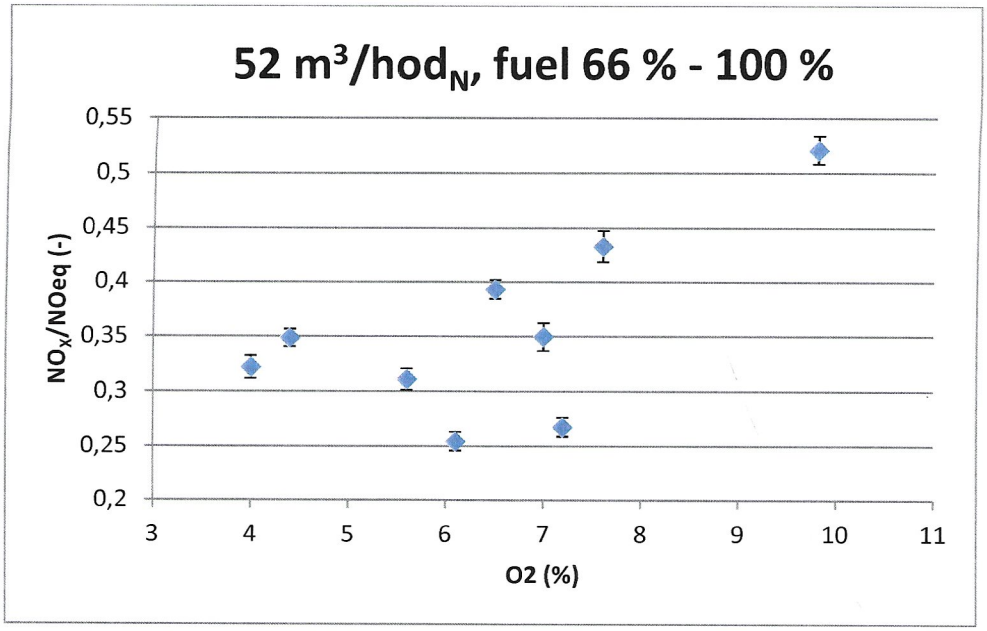

2) Temperature, measurements batch 1 - 3

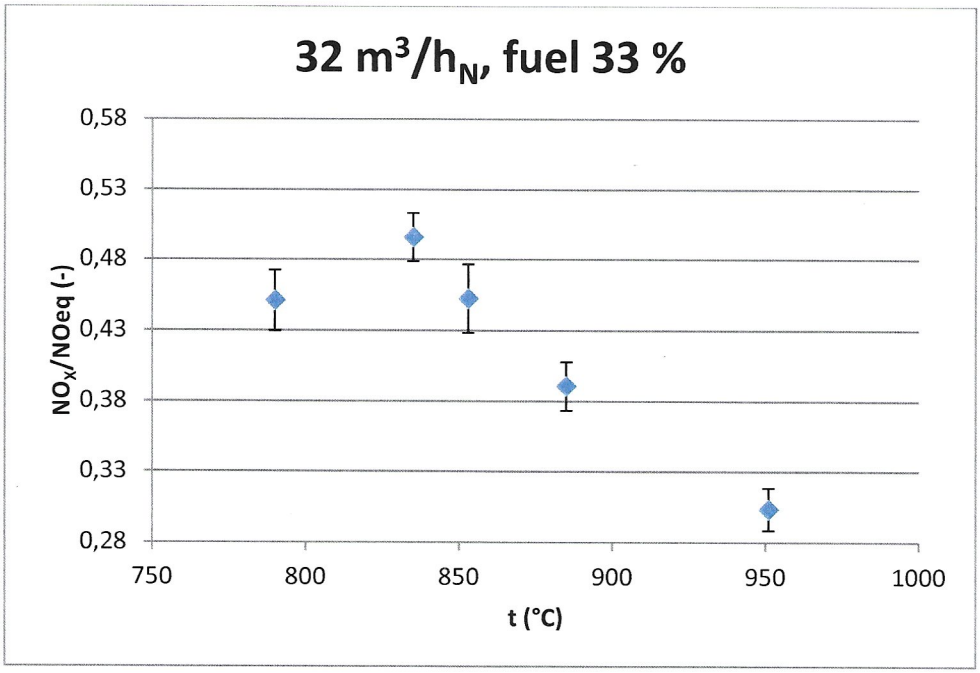

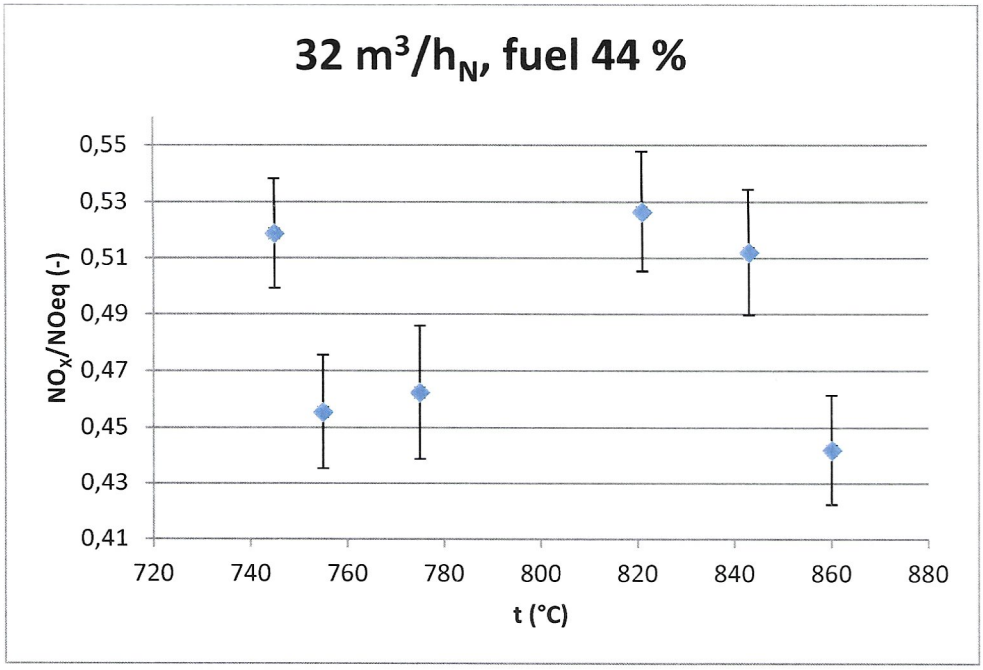
32 m³/h_N, fuel 44 %
NO_X/NOeq (-)
0,55
0,53
0,51
0,49
0,47
0,45
0,43
0,41
720
740
760
780
800
820
840
860
880
t (°C)

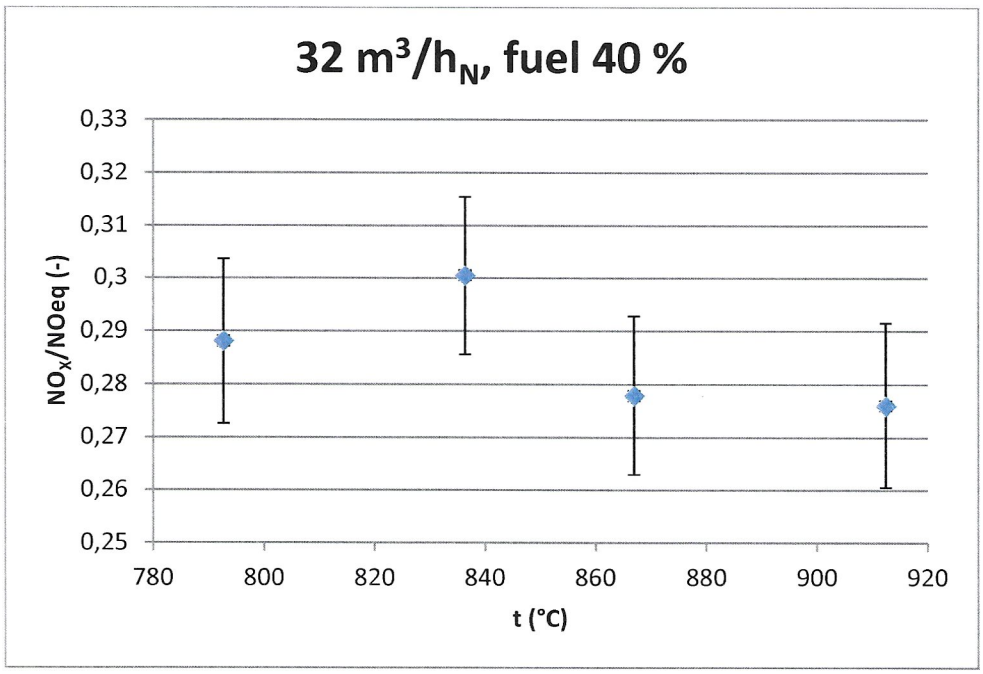
32 m³/h_N, fuel 40 %
NO_X/NOeq (-)
0,33
0,32
0,31
0,3
0,29
0,28
0,27
0,26
0,25
780
800
820
840
860
880
900
920
t (°C)

3) Total oxygen concentration (air staging) – measurements batches 1 - 3

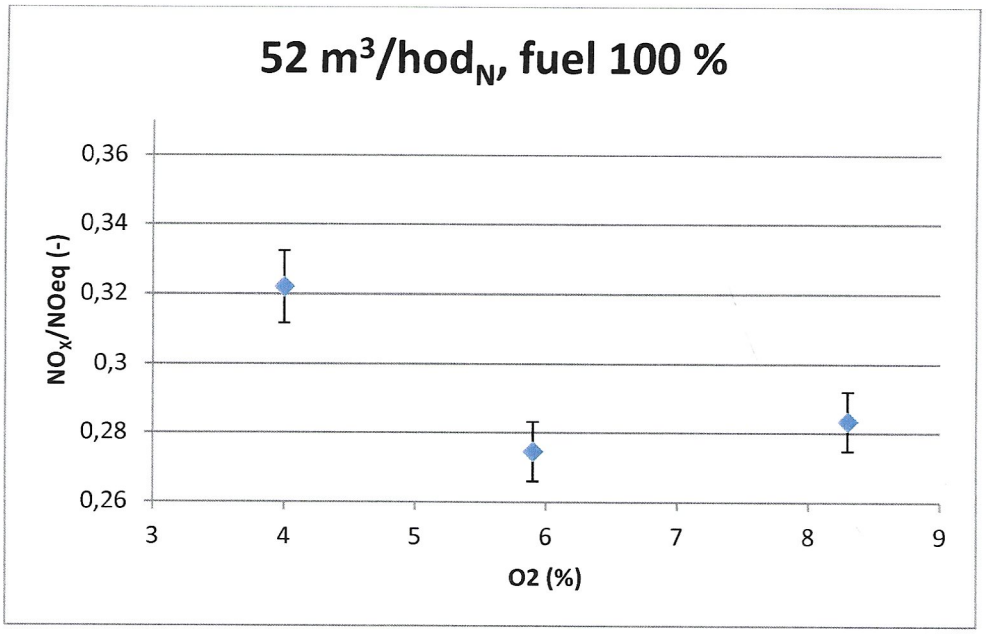

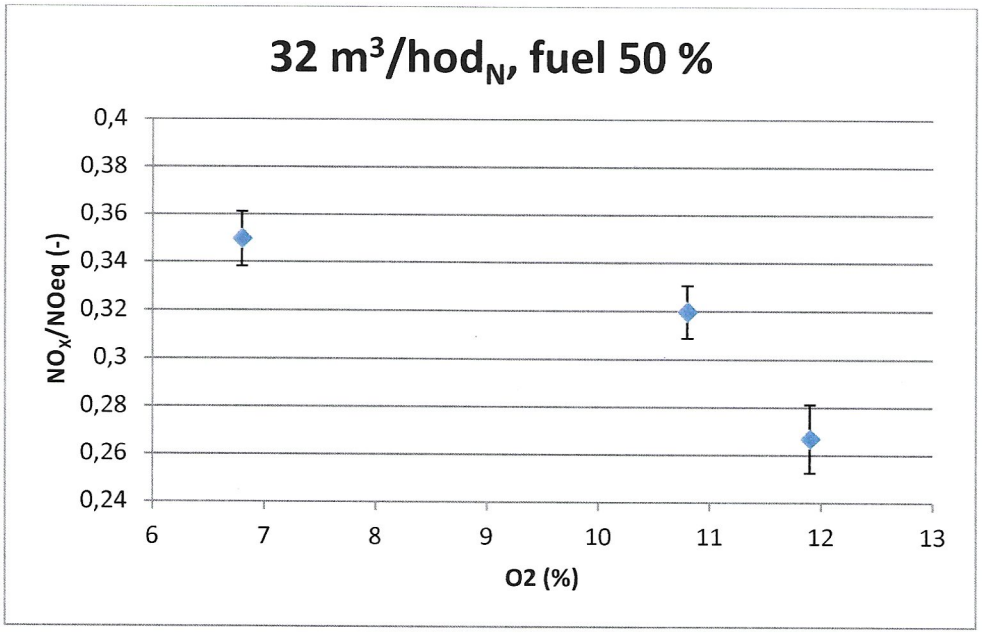

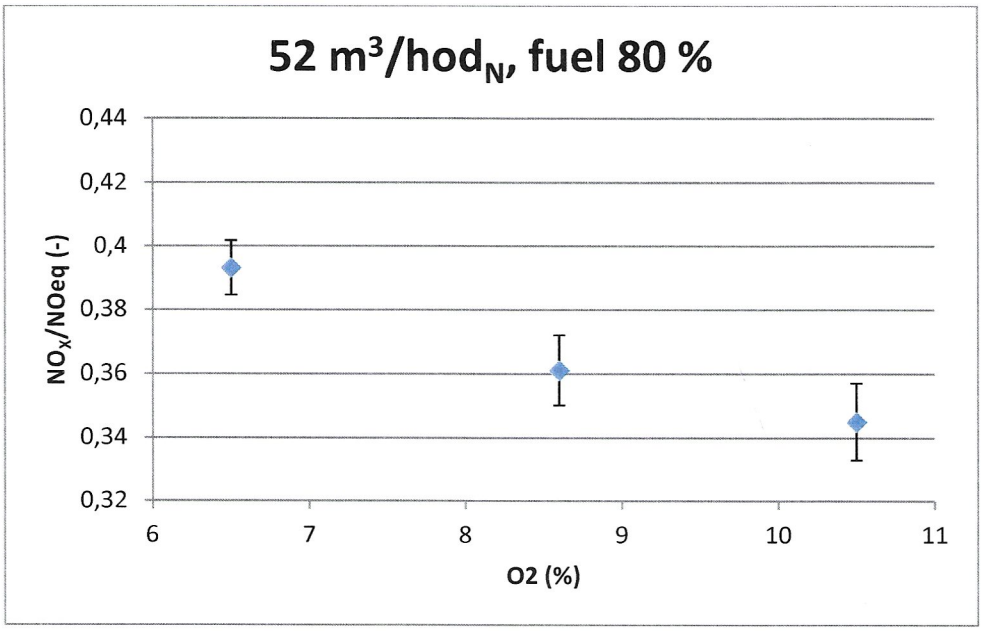

4) Reynolds number of particles, measurements batches 1 - 2

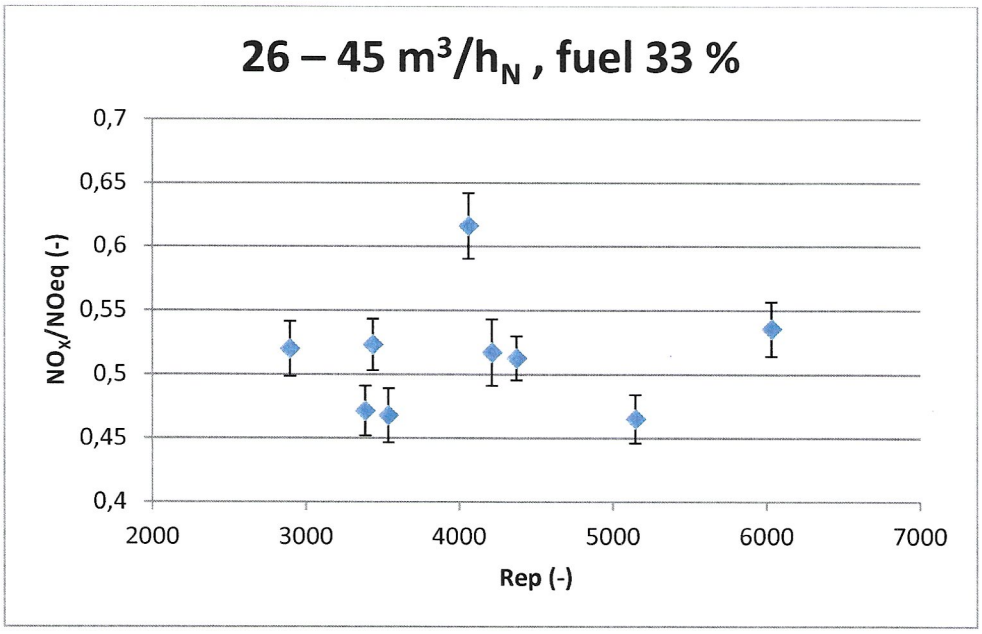

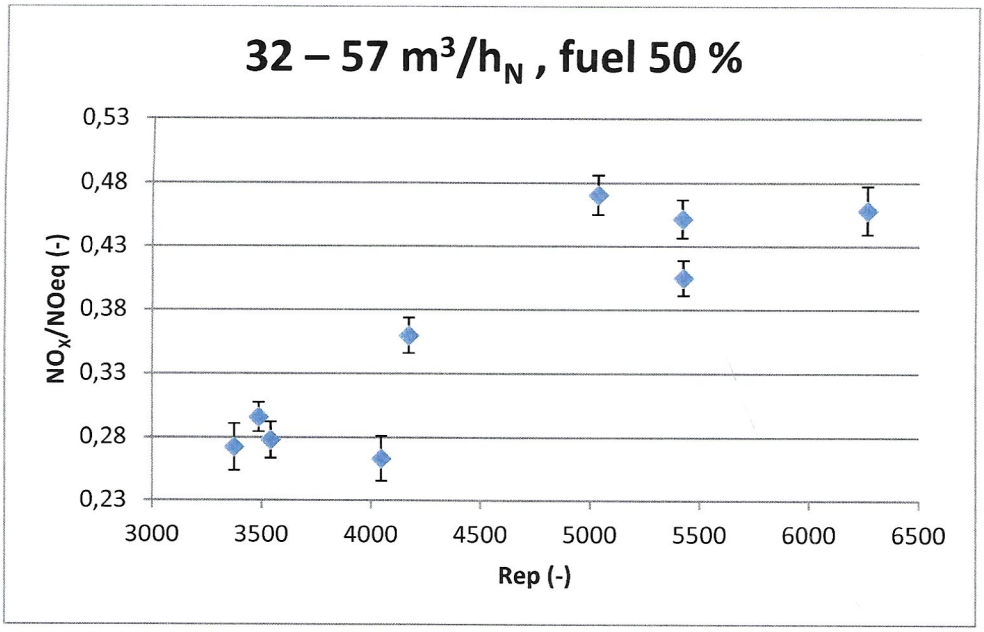

5) Flue gas recirculation coefficient – measurement batches 1 - 2

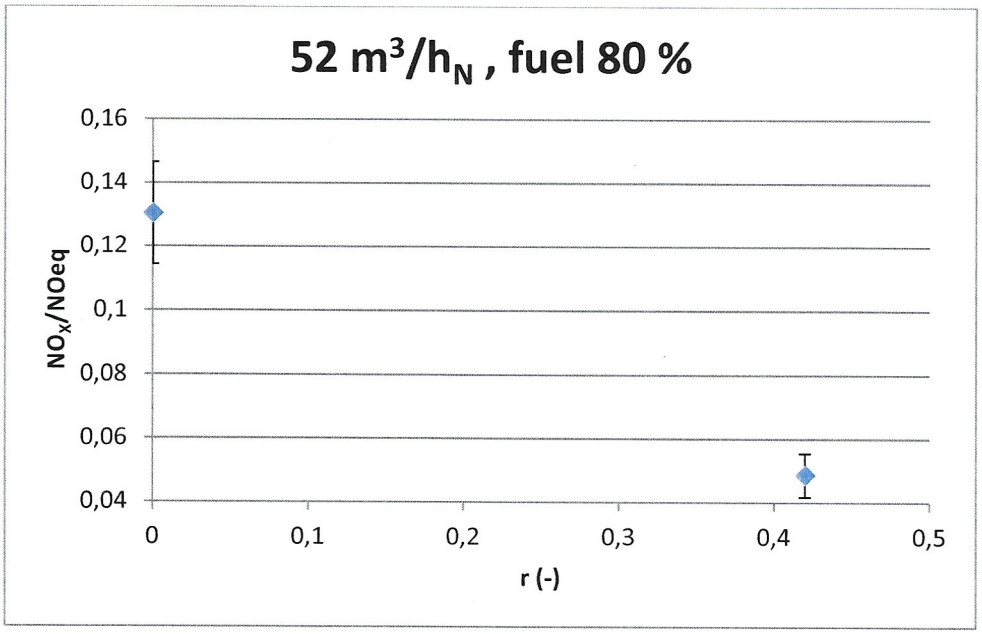

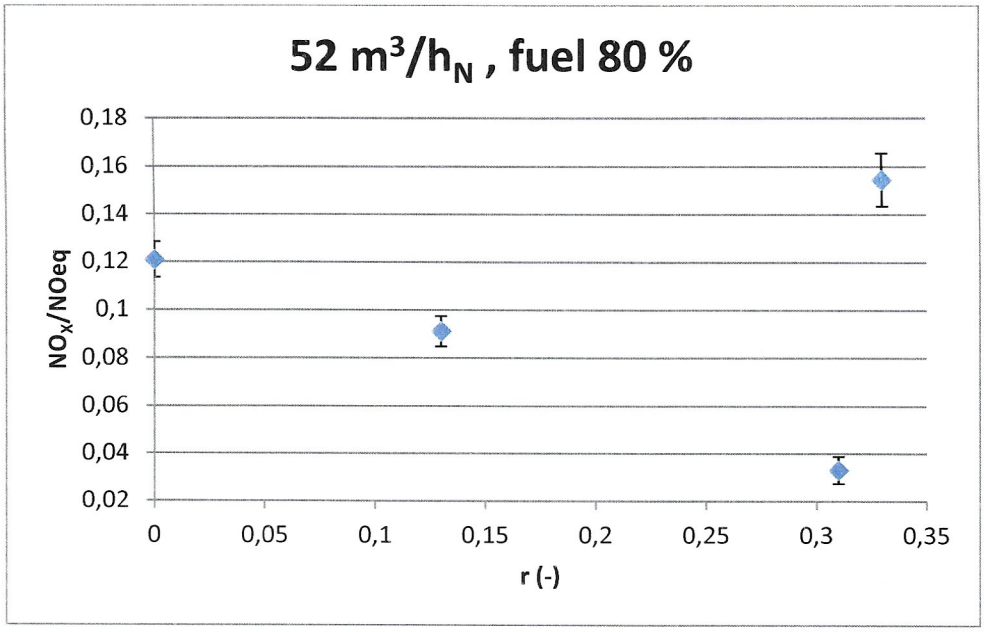
52 m³/h_N , fuel 80 %
0,18
0,16
0,14
0,12
0,1
0,08
0,06
0,04
0,02
NOx/NOeq
0
0,05
0,1
0,15
0,2
0,25
0,3
0,35
r (-)